Apr. 7 1947

THE JOURNAL OF CHEMICAL PHYSICS

VOLUME 15 NUMBER 6

JUNE, 1947

Published by the

AMERICAN INSTITUTE OF PHYSICS

Lancaster, Pa. and New York, N. Y.

...ould be used wherever ...ssible for fractions.

All illustrations should accompany manuscript and should always be referred to in the text. Line drawings must be made with India ink on plain white paper or on tracing cloth. Coordinate paper is not desirable, but if used must be blue-lined with all coordinates to be reproduced drawn with India ink. Lettering should be of sufficient size to be legible after reduction.

Proof and all correspondence concerning papers in the process of publication should be addressed to the Publications Manager, American Institute of Physics, 57 East ...Street, New York 22, New York.

Subscription Price

...*United States and Possessions, Canada and* ...Mexico $10.00
...Foreign 11.00

Back Numbers

Complete set: Vol. 1, 1933—Vol. 14, 1948 (except Vol. 1, No. 1) $140.00
Yearly price: $11.00.
Single copies: $1.00 each.

Subscriptions and orders for single copies should be addressed to Prince and Lemon Streets, Lancaster, Pennsylvania, or to the American Institute of Physics, 57 East ...Street, New York 22, New York.

Changes of address should be sent to the Business Manager, American Institute of Physics.

...Prince and Lemon Streets, Lancaster, Pennsylvania.

...Entered as second-class matter ... at the post office at Lancaster, Pa., under the Act of ... 1912. Acceptance for ... provided for in paragraph (d) Section ... P. L. & R., authorized

THE JOURNAL
OF
CHEMICAL PHYSICS

VOLUME 15, NUMBER 6 JUNE, 1947

On the Concentration Dependence of the Rates of Sedimentation and Diffusion of Macromolecules in Solution. Preliminary[1]

SEYMOUR J. SINGER[2]
Polytechnic Institute of Brooklyn, Brooklyn, New York

(Received February 12, 1947)

The concentration dependence of the osmotic pressure, rate of diffusion, and sedimentation velocity for solutions of high molecular weight solutes, on the basis of certain assumptions, have been shown to be interrelated. Experimental confirmation, however, has been lacking. Preliminary data are given in this article which satisfy these interrelationships, with fractions of cellulose acetate in acetone; however, more cooperative osmotic pressure, diffusion, and sedimentation experiments on a variety of well-defined systems are necessary to confirm the hypothesis.

If and when this additional confirmation is produced, the assumptions involved in the hypothesis may be considered correct; these are: (1) that the frictional coefficient in diffusion is the same (barring special cases of orientation during transport) as the frictional coefficient in sedimentation; and (2) that the driving force of diffusion is the gradient of the free energy of dilution of the system.

For solutions with no heat of mixing, the slight dependence of the diffusion constant on concentration has its molecular basis in the fact that the size and shape of the molecules affect the thermodynamic and hydrodynamic contributions to the variation of the diffusion rate to a comparable extent, and these contributions partially cancel one another. This is quantitatively so in the simple case of rigid spheres in an athermal solution.

A. INTRODUCTION

THE dependence of the rates of sedimentation and diffusion of solutes of high molecular weight on their concentrations in solution has long been of considerable empirical and theoretical interest. These rates, for example, have to be extrapolated to zero concentration in order for the Svedberg molecular weight equation to hold. It has been found that the sedimentation velocity is generally much more marked a function of concentration than the rate of diffusion, and that the dependence is more pronounced the more asymmetric the solute molecule. Certain independent empirical relations have been adduced to account for these rate variations with concentrations, and these generally satisfy the experimental data. The purposes of this paper are to discuss the investigation of Beckmann and coworkers, who have related these rate dependences to one another and to the variation of the thermodynamic properties of the solution with concentration; to present experimental data substantiating their hypothesis; and to develop in more detail the explanation of these rate phenomena in the light of recent advances in the theory of solutions.

B. THEORY

A brief account of the pertinent theory of the ultracentrifuge is necessary in order to discuss the material covered in this article. More detailed general information may be found elsewhere.[3,4]

[1] This paper was presented at the Twentieth Colloid Symposium, University of Wisconsin, May 1946.
[2] Du Pont Research Fellow, 1946–1947.
[3] T. Svedberg and K. O. Pedersen, *The Ultracentrifuge* (Oxford University Press, London, 1940).
[4] E. G. Pickels, Chem. Rev. **30**, 341 (1942).

When molecules in solution are acted upon by a centrifugal field of sufficient strength, the random Brownian motion, tending to keep the average concentration of the solution uniform, is partially overcome, and the molecules sediment in the direction of the field. The velocity of sedimentation is small and nearly constant, and, thus, the resultant force on each molecule is almost zero. That is, the weight minus the buoyant force may be taken as equal to the force of resistance for each molecule. For a gram-molecular weight of such molecules we have the relation:

$$M(1-\bar{V}d)\omega^2 x = f dx/dt. \tag{1}$$

M is the molecular weight of the solute of partial specific volume $\bar{V}$, moving with an average velocity dx/dt in a fluid of density d; x is the distance from the axis of rotation and ω is the angular velocity with which the centrifuge rotor is spinning. The force of resistance acting on the molecule may be taken as proportional to the velocity with which the molecule moves in the fluid; the proportionality constant f, as written in Eq. (1), is called the molar frictional coefficient. The sedimentation constant, s, is defined as $(dx/dt)/\omega^2 x$, and Eq. (1) may be put in the form:

$$s_c = M(1-\bar{V}d_c)/f_{s,c}, \tag{1a}$$

where the subscript c indicates a finite concentration, and the subscript s refers to sedimentation. Many investigators[5–11] have found the sedimentation constant to be a quantity strongly dependent on concentration, and it is well understood that experiments must be performed at several concentrations, and the sedimentation constant extrapolated to infinite dilution. Empirically, it has been shown that for most high polymer solutions, and for solutions of asymmetric protein molecules, the sedimentation data fit the equation:

$$s_c = s_\infty/(1+k_s c), \tag{2}$$

where k_s is a constant. It has been demonstrated that $\bar{V}$ is essentially independent of concentration in dilute solutions.[6,7] The problem of what value of d_c to use in Eq. (1a) is not yet settled: the appropriate value is probably in between that for the macroscopic density of the solution and the density of the pure solvent. In any event the magnitude, Δd, of the change of density in going from solvent to a dilute solution is generally small compared to the magnitude of k_s. *Therefore, when $k_s \gg \Delta d$, the dependence of s upon c is entirely caused by the variation of $f_{s,c}$ with c.*[12] If we write

$$f_{s,c} = f_{s,\infty}(1+k_s c), \tag{3}$$

we then obtain Eq. (2) from Eq. (1a).

The Einstein gas law of diffusion:[13]

$$D_\infty = RT/f_{D,\infty} \tag{4}$$

holds at infinite dilution, where D_∞ is the diffusion constant extrapolated to zero concentration, R the gas constant, T the absolute temperature, and $f_{D,\infty}$ the molar frictional coefficient acting during the diffusion process. If $f_{D,\infty} = f_{s,\infty}$, combination of Eqs. (1a) and (4) yields the well-known Svedberg equation for molecular weights obtained with the aid of the velocity ultracentrifuge:

$$M = RTs_\infty/D(1-\bar{V}d). \tag{5}$$

At any finite concentration, however, the gas law of diffusion cannot be expected to hold, except for ideal solutions. *If the driving force of the diffusion process is the gradient of the free energy of dilution of the system*, i.e., the gradient of $\Delta\bar{F}_1$, the partial molar free energy of the solvent in the solution minus the partial molar free energy of the solvent at infinite dilution, Onsager and Fuoss[14] have shown that the diffusion constant at a finite concentration depends on the activity coefficient of the solute. Equivalently, since $\Delta\bar{F}_1 = -\pi\bar{V}_1$, giving the osmotic pressure of the solution by a convergent power series in the solute concentration:

$$\pi = (RT/M)c + Bc^2 + \cdots, \tag{6}$$

[5] R. O. Carter, J. Am. Chem. Soc. **63**, 1960 (1941).
[6] N. Gralen, *Inaugural Dissertation*, Uppsala (1944).
[7] I. Jullander, Arkiv. f. Kemi Min. Geol. **A21**, 1 (1945).
[8] M. Lauffer, J. Am. Chem. Soc. **66**, 1189 (1944).
[9] H. Mosimann, Helv. Chim. Acta **26**, 61 (1943).
[10] R. Signer and H. Gross, Helv. Chim. Acta **17**, 59, 335 (1934).
[11] K. G. Stern, S. Singer, and S. Davis, Polymer Bull. **1**, 31 (1945).

[12] For solutions of symmetrical protein molecules, s_c varies more slowly with c than described by Eq. (2). This is probably due to the fact that Δd is beginning to make a significant contribution.
[13] A. Einstein, Ann. d. Physik **17**, 549 (1905).
[14] L. Onsager and R. M. Fuoss, J. Phys. Chem. **36**, 2689 (1932).

where B is a constant[15] independent of the molecular weight of the solute, and $\bar{V}_1$ is the partial molar volume of the solvent, we may write:

$$D_c=(RT/f_{D,c})[1+(2BM/RT)c]. \quad (7)$$

Most dilute solutions (up to concentrations of 1 percent or so) of solutes of high molecular weight have osmotic pressures that are satisfactorily represented by the first two terms in Eq. (6), and so Eq. (7) should represent their diffusion behavior.[16–18]

Assuming now that $f_{D,c}=f_{s,c}$, an assumption analogous to the one previously made for the frictional coefficients at zero concentration, we obtain Eq. (8):

$$D_c=\frac{RT[1+(2BM/RT)c]}{f_\infty(1+k_sc)}$$

$$=D_\infty\frac{[1+(2BM/RT)c]}{1+k_sc}\cong D_\infty(1+k_Dc). \quad (8)$$

It has been found empirically that the diffusion constant generally varies linearly with concentration[6,7,19] represented by the right side of Eq. (8); k_D is some small constant which is most often positive but may be negative, and which is somewhat a function of the molecular weight in a homologous series of polymers.[7]

According to this treatment of the problem, a modification of that credited to Beckmann and Rosenberg,[19,20] the slight dependence of the diffusion constant on concentration is attributable to the balancing of two effects: the thermodynamic, usually tending to increase the diffusion constant at a finite concentration, and the hydrodynamic, always tending to decrease it.[21] "In general, we should suppose that the effect of mutual influence of particles sedimenting in a solution will be a retardation of the motion; . . . so that apparently for every molecule the frictional forces will become somewhat greater than they are for a single molecule in an unlimited field." [22] The sign and magnitude of k_D depends on the relative magnitudes of the two factors. Moreover, the variation of the frictional coefficient with concentration should be the same during sedimentation and diffusion, and we expect the relation

$$[1+(2BM/RT)c]/[1+k_sc]=1+k_Dc+\cdots. \quad (9)$$

It should be emphasized that k_s has not been made any the less empirical; it is still not derivable from molecular parameters except for spherical particles (see below). What this treatment does is to relate in a reasonable fashion the variations of osmotic pressure, rate of diffusion, and sedimentation velocity, with concentration in dilute solutions.

C. EXPERIMENTAL

One of the aims of this communication is to provide some experimental confirmation of the hypothesis just outlined by testing the validity of Eq. (9), through independent sedimentation, diffusion, and osmotic pressure measurements on the same systems. Unfortunately, heretofore there have been no published data in which all three types of experiments were performed on the same solutions. However, with some severe assumptions, the sedimentation data of Signer and Gross[10] on unfractionated polystyrenes in chloroform may be subjected to analysis.

We take for the value of B in this system a modification of that reported by Boyer,[23,24] obtained by swelling measurements. This value is somewhat dependent on the method of

[15] Over a very wide range of molecular weights, however, theory predicts some variation of B with M.

[16] T. Alfrey, A. Bartovics, and H. Mark, J. Am. Chem. Soc. **65**, 2319 (1943).

[17] P. M. Doty and E. Mishuk, J. Am. Chem. Soc., in press.

[18] H. M. Spurlin, in *High Polymers*, Volume V (Interscience Publishers, Inc., New York, 1943), p. 910.

[19] C. O. Beckmann and J. Rosenberg, Ann. N. Y. Acad. Sci. **46**, 209 (1945).

[20] A similar interrelationship was proposed by R. Simha at a meeting of the American Physical Society, Columbia University, New York, January 1946.

[21] An exception will occur if the particles are oriented during transport. Orientation must be avoided, so that this exception is trivial.

[22] J. M. Burgers, in *Second Report on Viscosity and Plasticity* (Amsterdam, 1938), p. 178.

[23] R. F. Boyer, paper presented before the Columbia University meeting of the American Physical Society, January 1946; see also R. F. Boyer, J. Chem. Phys. **13**, 363 (1945). The μ value was given as 0.43; we have used 0.41 to correct for the effect of the cross-linking in the swelling measurements. In the Huggins theory for the osmotic pressures of polymer solutions,

$$B=(RT/V_1\rho_2^2)(\tfrac{1}{2}-\mu),$$

where ρ_2 is the density of the polymer. For ρ_2, the value 1.06 was used, and as a result $(2BM/RT)=2.0\pm10^{-3}M$. V_1 is the molar volume of solvent.

[24] M. L. Huggins, J. Chem. Phys. **9**, 440 (1941).

TABLE I. Polystyrene-chloroform sedimentation data (Signer and Gross).

$\eta sp/c$	M	k_s	$2BM/RT$
110	1,100,000	1990	2200
47	550,000	1110	1100
24	270,000	523	540
5.6	80,000	83	160

preparation of the polymer,[18] but this is disregarded here. For M we use the weight average values given by the authors: a number average is desirable, but there is no way to determine it from the given data. The assumption is made, moreover, that $k_D \ll 2BM/RT$, as is probably true for the higher molecular weight polystyrenes in chloroform. In toluene, a polystyrene fraction of molecular weight 200,000 gave a value[19] of $k_D = 10$, which is relatively small (see Table I), and in chloroform, also a good polystyrene solvent, the value is probably similar.

With these assumptions: that k_D is negligible; that the value of B obtained from swelling measurements is applicable; and that the molecular weights of the unfractional polymers given by equilibrium centrifuge measurements are suitable for our purposes, we obtain the values listed in Table I. The close agreement between k_s and $2BM/RT$ is no doubt fortuitous, considering the assumptions made in order to employ the excellent sedimentation data. Nevertheless, the confirmation of the development given above is striking.

We have studied the behavior of four fractions of cellulose acetate in acetone. The samples of fractions 2, 9, and 15 were from the well-known fractions of Sookne and Harris;[25] fraction 2c was prepared by Dr. W. Badgley, from a different batch of cellulose acetate, but using a similar fractionation procedure.[26]

Beckmann and Rosenberg[19] have found $k_D = 0$ at 25°C for an acetone solution of another cellulose acetate fraction prepared by Badgley, with a molecular weight 100,000. Since k_D is not strongly a function of molecular weight, we may assume that $k_D = 0$ for our fractions dissolved in acetone. The value of B at 27°C is available from the osmotic pressure measurements of Badgley[27] which were performed with a series of fractions; the slopes of the straight lines in the π/c against c graphs were the same within experimental error over a range of molecular weights 50,000–230,000.

The sedimentation measurements were performed with an air-driven ultracentrifuge; our installation is described elsewhere.[11] Several considerations, however, pertaining to the accuracy of the measurements are mentioned here.

The rotor, enclosed in a vacuum chamber, spins in an atmosphere of about 5-mm hydrogen gas, which serves to conduct away any heat generated during rotation to the cooling coils in the periphery of the chamber. A cold alcohol-water mixture is circulated through the coils during an experiment. The temperature of the rotor is determined by a thermocouple circuit, one junction of which is a silver leaf situated in the slip-stream of the spinning rotor. The slip-stream temperature was calibrated by observing the melting points of pure, low melting solids under experimental conditions, as suggested by Svedberg.[3] The rotor temperature was found to be 2.5°–4.0° above the slip-stream temperature as recorded by a galvanometer deflection, over the temperature interval 20°–40°C. Since most of the experiments were run at one speed, 720 r.p.s., and the temperatures were always near 30°, the correction necessary to obtain the actual rotor temperature was about 3°. During a run, the temperature variation was less than 2°, and no convection effects were noticed.

The speed is measured stroboscopically with a Strobotak,[28] the light from which is reflected from the top surface of the centrifuge air turbine. This surface is half-covered with a dull black paint, the other half retaining a metallic sheen. Runs are performed only at a multiple of the calibrated reed frequency, and the speed is measured and manually maintained constant to within ±10 r.p.s. without difficulty.

To calibrate the performance of the centrifuge, a 1 percent solution of bovine serum albumin in phosphate buffer was investigated. This protein is available in crystalline form from the Armour Company, Chicago, and was found to be electrophoretically and ultracentrifugally homogeneous. It was dissolved in phosphate buffer of pH 7.7, $\mu = 0.2$. A sedimentation experiment performed at 840 r.p.s. gave, when corrected to water at 20°,[3] $S_W^{1\%} = 4.04$; values reported in the literature are 4.0, by Cohn *et al.*[29] and 4.06 by Lauffer.[30]

[25] A. Sookne, H. Rutherford, H. Mark, and M. Harris, J. Research Nat. Bur. Stand. **29**, 123 (1942).

[26] W. Badgley, Ph.D. Thesis, Polytechnic Institute of Brooklyn, 1945. No chemical analyses were performed on fraction 2c; fractions 2, 9, and 15 analyzed for 38.6 percent acetyl.

[27] W. Badgley and H. Mark, J. Phys. Coll. Chem. **51**, 58 (1947).

[28] General Radio Company, Cambridge, Massachusetts.

[29] E. J. Cohn, J. A. Leutscher Jr., J. L. Oncley, S. H. Armstrong Jr., and B. D. Davis, J. Am. Chem. Soc. **62**, 3396 (1940).

[30] M. Lauffer, data published in F. W. Putnam, J. O. Erickson, E. Volkin, and H. Neurath, J. Gen. Physiol. **26**, 513 (1943).

The molecular weights of fractions 2, 9, and 15 were determined by osmotic pressure measurements, and of all four fractions by velocity ultracentrifuge and free diffusion measurements, with Eq. (5). Kraemer's value of $\bar{V}=0.68$ was utilized.[31] The diffusion technique employed is described in a forthcoming publication;[32] the experiments are performed in a modified Lamm diffusion cell[33] adapted to the Longsworth-Tiselius apparatus,[34] and the second moment method of calculating the diffusion constant is employed.[6]

In our experiments, however, the base-lines of the diffusion curves were slightly skewed, because the optical apparatus was focused for water and not acetone solutions. Therefore, we preferred not to calculate k_D; the curves we obtained appeared symmetrical, however, indicating a value of k_D very near zero.[6,19]

Since the molecular weight distribution of the cellulose acetate fractions appears quite sharp, there is little question as to the experimental value of M to insert in Eq. (9). We have consistently used the value determined ultracentrifugally, however.

In the calculation of the sedimentation constant, there are several fine points that deserve consideration. Under the influence of the high pressures built up in the centrifuge cell during an experiment, the viscosity of acetone changes noticeably from its value at atmospheric pressure. This has been demonstrated by Mosimann and Signer.[35] In our experiments, however, the sedimenting boundary was observed for only a short distance in the cell, never beyond 6.30 cm from the axis of rotation. (The distance to the top of the cell is 5.77 cm.) Moreover, at 720 r.p.s. the pressures are much less than at 1150 r.p.s., the speed used in the calculations of Mosimann and Signer. Therefore, while the viscosity corrections were always made because of pressure, they never exceeded 4 percent. The variation of the density of solvent with pressure was even smaller.

There is still another factor, however, which must be taken into account. It is well known that during sedimentation there occurs a dilution effect[3] caused by the sector shape of the cell, and the continual increase in the centrifugal force with distance from the axis of rotation. The magnitude of this effect is given by the relation: $c_t=c_0(x_0/x_t)^2$, where c_t is the concentration of the solution at the distance x_t in the cell, c_0 is the initial concentration, and x_0 the distance to the top of the cell. If the sedimentation boundary is observed at 6.30 cm, the effective concentration of the solution will be 16 percent less than the original value, a serious effect in all cases where an appreciable concentration dependence of the sedimentation constant exists. In our experiments the average concentration during an experiment was never different by more than 8 percent from the original, and this average value was employed in evaluating the data. Under these circumstances, no systematic variation of the sedimentation constants during a run was observed.

In Fig. 1, the Philpot sedimentation diagrams[36] of the bovine serum albumin experiment, and of experiments on two of the cellulose acetate fractions, are reproduced. The results of our measurements are listed in the first three columns of Tables II, III, IV, and V and are represented graphically in Fig. 2. In Table VI are recorded

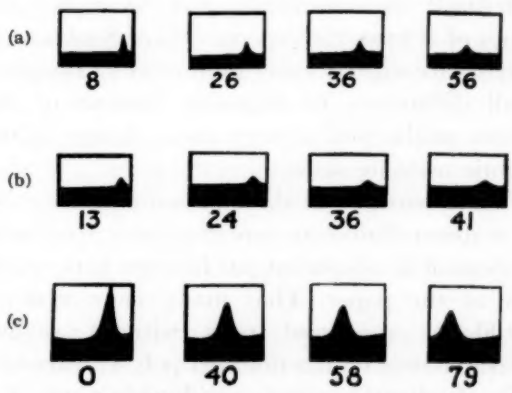

FIG. 1. Philpot sedimentation diagrams of: (a) fraction 2 in acetone at 0.181 percent; (b) fraction 9 in acetone at 0.167 percent; and (c) bovine serum albumin in phosphate buffer pH 7.7, $\mu=0.2$ at 1 percent. The ordinate of each diagram is the refractive index gradient in the solution, and the abscissa the distance in the cell. The numbers under the diagrams refer to the times in minutes after the first reference exposure.

[31] E. O. Kraemer and W. D. Lansing, J. Phys. Chem. **39**, 153 (1935).

[32] K. G. Stern, S. Singer, and S. Davis, J. Biol. Chem., in press.

[33] O. Lamm, Nova Acta Reg. Soc. Sci. Upsal. **IV, 10**, 1 (1937).

[34] L. G. Longsworth, Ind. Eng. Chem. A. E. **18**, 219 (1945).

[35] H. Mosimann and R. Signer, Helv. Chim. Acta **27**, 1123 (1944).

[36] J. St. L. Philpot, Nature **141**, 283 (1938).

TABLE II. Fraction 15.

c_{av} g/100 cc	$s_{20} \times 10^{13}$	$(1/s_{20}) \times 10^{-12}$	η_{sp}/c*
0.925	3.83	2.61	0.241
0.694	3.93	2.54	0.238
0.463	3.94	2.54	0.235
0.000	4.07**		0.230**

* Extrapolated from data of A. Sookne and M. Harris, Ind. Eng. Chem. **37**, 475 (1945).
** Extrapolated.

TABLE III. Fraction 9.

0.483	5.9	1.70	1.75*
0.344	6.3	1.59	1.64
0.243	6.8	1.47	1.56
0.230	6.5	1.54	1.55
0.173	6.7	1.49	1.50
0.173	6.6	1.51	1.50
0.117	7.2	1.39	1.45
0.000	7.5**		1.37**

* Interpolated in the data of A. Sookne and M. Harris, Ind. Eng. Chem. **37**, 475 (1945).
**Extrapolated.

the calculations concerning the validity of Eq. (9), with k_D taken as zero.

It is to be noted that while the deviations of k_s from $2BM/RT$ are within experimental error for all three fractions, the values of k_s are very closely proportional to the values of M. It may be possible, therefore, to ascribe the observed slight discrepancies to somewhat different values of B, resulting from the use of different batches of c.p. acetone in the osmotic pressure and ultracentrifugal measurements. For example, the values of B from the experiments of Sookne and Harris[37] are slightly lower than those of Badgley. Small differences in impurity content of the solvent might well account for a change in the osmotic pressure slope.

Consequently, the data presented above for the system cellulose acetate in acetone agree with the general development put forward in the early part of the paper. That many more systems should be measured goes without saying. Measurements on fractionated polystyrenes in a series of solvents, over a considerable range of B values are being initiated in our laboratories. Not until more data over a large interval of B and k_s values are obtained will the quantitative considerations given above be generally confirmed. At the moment, however, the available data do agree with the hypothesis.

D. DISCUSSION

Up to this point no reference has been made to any of the theories concerning the value of B, the slope of the π/c against c lines, measuring the departure of the solution from the ideal. The quantitative interrelationships of the concentration dependences of the diffusion rate, the sedimentation velocity, and the osmotic pressure are independent of the interpretation placed upon B, only its magnitude being significant. However, in order to gain greater insight into the molecular parameters which so often cause the diffusion constant to be only lightly a function of concentration, some of these theories must be considered.

Many papers have been written in the past few years on the free energy of dilution of dilute macromolecular solutions, but for the particular purposes of this communication, two of the most recent are significant. Flory,[38] in a treatment which improves on previous calculations made with the quasi-lattice model of polymer solutions, and Zimm,[39] by the more rigorous and general method of molecular distribution func-

TABLE IV. Fraction 2.

0.329	7.4	1.35	4.08*
0.293	7.7	1.30	3.91
0.167	8.9	1.12	3.32
0.147	9.0	1.11	3.22
0.111	9.3	1.08	3.06
0.075	9.8	1.02	2.89
0.000	10.9**		2.75**

* Interpolated in the data of A. Sookne and M. Harris, Ind. Eng. Chem. **37**, 475 (1945).
** Extrapolated.

TABLE V. Fraction 2c.

0.353	7.5	1.34	5.20*
0.230	8.6	1.16	4.38
0.173	9.2	1.09	4.03
0.124	10.2	0.98	3.74
0.116	10.5	0.95	3.69
0.100	10.4	0.96	3.60
0.000	12.5**		3.05**

* Interpolated in the data of W. Badgley, private communication.
** Extrapolated.

[37] A. Sookne and M. Harris, Ind. Eng. Chem. **37**, 475 (1945).

[38] P. J. Flory, J. Chem. Phys. **13**, 453 (1945).
[39] B. H. Zimm, J. Chem. Phys. **14**, 164 (1946).

tions, come to roughly similar conclusions. Since the former treatment lends itself more readily to qualitative discussion, we will make more frequent use of it in the following paragraphs.

The free energy of dilution, $\Delta\bar{F}_1$, is made up of a heat and an entropy contribution:

$$\Delta\bar{F}_1=\Delta\bar{H}_1-T\Delta\bar{S}_1,$$

at constant temperature. *In athermal solutions*, $\Delta\bar{H}_1=0$, $\Delta\bar{F}_1=-T\Delta\bar{S}_1$, and $\pi=T\Delta\bar{S}_1/\bar{V}_1$; moreover, the entropy of dilution may be calculated without the necessity for any weighting of certain molecular configurations because of energy considerations. Without going into any details, for which the reader is referred to the original publication, the osmotic pressure term which is quadratic in the solute concentration is proportional to a "swelling factor," s, the ratio of lattice cells pervaded by the solute molecule to the number of segments in the molecule. In other words, in an athermal solution, B is proportional to a factor which is determined by the shape and rigidity of the molecule: the more compact the molecule, the smaller the value of B. Therefore, the product BM is a function both of the shape and size of the solute particle.

Now, the decrement in the sedimentation velocity with increasing solute concentration is obviously a function of the dimensions and form of the solute molecules, since these variables determine the extent of intermolecular interference in kinetic processes.[40] In a crude manner, then, we can understand that in athermal solutions, the quantities k_s and $2BM/RT$, both depending on the size and shape of the dissolved molecules in approximately the same way, are often of the same order of magnitude.

This is actually the case for athermal solutions of spherical particles. A rigorous theoretical

TABLE VI. $B=0.00125\pm0.00012$.

Fract.	s_{20} $\times10^{13}$	D_{20} $\times10^{-7}$	Molecular weight Osm.[37]	Sed. and diff.	$2BM/RT$	k_s
15	4.07	20.7	11,000	10,350	14±2	6±10
9	7.5	7.7	53,000	51,000	64±6	56±15
2	10.9	4.0	130,000	143,000	179±17	143±20
2c	12.5	3.4	———	194,000	243±23	191±25

[40] J. M. Burgers, Proc. Acad. Sci. Amsterdam **44**, 1045, 1177 (1941); **45**, 9, 126 (1942).

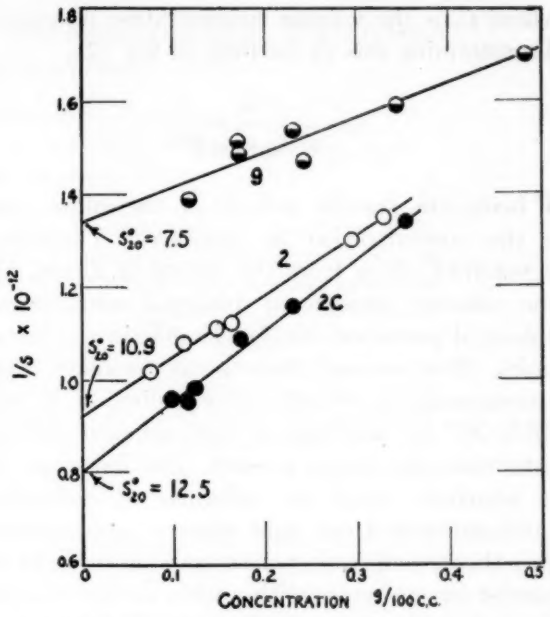

FIG. 2. Sedimentation data for three cellulose acetate fractions, 9, 2, and 2c, in acetone.

treatment of the problem of the concentration dependence of the sedimentation constant in such solutions is accredited to Burgers.[40] Since this paper is apparently not too well known as yet on this continent, a short section of it is quoted in the following paragraph.

"Under the influence of the field of flow produced by the falling particle A, the particle B is carried along with a velocity, the x-component of which is given by $u_m\cdots$; whereas the particle A, in consequence of the disturbance due to the presence of B, experiences an induced velocity $u_i\cdots$, which is of negative sign and thus evidently represents a retardation of the motion of $A\cdots$. Hence when we now consider two particles both of which experience the action of the same gravitational force, they will acquire the same resultant velocity, $u_{res}=(F/8\pi\eta)(4/3a+u_m+u_i)$." Here F is the weight minus the buoyant force acting on the particle of radius a, in a medium of viscosity η. Assuming the medium extends indefinitely in all directions, everywhere possessing the same average number of particles per unit volume, summations over the particles are performed, and neglecting terms of higher order,

$$u_{res}=\frac{F}{6\pi\eta a}\cdot\frac{1}{1+6.875C_v},$$

where C_v is the volume concentration of solute. Transforming this to the form of Eq. (2),

$$s_c=\frac{s_\infty}{1+6.875c\bar{V}},$$

$\bar{V}$ being the specific volume of the solute, and c the concentration in grams/cc. Therefore, $k_s=6.875\bar{V}$. Now from the theory of Zimm, for the osmotic pressure of athermal solutions of spherical particles, $2BM/RT=8\bar{V}$ in the same units. Thus we see that theory predicts close correspondence, though not equality, of k_s and $2BM/RT$ for solutions of rigid spheres with no intermolecular forces present. The fact that k_D is relatively small for solutions of molecules quite different from rigid spheres suggests that this theoretical correspondence will be found to persist for molecules with a wide variety of configurations in athermal solutions.

In dealing with solutions for which $\Delta\bar{H}_1\neq 0$, but is not large enough to alter significantly the shapes and distributions of the molecules from their characteristics in the athermal solution, it may be assumed as a first approximation[24] that the entropy and heat contributions to the free energy of dilution are independent, and that the entropy of dilution has the same value as it had in the previous case. For such solutions, according to the development just given, k_s should be of about the same magnitude as in the corresponding athermal solution, while k_D, a function of the free energy of dilution, should be somewhat different from its athermal value; larger if $\Delta\bar{H}_1<0$, smaller if $\Delta\bar{H}_1>0$. The value of $\Delta\bar{H}_1$ is given by the relation:

$$\Delta\bar{H}_1=\frac{\partial(\Delta\bar{F}_1/T)}{\partial(1/T)};$$

it may therefore be determined from the temperature dependence of the osmotic pressure.

For solutions with a large heat of mixing, where the heat and entropy of dilution are not independent, the quasi-lattice model becomes less significant, and the method of molecular distributions is at least hypothetically capable of predicting the osmotic pressure. However, the theory of the concentration dependence of the sedimentation constant for solutions of thread-like molecules is as yet so undeveloped that it is not profitable to attempt even qualitative correlations of k_s with the entropy of heat of dilution in such solutions. Moreover, there are practically no data concerned with this phase of the subject. Indeed, only in a very few polymer systems has the heat of dilution been determined. Evidently, investigations are required concerning the variation of k_s and k_D with $\Delta\bar{S}_1$ and $\Delta\bar{H}_1$ of solutions.

ACKNOWLEDGMENT

It is a pleasure of acknowledge the aid and advice given us by Drs. K. G. Stern, B. H. Zimm, P. M. Doty, and T. Alfrey of this Institute, during the course of this investigation. We are also grateful to Drs. M. Harris, A. Sookne, and W. Badgley for supplying the cellulose acetate fractions used in these experiments.

The Non-Degenerate Vibrations of Dimethylacetylene, Diacetylene, and Dimethyldiacetylene

ARNOLD G. MEISTER* AND FORREST F. CLEVELAND**
Department of Physics, Illinois Institute of Technology, Chicago 16, Illinois

(Received January 22, 1947)

By using force constants obtained from the observed non-degenerate frequencies of dimethylacetylene and diacetylene, the non-degenerate frequencies of dimethyldiacetylene were calculated. It was found that when several of these force constants were modified, agreement to within 2 percent of the observed values of the frequencies was possible. In order to check the values of the modified force constants the non-degenerate frequencies of diacetylene were recalculated. The central C−C stretching force constant was found to have a value of $3.234_2 \times 10^5$ dynes/cm which is much less than the normal value (5×10^5 dynes/cm) for a C−C stretching force constant. Finally, the previous tentative assignment of the observed Raman frequencies of dimethyldiacetylene has been revised as a result of the calculations.

INTRODUCTION

IN their analysis of the vibrational spectrum of diacetylene, Wu and Shen[1] found that the value of the stretching force constant for the carbon-carbon single bond was much lower than the value usually obtained for a C−C stretching frequency. They obtained a value of 3.58×10^5 dynes/cm which seems low when compared with a normal value of about 5×10^5 dynes/cm. Since Meister and Cleveland[2] have obtained the Raman spectrum of dimethyldiacetylene, and because a calculation of the fundamental frequencies of this molecule was necessary in order to check the tentative assignments of the observed frequencies made by the same investigators, it seemed possible that such a calculation should indicate whether this lowering of the value of the C−C stretching force constant also occurs for dimethyldiacetylene.

In order to calculate the non-degenerate fundamental frequencies for dimethyldiacetylene, it was necessary to obtain force constants for the potential energy function. These were obtained from molecules having a structure similar to that of dimethyldiacetylene. For the carbon chain force constants the diacetylene molecule was used, while the methyl group force constants were obtained from the dimethylacetylene molecule.

It was hoped that a similar method could be used for the doubly degenerate vibrations of dimethyldiacetylene but, unfortunately, this was not the case. The assignments of the doubly degenerate vibrations of diacetylene are still uncertain and no meaningful set of force constants could be obtained with the present assignments.[3] Either selection rules had to be violated in order to obtain reasonable force constants or if the selection rules were obeyed meaningless force constants resulted. It seems that it will be necessary to obtain the Raman spectrum of gaseous diacetylene since the Raman data now available is for the liquid state. Also, an investigation of the infra-red spectrum of dimethyldiacetylene would be very helpful in determining the doubly degenerate vibrations of both dimethyldiacetylene and diacetylene. So, for these reasons, no treatment will be made of the doubly degenerate vibrations of dimethylacetylene, diacetylene, or dimethyldiacetylene.

The Wilson *FG* matrix method[4] was used in all the calculations. It was very convenient because certain sections of the matrices involved were identical for some of the molecules being considered. As a further simplification, the C−H stretching frequencies for the methyl group (*ca.* 3000 cm^{-1}) were "split out" from the rest of the frequencies by making the appropriate force constants become infinite.[4] This procedure reduced considerably the number of determinants

* This paper is a report on an investigation carried out by Mr. Arnold G. Meister in partial fulfillment of the requirements for the degree of Doctor of Philosophy at Illinois Institute of Technology.

** Now at Lynchburg College, Lynchburg, Virginia.

[1] T. Y. Wu and S. T. Shen, Chin. J. Phys. **2**, 128 (1936).

[2] Arnold G. Meister and Forrest F. Cleveland, J. Chem. Phys. **12**, 393 (1944).

[3] G. Herzberg, *Infrared and Raman Spectra of Polyatomic Molecules* (D. Van Nostrand Company, Inc., New York, 1945), p. 325.

[4] E. B. Wilson, Jr., J. Chem. Phys. **7**, 1047 (1939); **9**, 76 (1941).

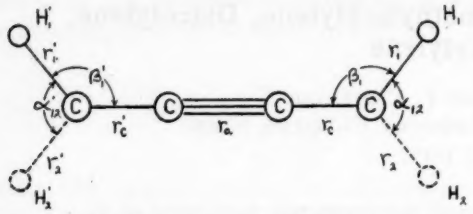

FIG. 1. Bond distances and interbond angles for dimethylacetylene. (Atoms H_3 and H_3' are omitted for clarity and simplicity.)

which had to be evaluated since each secular equation of the nth degree was reduced to one of the $(n-1)$th degree.

NORMAL COORDINATE TREATMENT

Dimethylacetylene Molecule

Although Crawford[5] has calculated the fundamental frequencies for dimethylacetylene, it was felt that the force constants should be recalculated since Crawford used the old value of Avogadro's number (6.06×10^{23}) in his work. Furthermore, he did not calculate all the force constants from the observed frequencies, since he was interested only in establishing the frequencies using calculations involving force constants most of which were transferred from ethane and acetylene. Following Crawford,[5] the dimethylacetylene molecule was assumed to have the symmetry D_{3h}'. Such a symmetry permits only four type A_1 non-degenerate vibrations and three type $\bar{A}_2$ non-degenerate vibrations. The various bond distances and interbond angles used to determine the internal coordinates are shown in Fig. 1, except those associated with H_3 and H_3' which are omitted for clarity and simplicity.

From the internal coordinates the following symmetry coordinates were formed: for the A_1 vibrations

$$R_1=\Delta r_a,$$

$$R_2=\frac{1}{\sqrt{2}}(\Delta r_C+\Delta r_C'),$$

$$R_3=\frac{1}{(6)^{\frac{1}{2}}}(\Delta r_1+\Delta r_2+\Delta r_3+\Delta r_1'+\Delta r_2'+\Delta r_3'),$$

$$R_4=\frac{1}{(12)^{\frac{1}{2}}}(\Delta\alpha_{12}+\Delta\alpha_{23}+\Delta\alpha_{31}+\Delta\alpha_{12}'+\Delta\alpha_{23}'+\Delta\alpha_{31}'-\Delta\beta_1-\Delta\beta_2-\Delta\beta_3-\Delta\beta_1'-\Delta\beta_2'-\Delta\beta_3');$$

and for the $\bar{A}_2$ vibrations

$$R_1=\frac{1}{\sqrt{2}}(\Delta r_C-\Delta r_C'),$$

$$R_2=\frac{1}{(6)^{\frac{1}{2}}}(\Delta r_1+\Delta r_2+\Delta r_3-\Delta r_1'-\Delta r_2'-\Delta r_3'),$$

$$R_3=\frac{1}{(12)^{\frac{1}{2}}}(-\Delta\alpha_{12}-\Delta\alpha_{23}-\Delta\alpha_{31}+\Delta\alpha_{12}'+\Delta\alpha_{23}'+\Delta\alpha_{31}'+\Delta\beta_1+\Delta\beta_2+\Delta\beta_3-\Delta\beta_1'-\Delta\beta_2'-\Delta\beta_3').$$

The potential energy function for the non-degenerate vibrations was the same as the one used by Crawford.[5] It was

$$2V=k_H\sum_6(\Delta r_i)^2+k_\alpha r_1^2\sum_6(\Delta\alpha_{ij})^2+k_\beta r_1^2\sum_6(\Delta\beta_i)^2+2k_{\alpha\beta}r_1^2\sum_{12}(\Delta\beta_i)(\Delta\alpha_{i,\,i\pm1})$$
$$+2k_{C\alpha}r_1\sum_6(\Delta r_C)(\Delta\alpha_{ij})+2k_{C\beta}r_1\sum_6(\Delta r_C)(\Delta\beta_i)+k_C[(\Delta r_C)^2+(\Delta r_C')^2]+k_a(\Delta r_a)^2$$
$$+2k_{CC}(\Delta r_C)(\Delta r_C')+2k_{Ca}(\Delta r_a)(\Delta r_C+\Delta r_C'),$$

[5] B. L. Crawford, Jr., J. Chem. Phys. 7, 555 (1939).

where $r_1 = 1.093$A (the equilibrium value of the C−H bond distance[5]), $i = 1, 2$, or 3, the subscript to the summation sign indicates the number of terms in the summation, and the summations are taken over primed and unprimed variables.

From the potential energy matrix and the matrix formed from the coefficients of the internal coordinates as obtained from the symmetry coordinates, one gets the following F matrices: for the A_1 vibrations

$$F = \begin{array}{c|cccc} A_1 & & & & \\ \hline & k_a & \sqrt{2}k_{Ca} & 0 & 0 \\ & \sqrt{2}k_{Ca} & k_C + k_{CC} & 0 & \frac{(6)^{\frac{1}{2}}}{2} r_1 k_{C\gamma} \\ & 0 & 0 & k_H & 0 \\ & 0 & \frac{(6)^{\frac{1}{2}}}{2} r_1 k_{C\gamma} & 0 & \frac{1}{2} r_1^2 K_{\alpha\beta} \end{array} ;$$

and for the $\bar{A}_2$ vibrations

$$F = \begin{array}{c|ccc} \bar{A}_2 & & & \\ \hline & k_C - k_{CC} & 0 & -\frac{(6)^{\frac{1}{2}}}{2} r_1 k_{C\gamma} \\ & 0 & k_H & 0 \\ & -\frac{(6)^{\frac{1}{2}}}{2} r_1 k_{C\gamma} & 0 & \frac{1}{2} r_1^2 K_{\alpha\beta} \end{array} ,$$

where $k_{C\gamma} = k_{C\alpha} - k_{C\beta}$ and $K_{\alpha\beta} = k_\alpha + k_\beta - 4k_{\alpha\beta}$.

The G matrices were obtained from relations given by Wilson.[4] They were the following, assuming tetrahedral angles for the methyl groups: for the A_1 vibrations

$$G = \begin{array}{c|cccc} A_1 & & & & \\ \hline & 2\mu_C & -\sqrt{2}\mu_C & 0 & 0 \\ & -\sqrt{2}\mu_C & 2\mu_C & -\frac{\sqrt{3}}{3}\mu_C & \frac{4}{3}\sqrt{3}a\mu_C \\ & 0 & -\frac{\sqrt{3}}{3}\mu_C & \mu_H + \frac{\mu_C}{3} & -\frac{4}{3}a\mu_C \\ & 0 & \frac{4}{3}\sqrt{3}a\mu_C & -\frac{4}{3}a\mu_C & 2a^2\left(\mu_H + \frac{8}{3}\mu_C\right) \end{array} ;$$

TABLE I. Force constants for the non-degenerate vibrations of dimethylacetylene.

Type	Present value (10^5 dynes/cm)	Crawford's value[5] (10^5 dynes/cm)
k_a	16.31_2	15.587
k_C	5.129_6	5.183
k_H	5.014_1	4.79
k_{Ca}	0.4705_9	0.22
k_{CC}	0.1153	0.193
$k_{C\gamma}$	-0.2618_6	−0.235
$K_{\alpha\beta}$	0.9640_9	0.97

and for the $\bar{A}_2$ vibrations

$$G = \begin{array}{c|ccc} \bar{A}_2 & & & \\ \hline & 2\mu_C & -\frac{\sqrt{3}}{3}\mu_C & -\frac{4}{3}\sqrt{3}a\mu_C \\ & -\frac{\sqrt{3}}{3}\mu_C & \mu_H + \frac{\mu_C}{3} & \frac{4}{3}a\mu_C \\ & -\frac{4}{3}\sqrt{3}a\mu_C & \frac{4}{3}a\mu_C & 2a^2\left(\mu_H + \frac{8}{3}\mu_C\right) \end{array} ,$$

where $a = 1/r_1$.

When the observed frequencies, as given by Crawford,[5] were used with the F and G matrices, the force constants given in Table I were obtained with $\mu_C = 5.0183 \times 10^{22}$ g^{-1} and $\mu_H = 5.9742 \times 10^{23}$ g^{-1}. The value of $k_{C\gamma}$ is a mean value obtained from the observed frequencies of methyl deuteride and ethane as determined by the authors in an unpublished investigation. It is to be noted that most of the force constants are given to five significant figures. While the experimental data do not warrant this accuracy, since most of the data were given to only four significant figures, such a procedure was followed in order to be consistent in the calculations and in order to establish four significant figure frequency values. Frequency values obtained from such force constants were always rounded off to four significant figures.

Diacetylene Molecule

Although Wu and Shen[1] obtained force constants for the non-degenerate vibrations of diacetylene, a different type of potential energy function was used in their work so that it was necessary to redetermine the force constants. The symmetry of the diacetylene molecule is

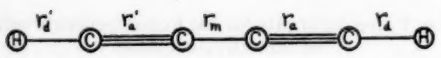

FIG. 2. Bond distances and interbond angles for diacetylene.

$D_{\infty h}$. For this symmetry, one finds that diacetylene has three non-degenerate type A_g vibrations and two non-degenerate type A_u vibrations. The various bond distances and interbond angles used to determine the internal coordinates are given in Fig. 2.

From the internal coordinates the following symmetry coordinates were formed: for the A_g vibrations

$$R_1=\Delta r_m,$$

$$R_2=\frac{1}{\sqrt{2}}(\Delta r_d+\Delta r_d'),$$

$$R_3=\frac{1}{\sqrt{2}}(\Delta r_a+\Delta r_a');$$

and for the A_u vibrations

$$R_1=\frac{1}{\sqrt{2}}(\Delta r_d-\Delta r_d'),$$

$$R_2=\frac{1}{\sqrt{2}}(\Delta r_a-\Delta r_a').$$

The potential energy function used was of the following form:

$$\begin{aligned}2V=&k_m(\Delta r_m)^2+k_d[(\Delta r_d)^2+(\Delta r_d')^2]\\&+k_a[(\Delta r_a)^2+(\Delta r_a')^2]\\&+2k_{ac}[(\Delta r_a)(\Delta d+\Delta r_m)\\&+(\Delta r_a')(\Delta d'+\Delta r_m)]+2k_{aa}(\Delta r_a)(\Delta r_a').\end{aligned}$$

This expression for the potential energy leads to the following F matrices: for the A_g vibrations

$$F=\begin{array}{c|ccc} A_g & & & \\ \hline & k_m & 0 & \sqrt{2}k_{ac} \\ & 0 & k_d & k_{ac} \\ & \sqrt{2}k_{ac} & k_{ac} & k_a+k_{aa} \end{array},$$

and for the A_u vibrations

$$F=\begin{array}{c|cc} A_u & & \\ \hline & k_d & k_{ac} \\ & k_{ac} & k_a-k_{aa} \end{array}.$$

The G matrices obtained from the relations given by Wilson[4] were the following: for the A_g vibrations

$$G=\begin{array}{c|ccc} A_g & & & \\ \hline & 2\mu_C & 0 & -\sqrt{2}\mu_C \\ & 0 & \mu_H+\mu_C & -\mu_C \\ & -\sqrt{2}\mu_C & -\mu_C & 2\mu_C \end{array},$$

and for the A_u vibrations

$$G=\begin{array}{c|cc} A_u & & \\ \hline & \mu_H+\mu_C & -\mu_C \\ & -\mu_C & 2\mu_C \end{array}.$$

When the values of the observed frequencies for the type A_u vibrations as given by Herzberg,[3] and the values of k_a and k_{ac} as obtained from dimethylacetylene are used with the F and G matrices and the values of μ_C and μ_H already given, one obtains the following values for k_d and k_{aa}:

$$k_d=6.110_5\times10^5 \text{ dynes/cm},$$
$$k_{aa}=1.136\times10^5 \text{ dynes/cm}.$$

The value of k_m was obtained by using the 644 cm^{-1} type A_g fundamental frequency and the F and G matrices for the A_g vibrations. The value of k_m obtained was

$$k_m=3.234_2\times10^5 \text{ dynes/cm}.$$

Since only one type A_g frequency was used in obtaining the force constants, the remaining A_g frequencies were calculated. The results of this calculation are given in Table II as well as the observed values[3] for comparison purposes. The observed value of ν_1 is enclosed in parentheses, since this frequency was not actually observed but, according to Herzberg,[3] is believed to be very close to this value.

Dimethyldiacetylene Molecule

Since the dimethyldiacetylene molecule is very similar to the dimethylacetylene molecule and

TABLE II. Calculated and observed values of the A_g fundamental frequencies of diacetylene.

Designation	Calculated (cm^{-1})	Observed[3] (cm^{-1})
ν_1	3357	(3350)
ν_2	2219	2183
ν_3	644	644

because the methyl groups are much farther apart in dimethyldiacetylene, one would suspect that for dimethyldiacetylene very little hindered rotation occurs. So the symmetry of the dimethyldiacetylene molecule was assumed to be D_{3h}'. For this symmetry the molecule will have five type A_1 non-degenerate fundamental vibrations and four type $\bar{A}_2$ non-degenerate vibrations. The various bond distances and interbond angles used to determine the internal coordinates are shown in Fig. 3, except those associated with H_3 and H_3' which, as in Fig. 1, are omitted for clarity and simplicity.

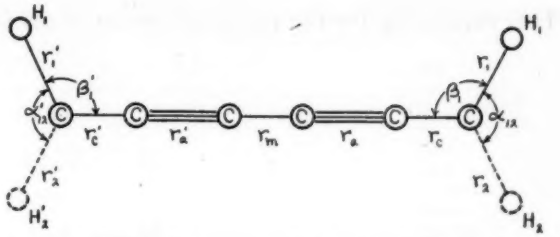

FIG. 3. Bond distances and interbond angles for dimethyldiacetylene. (Atoms H_3 and H_3' are omitted for clarity and simplicity.)

From the internal coordinates the following symmetry coordinates were formed: for the A_1 vibrations

$$R_1=\Delta r_m,$$

$$R_2=\frac{1}{\sqrt{2}}(\Delta r_a+\Delta r_a'),$$

$$R_3=\frac{1}{\sqrt{2}}(\Delta r_C+\Delta r_C'),$$

$$R_4=\frac{1}{(6)^{\frac{1}{2}}}(\Delta r_1+\Delta r_2+\Delta r_3+\Delta r_1'+\Delta r_2'+\Delta r_3'),$$

$$R_5=\frac{1}{(12)^{\frac{1}{2}}}(\Delta\alpha_{12}+\Delta\alpha_{23}+\Delta\alpha_{31}+\Delta\alpha_{12}'+\Delta\alpha_{23}'+\Delta\alpha_{31}'-\Delta\beta_1-\Delta\beta_2-\Delta\beta_3-\Delta\beta_1'-\Delta\beta_2'-\Delta\beta_3');$$

and for the type $\bar{A}_2$ vibrations

$$R_1=\frac{1}{\sqrt{2}}(\Delta r_a-\Delta r_a'),$$

$$R_2=\frac{1}{\sqrt{2}}(\Delta r_C-\Delta r_C'),$$

$$R_3=\frac{1}{(6)^{\frac{1}{2}}}(\Delta r_1+\Delta r_2+\Delta r_3-\Delta r_1'-\Delta r_2'-\Delta r_3'),$$

$$R_4=\frac{1}{(12)^{\frac{1}{2}}}(-\Delta\alpha_{12}-\Delta\alpha_{23}-\Delta\alpha_{31}+\Delta\alpha_{12}'+\Delta\alpha_{23}'+\Delta\alpha_{31}'+\Delta\beta_1+\Delta\beta_2+\Delta\beta_3-\Delta\beta_1'-\Delta\beta_2'-\Delta\beta_3').$$

The potential energy function used was a combination of those already given for dimethylacetylene and diacetylene. It was

$$\begin{aligned}2V=&k_H\sum_6(\Delta r_i)^2+k_\alpha r_1^2\sum_6(\Delta\alpha_{ij})^2+k_\beta r_1^2\sum_6(\Delta\beta_i)^2+2k_{\alpha\beta}r_1^2\sum_{12}(\Delta\beta_i)(\Delta\alpha_{i,\,i\pm1})\\&+2k_{C\alpha}r_1\sum_6(\Delta r_C)(\Delta\alpha_{ij})+2k_{C\beta}r_1\sum_6(\Delta r_C)(\Delta\beta_i)+k_C[(\Delta r_C)^2+(\Delta r_C')^2]+k_a[(\Delta r_a)^2+(\Delta r_a')^2]\\&+k_m(\Delta r_m)^2+2k_{aa}(\Delta r_a)(\Delta r_a')+2k_{mC}(\Delta r_m)(\Delta r_C+\Delta r_C')\\&+2k_{aC}[(\Delta r_a)(\Delta r_C+\Delta r_m)+(\Delta r_a')(\Delta r_C'+\Delta r_m)].\end{aligned}$$

This expression for the potential energy leads to the following F matrices: for the A_1 vibrations

$$F = \begin{array}{c|ccccc} A_1 & & & & & \\ \hline & k_m & \sqrt{2}k_{ac} & \sqrt{2}k_{mc} & 0 & 0 \\ & \sqrt{2}k_{ac} & k_a+k_{aa} & k_{ac} & 0 & 0 \\ & \sqrt{2}k_{mc} & k_{ac} & k_c & 0 & \frac{(6)^{\frac{1}{2}}}{2}r_1k_{c\gamma} \\ & 0 & 0 & 0 & k_H & 0 \\ & 0 & 0 & \frac{(6)^{\frac{1}{2}}}{2}r_1k_{c\gamma} & 0 & \frac{1}{2}r_1^2K_{\alpha\beta} \end{array};$$

and for the $\bar{A}_2$ vibrations

$$F = \begin{array}{c|cccc} \bar{A}_2 & & & & \\ \hline & k_a-k_{aa} & k_{ac} & 0 & 0 \\ & k_{ac} & k_c & 0 & -\frac{(6)^{\frac{1}{2}}}{2}r_1k_{c\gamma} \\ & 0 & 0 & k_H & 0 \\ & 0 & \frac{(6)^{\frac{1}{2}}}{2}r_1k_{c\gamma} & 0 & \frac{1}{2}r_1^2K_{\alpha\beta} \end{array}.$$

Assuming tetrahedral angles for the methyl groups, the G matrices obtained were the following: for the A_1 vibrations

$$G = \begin{array}{c|ccccc} A_1 & & & & & \\ \hline & 2\mu_c & -\sqrt{2}\mu_c & 0 & 0 & 0 \\ & -\sqrt{2}\mu_c & 2\mu_c & -\mu_c & 0 & 0 \\ & 0 & -\mu_c & 2\mu_c & -\frac{\sqrt{3}}{3}\mu_c & \frac{4}{3}\sqrt{3}a\mu_c \\ & 0 & 0 & -\frac{\sqrt{3}}{3}\mu_c & \mu_H+\frac{\mu_c}{3} & -\frac{4}{3}a\mu_c \\ & 0 & 0 & \frac{4}{3}\sqrt{3}a\mu_c & -\frac{4}{3}a\mu_c & 2a^2\mu_H+\frac{16}{3}a^2\mu_c \end{array};$$

and for the $\bar{A}_2$ vibrations

$$G = \begin{array}{c|cccc} \bar{A}_2 & & & & \\ \hline & 2\mu_c & -\mu_c & 0 & 0 \\ & -\mu_c & 2\mu_c & -\frac{\sqrt{3}}{3}\mu_c & -\frac{4}{3}\sqrt{3}a\mu_c \\ & 0 & -\frac{\sqrt{3}}{3}\mu_c & \mu_H+\frac{\mu_c}{3} & \frac{4}{3}a\mu_c \\ & 0 & -\frac{4}{3}\sqrt{3}a\mu_c & \frac{4}{3}a\mu_c & 2a^2\left(\mu_H+\frac{8}{3}\mu_c\right) \end{array}.$$

TABLE III. Calculated and observed values of the A_1 fundamental frequencies of dimethyldiacetylene.

Designation	Calculated value (cm^{-1}) Using original force constants	Using modified force constants	Observed value[2] (cm^{-1})
ν_1	2946	2946	2914
ν_2	2329	2265	2264
ν_3	1379	1375	1381
ν_4	1058	965	957
ν_5	461	473	475

Using the F and G matrices for the A_1 vibrations, the necessary force constants transferred from the dimethylacetylene and diacetylene molecules and the values of μ_H and μ_C already given, one obtains the calculated values of the frequencies as given in column two of Table III. For comparison purposes, the observed values as obtained by Meister and Cleveland[2] also are given in column four.

A glance at Table III indicates that for ν_2 and ν_4 the agreement between the observed and calculated values is not so good. However, it was found that if the values of k_a, k_{aa}, k_C, and k_{mC} were modified better agreement could be obtained. The modified force constants used are given in Table IV as well as the original values of the same constants. When these modified force constants are used with the F and G matrices for the type A_1 vibrations, one obtains the frequencies given in the third column of Table III. In all cases the agreement is very good and well within the 2 percent limit set by Crawford and Brinkley.[6]

In order to test the modified force constants given in Table IV, the $\bar{A}_2$ fundamental frequencies were calculated. These frequencies are given in Table V as well as the expected values for the same frequencies. It was necessary to use the expected values for comparison purposes, since the $\bar{A}_2$ frequencies are allowed only in the infra-red and the infra-red absorption spectrum of dimethyldiacetylene has not been obtained as yet.

The expected values of the $\bar{A}_2$ frequencies were obtained in the following manner. One would expect the methyl group frequencies to lie close to the values for the same frequencies for the $\bar{A}_2$ vibrations of dimethylacetylene, since

[6] B. L. Crawford, Jr. and S. R. Brinkley, Jr., J. Chem. Phys. 9, 72 (1941).

TABLE IV. Force constants for the non-degenerate vibrations of dimethyldiacetylene.

Type	Original value (10^5 dynes/cm)	Modified value (10^5 dynes/cm)
k_a	16.31_2	15.60_8
k_m	3.234_2	unchanged
k_C	5.129_6	4.705_0
k_H	5.014_1	unchanged
k_{aa}	1.136	0.5550
k_{mC}	0.1153	0.4505
k_{am}	0.4705_9	unchanged
$k_{C\gamma}$	-0.2618_6	unchanged
$K_{\alpha\beta}$	0.9640_9	unchanged

there is even less chance for interaction between the methyl groups in the case of dimethyldiacetylene. For dimethylacetylene these frequencies lie at 2976 and 1380 cm^{-1}, respectively, so that for dimethyldiacetylene it was assumed that ν_1 would lie in the 2950–3000 cm^{-1} region and ν_3 in the 1350–1400 cm^{-1} region. In going from diacetylene to dimethyldiacetylene the C≡C symmetrical stretching frequency is changed from 2183 to 2264 cm^{-1}, an increase of 81 cm^{-1}. If one assumes that the $\bar{A}_2$ antisymmetrical C≡C stretching frequency changes by the same amount, one would expect to find this frequency at $2023+81=2104$ cm^{-1}. For this reason ν_2 for dimethyldiacetylene was assumed to lie in the 2100–2150 cm^{-1} region. The expected value of ν_4 could not be determined so easily. However, it was assumed to lie in the 900–1100 cm^{-1} region where C−C stretching frequencies usually are found.

As a further check on the set of modified force constants given in Table IV the frequencies of the non-degenerate vibrations of diacetylene were again calculated using these force constants. A modified value of k_d was used, that is, instead of the value $6.110_5\times10^5$ dynes/cm as obtained previously from the diacetylene calculations, a value of $6.160_8\times10^5$ dynes/cm was used. The results of these calculations are given in Table VI and, for comparison purposes, the observed

TABLE V. Calculated and expected values of the $\bar{A}_2$ fundamental frequencies for dimethyldiacetylene.

Designation	Calculated value (cm^{-1})	Expected value (cm^{-1})
ν_1	2946	2950–3000
ν_2	2131	2100–2150
ν_3	1368	1350–1400
ν_4	903	900–1100

TABLE VI. Calculated and observed values of the non-degenerate vibrational frequencies of diacetylene.

Type	Designation	Calculated value (cm^{-1})	Observed value[3] (cm^{-1})
A_g	ν_1	3366	(3350)
	ν_2	2142	2183
	ν_3	644	644
A_u	ν_1	3350	3350
	ν_2	2023	2023

values[3] are also given. The agreement between the calculated and observed values is good with the exception of ν_2 of the type A_g vibrations which is about 2 percent below the observed value.

DISCUSSION

Probably the most significant result of this investigation is the fact that the value of the central C−C stretching force constant (k_m) was found to be the same for dimethyldiacetylene as for diacetylene. It seems difficult to account for such a behavior of this force constant since, if resonance between double and triple bond structures were to occur, one would expect this force constant to have a value greater than the normal value of about 5×10^5 dynes/cm. Furthermore, as Herzberg[7] has pointed out, electron diffraction data shows that the C−C bond distance for diacetylene is smaller than for ethane, which should indicate a tighter C−C bond for diacetylene than for ethane. For ethane the C−C stretching force constant is 4.50×10^5 dynes/cm.[8] Also, Pauling, Springall, and Palmer[9] found that the central C−C bond distance for dimethyldiacetylene was about the same as for diacetylene. However, despite all these reasons for expecting a value for k_m larger than the normal value, the calculations seem to indicate that the value of k_m for both diacetylene and dimethyldiacetylene is $3.234_2\times10^5$ dynes/cm which is considerably lower than the normal value of 5×10^5 dynes/cm.

According to the quantum theory of valence, the force of attraction between two atoms is caused by a concentration of negative electrical charge between the two atoms. Thus in ethane,

$$H_3C-CH_3,$$

the attraction between the two carbon atoms is caused by a large charge density in the region between the two atoms. In dimethylacetylene,

$$\overset{a}{H_3C}-\overset{b}{C}\equiv\overset{c}{C}-\overset{d}{CH_3},$$

the charge density between carbon atoms a and b and between carbon atoms c and d is still greater than in ethane, as is shown by the greater value of the carbon-carbon single bond force constant and the decreased value of the bond length obtained by electron diffraction investigations. This must be caused by electrostatic repulsion between electrons forming the triple bond between carbon atoms b and c, causing these electrons to spend part of their time in the regions between carbon atoms a and b or c and d, thus increasing the charge density between these atoms and accordingly increasing the strength of the two carbon single bonds.

For dimethyldiacetylene,

$$\overset{1}{H_3C}-\overset{2}{C}\equiv\overset{3}{C}-\overset{4}{C}\equiv\overset{5}{C}-\overset{6}{CH_3},$$

the unusually small value of the carbon-carbon single bond force constant, between carbon atoms 3 and 4, can be understood by supposing that the strong electrostatic repulsion of the negative charge concentrated between carbon atoms 2 and 3 and 4 and 5 prevents a normal concentration of charge between carbon atoms 3 and 4 of the central single bond. This would decrease the strength of this single bond.

The smaller than normal bond distance for this central carbon-carbon single bond may be explained by noting that there is an extraordinarily large charge concentration in the region between carbon atoms 2 and 5. It is thus probable that there are considerable attractive forces between carbon atoms 2 and 4, 3 and 5, and perhaps even between 2 and 5. This force of compression

TABLE VII. Comparison of the carbon-carbon force constants for dimethylacetylene and dimethyldiacetylene.

Bond	Dimethylacetylene (10^5 dynes/cm)	Dimethyldiacetylene (10^5 dynes/cm)
C≡C	16.31_2	15.60_8
End C—C	5.129_6	4.705_0

[7] See reference 3, p. 324.
[8] See reference 3, p. 193.
[9] L. Pauling, H. D. Springall, and K. J. Palmer, J. Am. Chem. Soc. 61, 927 (1939).

might well operate to shorten the distance between atoms 3 and 4, even though the strength of the bond between atoms 3 and 4 is itself less than normal.

One may notice also that the triple bond force constants and the end single bond force constants in dimethyldiacetylene are less than the corresponding values for dimethylacetylene (see Table VII). This is the result that would be expected if the unusually large concentration of charge along the axis of the molecule results, as seems probable, in strong electrostatic repulsions that force much of the charge off the axis and prevent the maximum concentration of charge in the space between the atoms.

Another result of this investigation was the disclosure that the tentative assignments of the observed Raman frequencies of dimethyldiacetylene, as made by Meister and Cleveland,[2] had to be revised. In their analysis they assigned the 475 cm^{-1} frequency as an $\bar{E}$ fundamental and the 686 cm^{-1} frequency as an A_1 fundamental. These assignments were based on a comparison with the diacetylene molecule. As a result of the calculations in this investigation, it appears that the 475 cm^{-1} frequency is an A_1 fundamental, and the 686 cm^{-1} frequency is assumed to be an E or $\bar{E}$ fundamental. Other minor changes in assignments were found to be necessary, so in Table VIII the revised assignment of the observed Raman frequencies of dimethyldiacetylene is given. It will be noticed that some frequencies have been given two possible assignments. In all such cases it will be seen that doubly degenerate frequencies are involved and the ambiguity cannot be removed until the doubly degenerate frequencies are calculated or otherwise determined.

In conclusion, one might point out the similarities which exist between the F and G matrices for the molecules considered. For example, the upper 3×3 matrix, formed from the F matrix for the type A_1 vibrations of dimethyldiacetylene, is much the same as the F matrix for the A_g vibrations of diacetylene. The lower 3×3 matrix, formed from the same type A_1 F matrix is almost the same as the lower 3×3 matrix formed from the F matrix for the type A_1 vibrations of dimethylacetylene. A similar behavior is exhibited by the G matrices for the A_1 and A_g vibrations for the molecules concerned and also the F and G matrices for the $\bar{A}_2$ and A_u vibration types. One would expect the F and G matrices to behave in this manner, since dimethyldiacetylene has a number of frequencies which are the same as those of diacetylene and dimethylacetylene.

TABLE VIII. Revised assignment of the Raman frequencies of dimethyldiacetylene.*

$\Delta\nu$	I	ρ	Assignment and symmetry
247	80	0.64	Fundamental E or $\bar{E}$
475	220	0.64	Fundamental A_1
686	*vw*		Fundamental E or $\bar{E}$
957	*vw*		Fundamental A_1
1020	*vw*		Fundamental $\bar{E}$
1151	*vw*		$686+475=1161$, E or $\bar{E}$
1185	*vw*		$1426-247=1179$, A_1+A_2+E or $\bar{A}_1+\bar{A}_2+\bar{E}$
1228	*vw*		$957+247=1204$, E or $\bar{E}$
1253	17		$1020+247=1267$, A_1+A_2+E or $\bar{A}_1+\bar{A}_2+\bar{E}$
1381	115	0.62	Fundamental A_1
1426	5		Fundamental $\bar{E}$
1458	*vw*		Fundamental E
2225	*vw*		C^{13} isotope
2264	1000	0.40	Fundamental A_1
2309	9		$957+1381=2338$, A_1
2502	*vw*		$2264+247=2511$, E or $\bar{E}$
2821	*vw*		$1381+1426=2807$, $\bar{E}$
2848	21		$1426^2=2852$, A_1+E
2914	400	0.17	Fundamental A_1
2954	39		Fundamental $\bar{E}$

* $\Delta\nu$ = Raman displacement in cm^{-1}, I is the relative intensity measured with a microdensitometer, *vw* = lines that were too weak to measure with the microdensitometer, ρ = depolarization factor, and the braces indicate a probable case of Fermi resonance.

THE JOURNAL OF CHEMICAL PHYSICS VOLUME 15, NUMBER 6 JUNE, 1947

The Entropy of Mixing of Binary Liquid Mixtures*

SCOTT E. WOOD
Sterling Chemistry Laboratory, Yale University, New Haven, Connecticut
(Received February 12, 1947)

Three factors which may contribute to the excess entropy of mixing of binary solutions have been explored. These are the relative volumes of the molecules, the spatial distribution of the molecules about a given reference molecule, and the lack of randomness of the orientational distribution of the molecules about a reference molecule. Of these, the spatial distribution, which depends upon the energy of mixing, is the smallest. It yields a negative value for the excess entropy and becomes zero at infinite dilution. The effect of differences in the volumes of the molecules of the components is positive and may be appreciable. The greatest effect is obtained from the orientational distribution. An estimation of the lack of randomness in this distribution for the pure components is obtained from the differences of the entropies of evaporation of the components and that of argon compared under corresponding conditions. This difference is positive and is comparable, at least in order of magnitude, to the observed partial molal excess entropy of mixing at constant pressure and at infinite dilution for the six binary mixtures composed of benzene, carbon tetrachloride, cyclohexane, and methanol. The contribution of the change in the orientational distribution of the components to the partial molal excess entropy at infinite dilution is then considered to be caused by two effects, one in which the orientational distribution of the solute becomes completely random when dissolved in a solvent at infinite dilution and the other in which the orientational distribution of the solvent is changed by the substitution of a solute molecule for a solvent molecule. The individual behavior of each solvent is very evident and is consistent with its molecular structure.

NUMEROUS determinations of the thermodynamic functions of binary liquid mixtures indicate that the change of the entropy on mixing non-polar components either at constant volume or constant pressure is greater than that of an ideal solution over the entire range of composition. Further, the excess change of entropy on mixing a polar and a non-polar component may have all positive values, positive and negative values, or all negative values. It is the purpose of this paper to consider, semi-quantitatively, three effects which may enter in an explanation of this excess entropy change on mixing.

The formal distribution function of molecules about a given reference molecule, based on statistical mechanics, is a function of the position coordinates of the molecules and of the angular coordinates required to describe the relative orientation of the molecules. Because of the complexity and consequent lack of knowledge of the liquid state, it is necessary to consider in this paper that the distribution function may be factored into three terms, the first of which involves the repulsive forces of the molecules, the second of which depends primarily on the attractive forces expressed in terms of the position coordinates alone, and the third of which involves the angular coordinates. Thus the excess change of the entropy on mixing, resulting from the difference of the entropy of the solution and that of the pure components, is discussed in terms of the relative volumes of the molecules, the spatial distribution, and the orientational distribution of the molecules about a reference molecule. It is evident that these three effects are not necessarily independent but yet it is unavoidable to consider them so. It appears that the smallest effect is that caused by the spatial distribution, the next is that caused by the differences in the volume of the molecules, and the largest is that caused by the orientational distribution. However, a generalization of the effect of the orientational distribution is not possible and indeed the partial molal excess entropy of mixing of a given solute at infinite dilution in various solvents depends upon the characteristic molecular structure of each solvent as well as on the properties of the solute.

THE VOLUME EFFECT

The effect of differences in the sizes of the molecules on the behavior of solutions has been the subject of several investigations. Guggen-

* Presented before the Division of Physical and Inorganic Chemistry of the American Chemical Society at Atlantic City, New Jersey, April 17, 1947.

heim[1] has shown that there is no basis for believing that solutions formed of molecules differing greatly in size should obey Raoult's law. Fowler and Guggenheim[2] obtained the thermodynamic functions for a mixture of double and single molecules, and Miller[3] has treated the similar problem of a mixture of two molecules, one occupying three sites on a lattice structure and the other occupying only one site. Further, Flory,[4] Huggins,[5] and Guggenheim[6] have obtained expressions for the thermodynamic functions for mixtures of two kinds of molecules, one of which occupies r sites of a lattice structure and the other only one site. In these treatments the energy of mixing is taken as zero. The results of all of these treatments are similar in that the change of the entropy on mixing at constant volume may be expressed as

$$S_V{}^M = -n_1 R \ln z_1 - n_2 R \ln z_2 + \text{higher terms} \quad (1)$$

where z_1 and z_2 are the volume fractions of the components. In order to obtain at least an approximate value of this volume effect on the entropy of mixing, one is led, as Huggins has already suggested, to assume that the change of the entropy on mixing molecules of ordinary size is given by Eq. (1) with the neglect of the higher terms, thus ignoring also the conditions under which this equation was derived. With these assumptions, the molal excess entropy of mixing is given by

$$S_X{}^E = x_1 R \ln(x_1/z_1) + x_2 R \ln(x_2/z_2) \quad (2)$$

where x_1 and x_2 represent the mole fractions of the components. The values of the excess entropy have been calculated according to this equation at 30° for the six possible binary mixtures formed from the four substances, benzene, carbon tetrachloride, cyclohexane, and methanol. The molal volumes in cc used for these calculations at 30° are: benzene 89.939, cyclohexane, 109.427, carbon tetrachloride, 97.673, and methanol 40.983. The partial molal excess entropies of mixing at infinite dilution of one component in each of the other components are given in the third column of Table I. These values do not change markedly with temperature. It will be observed that for mixtures of benzene, carbon tetrachloride, and cyclohexane these values are very small and in fact almost negligible. However, for solutions containing methanol the values are much larger since the molal volume of methanol is less than one-half that of the other three substances. It should be noted, however, that the excess entropy of mixing because of differences in the relative volumes of the molecules is always positive according to Eq. (2).

TABLE I. Partial molal excess entropies of mixing at infinite dilution at 30°.

Solute	Solvent	Volume effect	Orientational effect	Observed
C_6H_6	C_6H_{12}	+0.04	+1.09	+1.29
	CCl_4	+0.01		+0.14
	CH_3OH	+0.81		−1.85
C_6H_{12}	C_6H_6	+0.04	+0.89	+1.81
	CCl_4	+0.01		+0.25
	CH_3OH	+1.37		−2.41[b]
CCl_4	C_6H_{12}	+0.01	+0.14	+0.22
	C_6H_6	+0.01		+0.14
	CH_3OH	+1.02		−1.98
CH_3OH	C_6H_{12}	+0.69	+7.47[a]	+8.10[b]
	C_6H_6	+0.48		+1.99
	CCl_4	+0.57		−1.46

(a) The value given is at 35°.
(b) The value given is at 31°.

THE SPATIAL DISTRIBUTION

In the previous section the results were obtained assuming that the energy of mixing was zero. The effect of a non-zero energy of mixing has been considered by Orr[7] and Guggenheim,[8] who have obtained expressions for the thermodynamic functions of a mixture of non-polar molecules occupying different numbers of sites of a lattice.The results for the free energy are expressible in two parts, one independent of the energy of mixing and identical to that obtained when the energy of mixing is zero, and the other a function of the energy of mixing. Similar studies have been made by Rushbrooke[9] and Kirkwood[10] for mixtures consisting of rigid, spherical mole-

[1] E. A. Guggenheim, Trans. Faraday Soc. **33**, 151 (1937).
[2] Fowler and Guggenheim, *Statistical Thermodynamics* (Cambridge University Press, London, 1939), p. 366.
[3] A. R. Miller, Proc. Camb. Phil. Soc. **38**, 109 (1942); *ibid.* **39**, 54 (1943).
[4] P. J. Flory, J. Chem. Phys. **10**, 51 (1942); **12**, 452 (1944); **13**, 453 (1945).
[5] M. L. Huggins, Ann. N. Y. Acad. Sci. **43**, 1 (1942).
[6] E. A. Guggenheim, Proc. Roy. Soc. London **A183**, 203 (1944).
[7] W. J. C. Orr, Trans. Faraday Soc. **40**, 320 (1944).
[8] E. A. Guggenheim, Proc. Roy. Soc. London **A183**, 213 (1944).
[9] G. S. Rushbrooke, Proc. Roy. Soc. London **A166**, 296 (1938).
[10] J. G. Kirkwood, J. Phys. Chem. **43**, 97 (1939).

cules of equal size. The qualitative results of all these studies are similar in that the contribution to the excess entropy of mixing at constant volume is always negative, independent of the sign of the energy of mixing. This contribution is also very small as shown in the results of Scatchard, Wood, and Mochel[11–13] for the three systems: benzene—carbon tetrachloride, carbon tetrachloride—cyclohexane, and cyclohexane-benzene. Orr estimates that this ordering of the spatial distribution of the molecules about a reference molecule is about 20 percent of the volume effect. If the mixtures contained polar molecules, the magnitude of this effect might be larger but it would presumably still be negative.

Since, in the following sections, emphasis will be placed on the partial molal excess entropy of mixing at infinite dilution, it should be pointed out here that the contribution of this ordering in the spatial distribution to the partial molal excess entropy becomes zero at infinite dilution.

THE ORIENTATIONAL DISTRIBUTION

Scatchard, Wood, and Mochel[11] explained the positive excess entropy of mixing in the benzene-cyclohexane system as being caused by a lack of complete randomness in orientation in the pure liquids which became complete in the mixtures. This explanation became untenable when the excess entropy of mixing of the benzene-carbon tetrachloride[13] and cyclohexane-carbon tetrachloride[12] systems had been determined, since the sum of the excess entropies of the latter two systems was about one-fourth that of the first system rather than equal to or greater than that of the first system. In the more clear cut cases in which methanol is used as a component[14–16] the positive excess entropy was explained as an increase in the randomness of orientation of the methanol molecules and the negative excess entropy as being caused by a decrease in the randomness of orientation of the non-polar molecules and an ordering in the spatial distribution. The decrease of randomness of orientation is presumably of greater importance here.

It would seem that any positive excess entropy of mixing must be explained in terms of a lack of random orientation in the pure liquids and some estimation of this must be obtained. Pitzer[17] and Guggenheim[18] have shown that the law of corresponding states should be valid for liquids under certain conditions and that many liquids composed of simple molecules do follow this law. The conditions, in outline, are that (1) classical statistical mechanics are valid for the liquids, (2) the molecules are either spherical or freely rotating, (3) the intramolecular vibrations are the same in both the liquid and vapor phases, (4) the potential energy is a function of the distance only, and (5) the potential energy of a pair of molecules may be written as $E=A\phi(R/R_0)$ where ϕ is a universal function of the distance R, and A and R_0 constants characteristic of each substance. According to this law the entropy of evaporation, the reduced vapor pressure, and the ratio of the molal volume of the gas to that of the liquid should be the same for all substances at the same reduced temperature. Any substance whose properties deviate from the above conditions would be expected to have an entropy of evaporation different from that of a "perfect" liquid whose properties do fit these conditions, when compared under corresponding changes of states. Only the first condition is expected to be satisfied by the four substances compared in this paper. When the second, fourth, and fifth conditions are not satisfied a preferred orientation in the liquid phase would be expected and the difference in the entropies of evaporation of the substance under consideration and that of the "perfect" liquid under corresponding conditions would be positive. Except for the effect of the third condition, which will be mentioned later, this difference should be a measure of the lack of randomness of the orientational distribution in the pure liquid. In an infinitely dilute solution of a solute in a solvent, the orientational distribution between the solute molecules would be expected to be completely random, and thus the partial molal excess entropy of mixing

[11] G. Scatchard, S. E. Wood, and J. M. Mochel, J. Phys. Chem. **43**, 119 (1939).
[12] G. Scatchard, S. E. Wood, and J. M. Mochel, J. Am. Chem. Soc. **61**, 3206 (1939).
[13] G. Scatchard, S. E. Wood, and J. M. Mochel, J. Am. Chem. Soc. **62**, 712 (1940).
[14] G. Scatchard, S. E. Wood, and J. M. Mochel, J. Am. Chem. Soc. **68**, 1957 (1946).
[15] G. Scatchard, S. E. Wood, and J. M. Mochel, J. Am. Chem. Soc. **68**, 1960 (1946).
[16] S. E. Wood, J. Am. Chem. Soc. **68**, 1963 (1946).
[17] K. S. Pitzer, J. Chem. Phys. **7**, 583 (1939).
[18] E. A. Guggenheim, J. Chem. Phys. **13**, 253 (1945).

might be compared to this difference in the entropies of evaporation, provided that the solvent acted merely as an inert diluent and that no effects other than orientation entered into this difference. However, the solvent is certainly not an inert substance, and further, the orientational distribution in the pure solvent will probably not be random. Consequently, the substitution of a solvent molecule by a solute molecule may change this distribution such that the randomness of orientation of the solvent molecules surrounding the solute molecule may be either increased or decreased. Examples of these effects are evident in the six possible binary systems composed of the four compounds considered here. A qualitative discussion of the properties of several compounds based on the differences in their entropies of evaporation as determined from the Hildebrand rule has already been given by Hildebrand.[19]

In these suggested comparisons the validity of the third condition, that the intramolecular vibrations are the same in both the liquid and vapor phases, must be considered. If there is a difference in these vibrations, then this difference will enter into the entropy of evaporation along with the effect of orientation, and consequently, the entropy differences may not be comparable to the partial molal excess entropy at infinite dilution. This effect should be small for benzene, cyclohexane, and carbon tetrachloride. For methanol, however, it is well known that there is a distinct difference in the vibration of the O—H group in the pure liquid and vapor phases. But there is also a similar shift when methanol is dissolved at low concentrations in benzene and carbon tetrachloride. Thus the entropy change caused by this shift would be present in both the entropy of evaporation and the partial molal excess entropy, although it might not be identical in the two cases. It then seems that this third condition may be ignored at least qualitatively in these comparisons. Moreover, it seems that the influence of the dipolar field of methanol on the orientational distribution is of much greater importance.

For these comparisons it is then necessary to calculate the entropy of evaporation of these substances and that of a "perfect" liquid under corresponding conditions. Argon, being one of the substances which follow the law of corresponding states, has been chosen as an example of such a liquid. However, when a substance deviates from this law in one property, it deviates in all properties. Hence the question of what are corresponding conditions is presented. Various values of the difference of the entropy of evaporation of the liquid under consideration, and that of argon, are obtained depending upon what conditions are used. For this paper the entropy change has been calculated for the evaporation of benzene, cyclohexane, and carbon tetrachloride at 30° and methanol at 35° and at the vapor pressures of the liquids at these temperatures to an ideal gas at the same temperature and an arbitrary concentration. For argon the change in state is from the liquid at one atmosphere pressure and at a reduced temperature equal to the four reduced temperatures of the other liquids to an ideal gas at this temperature and the same arbitrary concentration. Values about two cal. per degree higher than those obtained with this change of state are obtained for the non-polar liquids if the comparisons are made at the same reduced temperatures and the same reduced vapor pressures. But in this case the concentration of the two substances in the vapor phase is not identical; this results in a difference in the entropies of the vapor phases even in the ideal gas state. Smaller values than those used in this paper, some of which are negative, are obtained if the comparisons are made either at temperatures at which the reduced vapor pressures are identical[18] or at temperatures at which the ratios of the molal volume of the vapor phase to that of the liquid phase are identical.[17] In these two cases the actual temperatures of argon are much lower than those corresponding to the same reduced temperature of the liquids resulting in a greater entropy of evaporation of argon; this entropy change increases about 12 percent for a ten degree decrease in temperature. Moreover, a large extrapolation of the vapor pressure of argon is necessary. It was because of these considerations that the changes of state stated above have been used. They do give the best agreement of the differences of the entropies of evaporation with the observed

[19] J. H. Hildebrand, J. Chem. Phys. **7**, 233 (1939).

values of the partial molal excess entropies of mixing, but it is not necessarily true as a consequence that they are the correct conditions. Nevertheless, no matter what conditions are used for comparison, the main conclusions drawn from this study will be the same.

The entropies of evaporation of benzene, cyclohexane, carbon tretrachloride, and methanol have been calculated from the vapor pressure equations of Scatchard, Wood, and Mochel[12,14] and the densities of benzene and cyclohexane given by them, of carbon tetrachloride given by Wood and Brusie,[20] and of methanol obtained from the International Critical Tables. The corrections for the non-ideality of the vapor have been obtained from the second virial coefficient only, using nine-tenths the value calculated by the theory of corresponding states for benzene, cyclohexane, and carbon tetrachloride using the equation of Keyes, Smith, and Gerry[21] and the full value of this quantity for methanol. The entropy of evaporation of argon has been determined from the calorimetric value of its heat of evaporation at the boiling point,[22] 1557.5 ± 1.5 cal. per mole, and the molal heat capacities of the vapor and liquid phases,[23] 5.3 and 10.6 cal. per degree, respectively. The necessary vapor pressures have been obtained from the equation given by Born,[24] and the corrections for the non-ideality of the vapor have been determined from the second virial coefficient given by Holborn and Otto.[25]

The differences of these entropies of evaporation of benzene, carbon tetrachloride, cyclohexane, and methanol from that of argon are given in the fourth column of Table I. In order to show the effect of temperature on these differences they have also been calculated at 70° for the non-polar compounds and at 55° for methanol and are 2.22 for benzene, 2.07 for cyclohexane, 1.84 for carbon tetrachloride, and 8.22 for methanol. The partial molal excess entropies of the solutes at constant pressure and at infinite dilution, determined from the data of the vapor-liquid equilibria[11–15] for all the systems except the cyclohexane-methanol system and from the liquid-liquid equilibria[16] for that system, are given in the last column of Table I. These observed entropies are independent of the temperature within the accuracy of the experimental data except those of the cyclohexane-methanol system. The values given for this system are at 31°. It should be pointed out here that the uncertainties in the entropies of this system are exceedingly large.

It is apparent that for the non-polar systems the orientational effect as calculated above is at least of the correct order of magnitude and has the correct sign. This is also true in the case where methanol is dissolved in cyclohexane, although here the comparison is much more uncertain. Thus the partial molal excess entropy of mixing at infinite dilution and constant pressure may be partly explained in terms of a lack of complete randomness in the orientational distribution of the pure solute which becomes complete at infinite dilution. However, with this concept, the observed quantities corrected for the volume effect should be approximately the same in all solutions of a given solute provided that the solvent acted as an inert diluent. But as previously suggested, this is not the case and the effect of substituting a solute molecule for a solvent molecule on the orientational distribution of the surrounding solvent molecules must be considered. These relationships can be discussed only qualitatively at the present time. An explanation of the behavior of the systems containing methanol, which is consistent with the concepts presented here, has already been suggested.[15,16] For the solutions in which benzene or cyclohexane are the solutes, the partial molal excess entropy is much smaller for solutions in which carbon tetrachloride is the solvent than for those in which cyclohexane or benzene, respectively, is the solvent and is larger for those solutions in which methanol is the solvent. Thus in the former solutions the interaction of the benzene or cyclohexane molecule with the surrounding carbon tetrachloride molecules apparently increases the lack of randomness of the orientation distribution of carbon tetrachloride,

[20] S. E. Wood and J. P. Brusie, J. Am. Chem. Soc. **65**, 1891 (1943).
[21] F. G. Keyes, L. B. Smith, and H. T. Gerry, Proc. Am. Acad. Arts and Sci. **70**, 319 (1936).
[22] A. Frank and K. Clusius, Zeits. f. physik. Chemie **B42**, 395 (1937).
[23] Landolt-Bornstein, *Tabellen* (Julius Springer, Berlin, 1923), 5, II, p. 1274, 1278.
[24] F. Born, Ann. d. Physik. [4], **69**, 473 (1922).
[25] L. Holborn and J. Otto, Zeits. f. Physik **33**, 1 (1925).

this effect being larger for benzene than for cyclohexane. The same relationship between benzene, cyclohexane, and carbon tetrachloride is observed in the three solutions in which methanol is the solute. Thus it would appear that the field of a carbon tetrachloride molecule should not be considered symmetrical, at least at intermolecular distances, and indeed is probably dipolar in nature, an effective dipole operating along each C—Cl bond. A preferred orientation in pure carbon tetrachloride has already been observed by Mencke[26] from x-ray diffraction patterns. The relative behavior of benzene and cyclohexane is evident in the solutions in which either carbon tetrachloride or methanol is the solute and is consistent with the concept of a larger electronic polarization of benzene in comparison to that of cyclohexane[15,16] and a possible closer approach of the neighboring molecules to the benzene molecule. The individual behavior of each solvent is thus very evident but is consistent with that expected from its molecular structure. At infinite dilution then, a qualitative but consistent explanation of the partial molal excess entropy of mixing at constant pressure is possible in terms of the lack of complete randomness in the orientational distribution of both the solute and solvent. However, the individual characteristics of each component are very important.

At finite concentrations the problem becomes exceedingly complex. It has been assumed that at infinite dilution the solute molecules are so far apart that the change in the orientational distribution of the solvent molecules is confined to those immediately surrounding the solute molecules and does not extend throughout the whole liquid. At finite concentrations, however, these regions of changed orientation will become close enough to have a mutual influence on each other, and further, the orientational distribution of the solute molecules themselves must be taken into account. No quantitative treatment of this problem is available at the present time.

This discussion has been based on the change of entropy on mixing at constant pressure. For the non-polar systems there is an increase in the volume of the mixture which might be expected to accompany an increase in the randomness of the orientational distribution, taking both components into account. Conversely, when there is a decrease in the total randomness of orientation, the volume decreases as is observed in the methanol solutions. Thus there is a correlation between the sign of the excess entropy of mixing and the volume of mixing as pointed out by Lacher.[27] Furthermore, on mixing at constant volume, the volume available for a single molecule in the non-polar systems would be less than on mixing at constant pressure. Thus an increase in the degree of orientation and a decrease in the excess entropy would be expected on mixing at constant volume in comparison to mixing at constant pressure. This is observed. However, since for non-polar molecules the interaction energy between unlike molecules is less than the geometrical mean of that between like molecules, an increase in the randomness of orientation and a positive excess entropy of mixing would be expected and is observed.

[26] H. Mencke, Physik. Zeits. **33**, 593 (1932).

[27] J. R. Lacher, J. Am. Chem. Soc. **63**, 2422 (1941).

Comparative Thermodynamic Properties of the Restricted Rotator and the Harmonic Oscillator

J. O. HALFORD
Department of Chemistry, University of Michigan, Ann Arbor, Michigan

(Received March 10, 1947)

The differences between the thermodynamic properties of the restricted internal rotator and a defined harmonic oscillator are expressed within narrow limits as a function of the single variable V/RT, where V is the height of the restricting potential barrier. As a result, a single table with one column for each of the four thermodynamic functions can be used in conjunction with standard harmonic oscillator tables to give the restricted rotator properties. This approximation is accurate within 0.02 cal./mole/deg. for nearly all cases to which it might be applied, and it is shown to be improbable that rotators will be found for which the error would rise appreciably above this limit. The harmonic oscillator chosen for comparison has a slightly lower frequency than the limiting one approached by the restricted rotator at very high values of V/RT.

IN connection with another problem the writer had occasion to make use of the tables of thermodynamic properties compiled by Pitzer[1] and by Pitzer and Gwinn[2] for the restricted internal rotator, and to look up a number of cases in which the restricting potential barrier has been evaluated from thermodynamic data with the aid of the entropy tables. With very few exceptions the barriers are above 2500 cal./mole, so that at ordinary and lower temperatures few molecules can acquire enough energy to rotate. Consequently, these systems can be regarded as vibrators possessing rather large anharmonicities.

It therefore seemed desirable to look into the question of tabulating the thermodynamic properties of the restricted rotator in relation to the harmonic oscillator rather than the free rotator, thus emphasizing the essentially oscillatory character of the motion and providing an alternative method of calculation.

When the differences between the thermodynamic properties of the restricted rotator and the limiting harmonic oscillator for which

$$h\nu/kT=(1/Q_f)(\pi V/RT)^{\frac{1}{2}} \qquad (1)$$

are examined, they prove to be small except at very low V/RT. They are also almost independent of Q_f, so that within limits of the order of 0.05 cal./mole/deg., these differences depend only upon V/RT. This is in accord with the relation proposed by Pitzer and Gwinn under the heading "A Useful Approximation," for which they give the equation

$$Q=Q_{\text{class}}(Q_{\text{HO, quant}}/Q_{\text{HO, class}}). \qquad (2)$$

Q is the partition function of the restricted rotator, Q_{HO} that of the harmonic oscillator, and the subscript quant or class refers to the quantum mechanical or classical variety of function. In Eq. (1), Q_f is the partition function of the free rotator and V is the height of the potential barrier or the maximum potential energy of the rotational degree of freedom.

Equation (2) implies that the ratio Q/Q_{HO} at a given value of V/RT is independent of Q_f and remains equal to its limiting or classical value. It follows that the differences between the thermodynamic functions should be similarly independent of Q_f. It is in this form that the approximation is accurate to about 0.05 cal./mole/deg. in the useful range of the variables. The error is somewhat less, as originally shown by Pitzer and Gwinn, for values of $1/Q_f$ below 0.4, but it becomes larger when $1/Q_f$ is high, even at the highest values of V/RT.

Two devices may be used to improve the accuracy of the approximation. The first is to change the frequency of the harmonic oscillator by substituting another constant for $\pi^{\frac{1}{2}}$ in Eq. (1). This change will affect the entropy and free energy more than the relatively insensitive heat content and heat capacity. The second is to tabulate at each value of V/RT an average dif-

[1] K. S. Pitzer, J. Chem. Phys. **5**, 469 (1937).
[2] K. S. Pitzer and W. D. Gwinn, J. Chem. Phys. **10**, 428 (1942).

ference rather than the limiting classical one, thereby cutting the maximum error approximately in half.

Exactly what harmonic oscillator is most suitable depends upon which of the thermodynamic functions is to be represented most accurately. Here the emphasis has been placed upon the entropy, for which 1.74 or 1.75 can be substituted for $\pi^{\frac{1}{2}}$ in Eq. (1) with about equally good results.

Table I shows the averaged increments to be added to the thermodynamic properties of the harmonic vibrator

$$h\nu/kT=(1.74/Q_f)(V/RT)^{\frac{1}{2}} \qquad (3)$$

to give the corresponding properties of the restricted rotator. Each row shows, consecutively for a given V/RT, the entropy, free energy, heat content, and heat capacity increments.

ACCURACY

The differences shown in Table I are in general consistent with the extended tables of Pitzer and Gwinn to within 0.01 cal./mole/deg. Interpolation in the least favorable regions should not increase this uncertainty beyond 0.02. For each value of V/RT, however, there is a limit to $1/Q_f$ beyond which the approximation becomes less accurate. When V/RT is high, the Pitzer and Gwinn tables are beginning to show similar uncertainties, but at low V/RT the larger deviations may appear well within the region in which the properties are accurately known. No attempt will be made to describe how the accuracy falls off under these circumstances because it can be shown that the region of large errors probably lies beyond the limit of useful application of the table.

In the region in question the reduced moment of inertia is low, and V/RT is relatively low. Since there are no molecules with symmetrical tops having reduced moments less than that of methanol, the methanol moment, a little above 1.0×10^{-40} c.g.s. units, will set an upper limit to the error. From Pitzer and Gwinn,

$$Q_f=(2.815/n)(10^{38}IT)^{\frac{1}{2}}. \qquad (4)$$

For $10^{40}I=1.0$ and $n=3$, $Q_f=0.094T^{\frac{1}{2}}$. A temperature is now chosen and for the resulting Q_f the value of V/RT is estimated below which the error in the free energy exceeds 0.02. This will give the minimum potential barrier which would permit calculation of the free energy within this limit. Table II shows the result of this estimate.

TABLE I. Comparative thermodynamic properties of the restricted rotator and the harmonic oscillator of Eq. (3).

V/RT	$S-S_H$	$-(F-F_H)/T$	$(H-H_H)/T$	$C-C_H$
0.6	−0.45	0.03	−0.48	−0.90
1.0	−0.02	.22	−0.24	−0.76
2.0	0.37	.27	0.10	−0.29
3.0	.41	.20	.21	0.10
4.0	.35	.14	.21	.30
6.0	.21	.08	.13	.32
9.0	.11	.03	.08	.19
12.0	.06	.02	.04	.12
16.0	.04	.01	.03	.07
20.0	.02	.0	.02	.05

In round figures, it appears that a potential barrier above 2000 cal./mole will permit accurate calculation. The situation is about the same with the heat content and heat capacity and is considerably more favorable with the entropy. It is probable that the correct barrier for methanol is at least this high. For all other organic molecules the limiting barrier will be lower. The case of dimethylacetylene should perhaps be mentioned because the potential barrier is low. Here the limiting barrier for accurate calculation is about 1000 cal./mole, but the question of an approximate calculation is less important because the internal rotation in this case is almost free.

It is interesting that this consideration also shows that the region in which the Pitzer and Gwinn tables are beginning to show inaccuracies lies outside the probable limit of usefulness.

USE OF TABLE I

When the temperature and the potential barrier are known, a thermodynamic property can be quickly evaluated. The ratio $h\nu/kT$ is determined from Eq. (3), and the property is obtained for the harmonic oscillator from standard tables such as those in Mayer and

TABLE II. Minimum potential barrier for calculation of the free energy within 0.02 unit at $10^{40}I=1.0$.

T	$1/Q_f$	V/RT (min.)	V (min.)
900	0.354	0.7	1250
625	.427	1.5	1860
400	.532	2.0	1600
225	.708	3.5	1600

TABLE III. Potential barrier for ethane. $10^{40}I=2.7$ and $S=1.70$ at $T=298$.

Approx.	δS	$h\nu/kT$	V/RT	δS (new)
1	0.20	1.378	4.44	0.32
2	.26	1.428	4.77	.30
3	.28	1.445	4.886	.288
4	.284	1.448	4.906	.286

Mayer.[3] Addition of the increment from Table I for the correct level of V/RT gives the approximate value of the property for the restricted rotator.

For example, take $V/RT=3.3$ and $1/Q_f=0.38$. Then $h\nu/kT=1.201$ and $S_H=0.876R=1.742$. Add 0.39 from Table I for a total entropy of 2.132. From Pitzer and Gwinn, Table III, a double linear interpolation gives the value 2.138.

To determine the height of the potential barrier from the entropy requires a series of approximations, since both the barrier and the increment from Table I depend upon V/RT. For ethane, take $10^{40}I=2.7$ and $S=1.70$ at $T=298$. This gives $1/Q_f=0.376$. First an average increment of 0.20 from the entropy column of Table I is subtracted, leaving 1.50 for the harmonic oscillator and giving $h\nu/kT=1.38$. Then $V/RT=(Q_f/1.74)^2(h\nu/kT)^2=2.340(h\nu/kT)^2=4.44$. This yields a new correction from Table I and the calculation is repeated. Rapid convergence is obtained by taking for each new approximation the numerical mean of the newly indicated increment and the one just previously used. The approximations are summarized in Table III.

The result is $V/RT=4.92$ and $V=2913$ cal./mole. From Table III of Pitzer and Gwinn, again by means of a double linear interpolation, for $S=1.70$ and $1/Q_f=0.376$, $V/RT=4.934$ and $V=2921$.

The approximation yields results almost as good as the extended tables of Pitzer and Gwinn and appears to be accurate enough for use with any data now available or in prospect. The calculation, however, is not always as convenient as could be desired, but in compensation has the advantage of emphasizing that the thermodynamic properties of the restricted rotator are related in a simple way to those of the harmonic oscillator.

[3] Mayer and Mayer, *Statistical Mechanics* (John Wiley and Sons, Inc., New York, 1946), p. 445.

APPENDIX

Setting up an approximate method of reproducing the values in the Pitzer and Gwinn tables implies dependence upon the potential energy function $V=V_0(1-\cos n\theta)/2$. The potential barrier is now represented by V_0 and n is the symmetry number of the number of potential minima in the cycle. θ is a combination coordinate in which a single rotator of moment of inertia I, equal to the reduced moment of the internal rotator, would have the same properties as the rotator under consideration.

Since $\cos n\theta=1-n^2\theta^2/2+\cdots$, we may write for small values of θ, $V=V_0n^2\theta^2/4$ for the limiting harmonic or parabolic potential energy at high levels of V/RT. The corresponding force constant is $V_0n^2/2$ and, consequently, $h\nu/kT=(nh/2\pi kT)(V_0/2I)^{\frac{1}{2}}$. When this expression is combined with $Q_f=(8\pi^3IkT)^{\frac{1}{2}}/nh$, we obtain Eq. (1).

To calculate the increments of Table I, a set of frequencies according to Eq. (3) was first tabulated as a function of V/RT and $1/Q_f$. The four thermodynamic properties of the harmonic oscillator were then tabulated in the same framework. Next, those parts of the entropy and free energy tables which are given only as deficiencies below free rotation were converted, except at $1/Q_f=0$, to read these properties directly. For this purpose, $F_f=RT\ln(1/Q_f)$ and $S_f=R/2-F_f/T$. The differences between harmonic oscillator and restricted rotator could then be tabulated and used to find the increments shown in Table I. The gas constant R has been taken as 1.9869.

At $1/Q_f=0$, the limiting ratio

$$Q_f/Q_H=1.74(V/RT)^{\frac{1}{2}}$$

was used in conjunction with the tabulated differences S_f-S and $(F-F_f)/T$ to find $S-S_H$ and $(F_H-F)/T$.

Finally, the effects produced by changing the constant a in the equation

$$h\nu/kT=(a/Q_f)(V/RT)^{\frac{1}{2}}$$

will be considered. For the harmonic oscillator,

$$F_H/T=R\ln(1-e^{-h\nu/kT}),$$

and

$$H_H/T=(Rh\nu/kT)/(e^{h\nu/kT}-1).$$

A small change in a at constant Q_f and V/RT affects these functions as follows:

$$\delta(F_H/T)/\delta a = H_H/aT$$

and

$$\delta(H_H/T)/\delta a = H_H/aT - C_H/a.$$

Since $S=(H-F)/T$, it follows that

$$\delta S_H/\delta a = -C_H/a$$

Thus the changes in the harmonic oscillator properties, and therefore also in the differences of Table I, are related in a simple way to the properties themselves. At $1/Q_f=0$, a given small change in a will produce the same effect upon the entropy and free energy at all values of V/RT, while at the same time the heat content will remain unchanged at the classical value. When V/RT is low, the frequency remains low through the whole useful range of $1/Q_f$, and the effect of changing a will change only slightly as $1/Q_f$ increases. If V/RT is high, a change in a will change the entropy and free energy by amounts varying from zero at high $1/Q_f$ to R times the percentage change in a at low $1/Q_f$.

This shows how the trend of 0.05 to 0.06 in the entropy and free energy differences found for the limiting harmonic oscillator at high V/RT can be effectively leveled out by the small change in a from $\pi^{\frac{1}{2}}$ to 1.74. The effect on the heat content and heat capacity is zero at both ends of the $1/Q_f$ scale and reaches a low maximum at some intermediate but fairly high $1/Q_f$. This maximum is less than one-half the maximum effect on the entropy and free energy.

It is reasonable that the most suitable harmonic oscillator for the comparison should have frequencies below the limiting ones, because in the useful range of the variables RT is always an appreciable fraction of V and, as a consequence, the average spacing of the more important energy levels will be less than that of the limiting oscillator.

THE JOURNAL OF CHEMICAL PHYSICS VOLUME 15, NUMBER 6 JUNE, 1947

Intermolecular Forces and Energies of Vaporization of Liquids

SIDNEY W. BENSON
Chemical Laboratories, University of Southern California, Los Angeles, California

(Received April 4, 1947)

By using a "smoothed potential" model for the liquid state and assuming isotropic, homogeneous expansion with temperature which involves no change in coordination, it is shown that it is possible to reduce the expression for the configurational energy of the liquid to a function of a single parameter, the density. If the intermolecular forces can be put into a polynomial form then the expression for the configurational energy can be factored, resulting in an algebraic equation of the form:

$$E_c = -B_1D^2 - B_2D^{8/3} - B_3D^{-10/3} + B_4D^4$$

in which D is the molar density and the B's are constants independent of temperature. For the distances occurring in liquids, the last three terms can be either dropped or combined with the first, leaving as an approximation: $E_c = AD^{x/3}$. The energy of vaporization is given by: $E_v = A(D_1^{x/3} - D_g^{x/3})$. Values calculated from this last equation show excellent agreement with experimental values for a large number of both normal and "abnormal" liquids. Values of $x=5$ or 6 both work, the latter being better up to the critical temperature.

INTRODUCTION

IN recent years, the problem of expressing analytically the thermodynamic properties of liquids has been shown capable of treatment using the methods of statistical mechanics. The most general and rigorous treatment made by Mayer and other workers,[1] has thrown considerable light on the phenomenon of condensation and raised fundamental questions concerning the region of the critical temperature. However, while fundamental in its approach, this method has not yielded functions susceptible to a simple, practical treatment.

Simpler models of the liquid state, based on

[1] Mayer and Mayer, *Statistical Mechanics*, Chaps. 13, 14 (John Wiley, 1940) (summarizes most of the recent work); see also: Band *et al.*, J. Chem. Phys. **9**, 123 (1941) and earlier papers.

somewhat crude formulations have yielded surprisingly good qualitative and even quantitative agreements with experimental data.[2-5] These models may be termed "cage" models. They assume a quasi-crystalline structure for the liquid in which the molecules are restricted to motions in a cage of nearest neighbors. The main differences between such models and a true solid, lies in the ability of the liquid molecules to exchange cages, in the slightly weaker central forces acting on the molecule of the liquid as it moves from the center of its cage, and in the anisotropy of the solid.

The crudest of these models which has given significant results is the one proposed by Guggenheim,[6] called the "smoothed potential" model. This model assumes that the liquid molecule, constrained to move within its cage, moves in a potential well with a flat floor and essentially infinite walls at the edges of the cage.

In this paper, it will be shown that the "smoothed potential" model for the liquid, when used in conjunction with intermolecular potentials of the London[7] form will yield a simple relation connecting the energy of vaporization and the density of the liquid. This relation is in excellent agreement with the experimental values for these quantities over most of the liquid range.

I. THE SMOOTHED POTENTIAL MODEL

If we assume a liquid composed of hard, spherical molecules of diameter d, moving in an average potential field $-U_c$, which is constant within the cage of a molecule, then we can write for the partition function of 1 mole:

$$Q_c = e^N v_f^N e^{NU_c/kT} = (ev_f e^{U_c/kT})^N. \tag{1}$$

N is Avogadro's number, v_f is the volume accessible to the center of the molecule (i.e., its free volume), and k is the Boltzmann constant.

For a rectangular potential well of the type which this model assumes, v_f may be represented by:

$$v_f = \tfrac{1}{6}\pi(a-d)^3 \tag{2}$$

in which a is the average distance between the central molecule and its nearest neighbors. (The radius of the cage is equal to a.) We see then that "a" will be some function of the molar volume of the liquid, V. Thus, the free volume v_f becomes a function of V only.

The total partition function, Q, which will include the contributions of the external and internal degrees of freedom may be written as:

$$Q = Q_{\text{trans}} \cdot Q_{\text{rot}} \cdot Q_{\text{int}} \cdot Q_c. \tag{3}$$

This assumes that the various energies, internal and external, are all separable. From Q, the thermodynamic functions of the liquid may be obtained:

$$A = -kT \ln Q; \quad E = kT^2(d \ln Q/dT)_v; \quad \text{etc.} \tag{4}$$

II. THE CONFIGURATIONAL ENERGY

The expression for the partition function, Q_c, has been termed the configurational partition function[6] since it represents that contribution to the total partition function which is caused by the intermolecular structure.

If we assume that the forces between molecules in a liquid are functions only of the distance of separation then it can be shown that U_c is a function only of the volume and Q_c will contribute exactly the quantity U_c to the total energy of the system. U_c is then the configurational energy of the system, and for molecules with no forces of interaction, U_c is equal to zero.

Let $E(r)$ represent the mutual potential energy averaged over-all configurations, of a pair of molecules, distant r from each other. Then the total potential energy of a molecule in the liquid, E_m will be the quantity $E(r)$ summed over all molecules in the liquid. This can be written as:

$$E_m = \sum_{i=1}^{N} n_i E(r_i). \tag{5}$$

In this equation n_i is the number of molecules at a distance r_i from the central molecule. Since n_i will increase roughly as r^2, $E(r_i)$ must decrease faster than r_i^{-3} if E_m is to remain finite.

U_c represents the energy required to separate all the molecules in the liquid. If we think of the liquid as being composed of bonds between each pair of molecules, then U_c would be the energy required to break all of these bonds. We

[2] Fowler and Guggenheim, *Statistical Thermodynamics*, Chaps. 7, 8. (Presents a review of the work with simple liquid models, Cambridge University Press, London, 1939.)
[3] Eyring and Hirschfelder, J. Phys. Chem. **41**, 250 (1937).
[4] Newton and Eyring, Trans. Faraday Soc. **33**, 73 (1936).
[5] H. S. Frank, J. Chem. Phys. **13**, 478–507 (1945).
[6] Guggenheim, Proc. Roy. Soc. **A135**, 181 (1932).
[7] London, Zeits. f. physik. Chemie **B11**, 222 (1930).

then have the relation:

$$U_c=\tfrac{1}{2}NE_m=\tfrac{1}{2}N\sum_{i=1}^{N}n_iE(r_i). \quad (6)$$

The factor of $\frac{1}{2}$ is introduced to avoid counting all the bonds twice. Equation (6) assumes that E_m is the same for all the molecules in the liquid. This cannot be the case for the molecules in the surface, but for any large number of molecules in the aggregate the contribution of the surface molecules may be neglected.

If we now make the assumption that temperature expansion of the liquid is a regular, homogeneous, isotropic change in which the coordination of the molecules is unchanged (an assumption which is compatible with the type of potential well employed), then the quantities n_i become independent of temperature and the entire temperature dependence of U_c is to be found in $E(r_i)$.

This assumption of homogeneous temperature expansion means that all of the intermolecular distances may be related to any configuration of the liquid (chosen as a standard) by a single parameter. If r_1 is equal to the distance between the central molecule and its nearest neighbors ($r_1=a$; see Eq. (2)) then it is possible to relate all the other distances in the liquid to r_1 by equations of the type:

$$r_i=c_ir_1. \quad (7)$$

The quantities c_i will be pure number ratios which will be independent of temperature and dependent only on the geometry or packing of the liquid.* If we choose a single temperature as a reference temperature, then for this standard state the ratios c_i are the ratios of the intermolecular distances to the distance r_1.

Replacing the r_i in Eq. (6) by their values from Eq. (7), we have:

$$U_c=\tfrac{1}{2}N\sum_{i=1}^{N}n_iE(c_ir_1). \quad (8)$$

It is desirable to relate r_1 to some property of the liquid, and the most convenient property for this purpose is the molar density D. Generally the density will be inversely proportional to r_1^3 and we can write,

$$r_1=gD^{-\frac{1}{3}}, \quad (9)$$

in which g is again a geometrical constant independent of temperature.**

Substituting the value of r_1 from Eq. (9) into Eq. (8), we will have

$$U_c=\tfrac{1}{2}N\sum_{i=1}^{N}n_iE(c_igD^{-\frac{1}{3}}). \quad (10)$$

In Eq. 10, U_c has been reduced to an expression which is a function of a single parameter, the molar density D, and it is now amenable to rather simple treatment.

III. ENERGY OF VAPORIZATION

The total energy E, of the liquid will be given by the expression (Eq. (4))

$$E=kT^2(d\ \ln Q/dT)_V.$$

If we assume that the various degrees of freedom are separable then, from Eq. (3) we have,

$$E=kT^2(d\ \ln Q_T\cdot Q_R\cdot Q_I)/dT)_v+U_c. \quad (11)$$

If we further assume that the rotation of the liquid is free or almost free (i.e., rotational barriers $<kT$) and that the internal modes of motion are the same in the liquid and vapor phases, then the partition functions Q_T, Q_R, and Q_I will be the same for both liquid and vapor.

To this degree of approximation then, we will have for the energy of vaporization,

$$E_{\text{vap}}=E(\text{gas})-E(\text{liq})=U_c(\text{gas})-U_c(\text{liq}). \quad (12)$$

At temperatures at which the density of the gas is small, the energy of the gas may be neglected and we can write,

$$E_{\text{vap}}=U_c(\text{liq}). \quad (13)$$

As a next approximation of Eq. (13), we may assume the gas capable of the same treatment as the liquid, and in this case we can use the same function in Eq. (12) for the configurational energy of gas and liquid.

IV. INTERMOLECULAR POTENTIALS

London[7] has shown that for non-polar molecules, the attractive forces are given by an

* If hexagonal packing is assumed, then $n_1=12$, $n_2=18$, $n_3=24$, etc., and $c_1=1$, $c_2=(3/4)^{\frac{1}{2}}$, $c_3=2$, etc. For simple cubic packing, $n_1=6$, $n_2=12$, $n_3=8$, $\cdots$ and $c_1=1$, $c_2=2^{\frac{1}{2}}$, $c_3=3^{\frac{1}{2}}$, etc.

** For hexagonal packing: $g=1.12N^{-\frac{1}{3}}$. For simple cubic packing; $g=N^{-\frac{1}{3}}$.

expression,

$$E(r) = -\alpha/r^6 - \beta/r^8 - \gamma/r^{10} \qquad (14)$$

in which the constants α, β, and γ are independent of temperature. Of these terms, the first (the "dipole-dipole" interaction) is dominant, although the other terms may become important at small distances. For molecules possessing dipole moments, the constant α is no longer temperature independent and has the form,

$$\alpha = \alpha_1 + \alpha_2/T. \qquad (15)$$

The first term α_1 in Eq. (15) represents the sum of the London dispersion forces and the "induction" effect. For most substances, this latter is usually negligible. The term α_2/T in Eq. (15) arises from the orientation effect caused by the permanent dipoles. For most polar substances this term is usually small compared to the dispersion term. Only for substances such as NH_3 and H_2O, which are strongly hydrogen-bonded, does the orientation effect exceed the dispersion term. However, the orientation effect is not additive, whereas the dispersion and induction terms are. It is not therefore unreasonable to use Eq. (14) to represent the attractive forces without considering the temperature dependence of α in the case of very polar molecules.[8]

In addition to the attractive forces, there exist repulsive forces at small distances which have been variously represented in the form δr^{-m}. With the aid of the quantum theory it has been shown[9–11] that the correct theoretical form for these repulsive forces is Ae^{-r/r_0}. Although A is a function of r, Slater[9] has shown that no large error is involved in assuming A to be a constant for a given molecule. In any case, these forces of repulsion fall off very rapidly with the distance, and excellent agreement with experimental data has been obtained using either form.[12–14]

A general expression may then be written for the total forces of interaction as follows:

$$E(r) = -\frac{\alpha}{r^6} - \frac{\beta}{r^8} - \frac{\gamma}{r^{10}} + \frac{\delta}{r^{12}}. \qquad (16)$$

For the distances which occur in liquids this may be approximated by assuming hard molecules with attractive forces of the form,

$$E(r) = -\alpha_0/r^x. \qquad (17)$$

This is justified to some extent by the fact that the higher dispersion terms in Eq. (16) are of about the order of magnitude and of opposite sign to the last repulsion term.[8] If over the range of distances in the liquid at different temperatures the cancellation of these terms is very close, then x would have the value of 6. Estimating more closely, most of the intermolecular potential caused by these higher order terms will arise from the nearest neighbors and for these small distances the contribution of the repulsive forces is larger[8] than the higher order dispersion terms, and we may expect to find values of x less than 6.

Substituting the value of $E(r)$ from Eq. (17) into Eq. (10), we find for the configurational energy,

$$U_c = -\tfrac{1}{2}N \sum_{i=1}^{N} n_i \alpha_0 c_i^{-x/3} g^{-x/3} D^{x/3} \qquad (18)$$

$$= -(\tfrac{1}{2}N\alpha_0 g^{-x/3}) D^{x/3} \sum_{i=1}^{N} n_i c_i^{-x/3} \qquad (19)$$

$$= -AD^{x/3}. \qquad (20)$$

In Eq. (20), A is a constant containing only temperature independent quantities and so U_c is reduced to a simple function of the density. It can be seen from the form of U_c given in Eq. (10) that so long as we can express $E(r)$ as a polynomial in r, U_c can always be reduced to a simple polynomial expression in terms of D.

In the general case, using all the terms for the potential energy we would have:

$$U_c = -B_1D^2 - B_2D^{8/3} - B_3D^{10/3} + B_4D^4.$$

The term B_1 might be expected to show some temperature dependence for very polar or hydrogen-bonded molecules, and terms B_2 and B_3 would be of smaller magnitude with B_3 probably

[8] Margenau, Rev. Mod. Phys. **11**, 1 (1939), reviews the theories of intermolecular forces and discusses the importance of the various terms.
[9] Slater, Phys. Rev. **32**, 349 (1928).
[10] Buckingham, Proc. Roy. Soc. **A161**, 476 (1937).
[11] Huggins, J. Chem. Phys. **5**, 143 (1937).
[12] Hirschfelder and Roseveare, J. Phys. Chem. **43**, 15 (1939).
[13] Buckingham, Proc. Roy. Soc. **A168**, 264 (1938).
[14] Lennard-Jones, Proc. Phys. Soc. **43**, 461 (1931).

TABLE I.*

Substance	M	T_c°C	D_c	A ($x=6$) A_{av}	Av. dev. %	Max. dev. %	Range −°C	A ($x=5$) A_{av}	Av. dev. %	Max. dev. %	Range −°C
Carbon dioxide	44	31.1	10.58	4.73	1.7	2.7	−60°/20°	13.6	2.4	4.1	−60°/20°
Sulfur dioxide	64	157.2	8.12	10.28	1.1	1.8	−40°/60°	28.9	2.5	5.9	−40°/60°
Ammonia	17	132.9	13.75	3.28	2.4	4.3	−50°/50°	10.97	0.6	1.3	−50°/50°
Water	18	374.4	17.72	3.29	2.3	4.5	0°/374.1°	11.68	1.3	3.6	0°/341°
Methyl alcohol	32	240.0	8.52	14.42	2.3	7.0	0°/238°	39.8	2.6	6.7	0°/210°
Ethyl alcohol	46	243.1	5.99	33.5	2.0	7.1	0°/230°	83.5	2.3	7.5	0°/200°
Propyl alcohol	60	263.7	4.55	59.0	3.1	9.5	0°/230°	135.5	4.4	11.2	0°/210°
Ethyl ether	74	193.8	3.55	65.1	1.9	4.0	0°/190°	134.8	0.5	3.1	0°/160°
Methyl formate	60	214.0	5.82	24.8	1.0	2.6	−20°/200°	68.2	1.5	4.0	−20°/170°
Ethyl formate	74	235.3	4.36	47.0	1.0	3.0	50°/220°	103.0	1.8	4.4	50°/200°
Propyl formate	88	264.9	3.52	79.3	1.1	3.5	70°/260°	160.5	1.7	4.0	70°/240°
Methyl acetate	74	233.7	4.40	48.2	1.5	2.8	50°/227°	105.5	1.8	6.0	50°/210°
Ethyl acetate	88	250.1	2.86	79.4	2.2	4.8	5°/245°	163.0	1.6	3.7	5°/210°
Propyl acetate	102	276.2	2.90	126.0	1.8	3.5	90°/266°	238	1.1	3.5	90°/250°
Methyl propionate	88	257.4	3.20	78.5	1.6	3.3	70°/250°	159.2	1.4	4.0	70°/230°
Ethyl propionate	102	272.9	2.91	121.8	1.7	3.5	0°/270°	238	2.0	4.7	0°/240°
Methyl butyrate	102	281.3	2.94	120.2	2.3	4.5	100°/278°	230	0.5	2.0	100°/250°
Methyl isobutyrate	102	267.6	2.95	116.3	1.0	3.8	90°/263°	223	1.3	3.2	90°/250°

* M = molecular weight, T_c = critical temperature in °C, D_c = critical density in moles/liter. $A_5 = E_{vap}/(D_{liq}^{5/3} - D_{gas}^{5/3})$ and $A_6 = E_{vap}/(D_{liq}^2 - D_{gas}^2)$ with E_{vap} in calories/mole and densities in moles/liter. Values for water from Keenan and Keyes, *Steam Tables*. Values for SO_2 and NH_3 from *International Critical Tables*. Values for CO_2 from *International Critical Tables*. The values at −60°C are for the super-cooled liquid. Values for the other substances are from Young, Proc. Roy. Soc. Dublin **12**, 374 (1910).

TABLE II. Hydrocarbons*

Substance	M	T_c°C	D_c	A ($x=6$) A_{av}	Av. dev. %	Max. dev. %	Range −°C	A ($x=5$) A_{av}	Av. dev. %	Max. dev. %	Range −°C
Propane	44	96.85	5.10	24.0	3.0	6.7	−62°/93.3°	54.8	0.7	1.6	−62°/80°
n-pentane	72	197.2	3.23	79.2	1.6	3.3	30°/190°	154.3	1.6	4.2	30°/170°
iso-pentane	72	187.4	3.07	75.0	1.9	3.6	10°/183°	147.2	0.8	3.7	10°/160°
n-hexane	86	234.8	2.73	124.5	1.2	2.7	60°/226°	231.0	1.7	4.1	60°/200°
Cyclohexane	84	280	3.16	90.2	1.4	5.3	10°/277°	179.0	1.7	4.3	10°/250°
Benzene	78	288.5	3.91	63.1	2.5	4.5	0°/280°	134.1	0.8	3.0	0°/250°
n-heptane	100	266.9	2.34	187	2.1	3.8	70°/264°	330	1.7	3.8	70°/250°
n-octane	114	296.2	2.04	258	2.9	6.3	10°/280°	445	1.1	3.0	10°/270°
Di-isopropyl	86	227.4	2.80	113.7	0.7	3.4	50°/220°	212	2.2	4.7	50°/200°
Di-isobutyl	114	276.8	2.08	242	1.7	4.1	90°/274°	405	1.0	3.5	90°/250°

* See footnote, Table I for units. Values for propane, Stearns and George, Ind. Eng. Chem. **35**, 602 (1943). All other hydrocarbons taken from Young (see reference to Table I).

negligible. Our assumption amounts to anticipating that the fourth term is of the same magnitude as the terms B_2 and B_3 or larger.

V. TEST OF EQ. (20) USING ENERGIES OF VAPORIZATION

We showed in Section III, Eq. (12) that the energy of vaporization of a liquid should be equal to the difference in configurational energies of the liquid and gas. Substituting the values of the configurational energies from Eq. (20) into Eq. (12), we have

$$E_{vap} = A(D_{liq}^{x/3} - D_{gas}^{x/3}). \quad (21)$$

For most of the liquid range, the density of the saturated vapor is small compared to the density of the liquid and Eq. (21) may be reduced to

$$E_{vap} = AD_{liq}^{x/3}. \quad (22)$$

To test Eq. (21), it is solved for the constant A and the ratio of E_{vap} to the difference in the $x/3$ power of the densities of liquid and vapor is computed from their experimental values. Values of x equal to 3, 4, 5, 6, 7 were tried for a number of different substances and the values for x of 3, 5, and 6 for all of the substances listed in Tables I, II, and III.

TABLE III. Halogen compounds.

Substance	M	T_c°C	D_c	A (x=6) A_{av}	Av. dev. %	Max. dev. %	Range −°C	A (x=5) A_{av}	Av. dev. %	Max. dev. %	Range −°C
Stannic chloride	260.5	318.7	2.85	131.0	1.2	2.8	100°/280°	242.0	1.5	4.3	100°/280°
Carbon tetrachloride	154	283.2	3.62	70.5	2.0	3.9	70°/280°	145.8	1.0	3.0	0°/260°
Methyl chloride	50.5	143.1	7.3	12.3	2.8	5.9	−62°/77°	32.4	0.3	2.0	−62°/77°
Dichloro-difluoro-methane	121	111.7		29.6	2.3	4.0	−40°/49°	67.0	0.4	1.3	−40°/49°
Trichloro-mono-fluoromethane	137.4	198.0		46.2	2.4	4.2	−40°/71°	103.0	0.7	1.5	−40°/71°
Dichloro-mono-fluoromethane	102.9	178.5		28.9	1.7	2.8	−40°/71°	68.8	0.2	1.0	−40°/71°
Difluoro-mono-chloro-methane	86.5	96.0		16.6	3.0	4.8	−104°/49°	41.6	0.6	2.6	−104°/49°
Unsymmetrical tri-chloro-trifluoro-ethane	187.4	214.1		90.5	2.3	3.9	−30°/105°	182.6	0.5	0.9	−30°/105°
Fluorobenzene	96	286.6	3.69	72.8	0.9	2.3	80°/280°	148.4	2.0	3.8	80°/260°
Chlorobenzene	112.5	359.2	3.08	104.0	2.1	4.3	130°/270°	207.5	0.4	1.1	130°/270°
Bromobenzene	157	397*	3.09*	118.5	2.0	3.6	150°/270°	235.0	0.5	1.2	150°/270°
Iodobenzene	204	448*	3.50*	149	1.4	2.8	180°/280°	290.5	0.6	1.3	180°/280°

* Values estimated by Young. See footnote, Table I for units. Values for methyl chloride and the chlorine-fluorine substituted compounds from the latest thermodynamic tables issued by the DuPont Company, Wilmington, Delaware. All other compounds taken from Young (see reference to Table I).

When the values 3, 4, or 7 are used for x, the values of A so obtained for a single liquid over a temperature range show considerable variation. Only the values for x of 5 and 6 will fit the data and give reasonably constant values for A.

In Table I are presented the data for CO_2, SO_2, and substances which are expected to show hydrogen bonding. Table II presents the data for hydrocarbons and Table III the data for halogenated compounds.

The energies of vaporization were usually not given directly in the literature cited in the footnotes to the tables, but were calculated by subtracting $P(V_g - V_l)$ from the heats of vaporization. The heats of vaporization given in the literature are not calorimetric heats but calculated values obtained from precise vapor pressure data and data on the molar volumes of liquid and vapor. The Clausius-Clapeyron relation—$H_v = T(V_g - V_l)dP/dT$—was used to obtain H_{vap} from this data. In almost every case where direct calorimetric data was available, the calculated values agree to within 1–2 percent. The values of the energy of vaporization calculated in this manner are probably good to about 1–2 percent over most of the temperature range and probably good to only about 5 percent in the neighborhood of the critical temperature.

For most of the substances over the temperature range for which data were available, the energies of vaporization changed by a factor of from 50 percent to 300 percent. In a few cases like that of water, the range is represented by a factor of 20.

In each case, values for A_5 and A_6 were calculated at 10°C intervals over the temperature range indicated in the tables. In a few cases where good data was available up to the critical, calculations were made at smaller intervals in this region. Because of the large number of individual calculations, only the average results presented in Tables I, II, and III are given.

From the tables it can be seen that both A_5 and A_6 represent the data to within a few percent. The detailed calculations show that A_5 gives a better fit for the data over a temperature range which extends from low temperatures (below the boiling point) up to temperatures not too close to the critical. For a temperature range which does not go beyond a reduced temperature of 0.9 the constancy of A_5 is within the limits of experimental error of the data. This is most evident for the halogenated compounds in Table III. For some of these compounds (e.g., the freons) the data does fall below $T_r < 0.9$ and for these A_5 is well within the limits of experimental error.

A_6 shows its largest deviations at temperatures below the boiling point. For temperatures near the boiling point and extending up to the critical temperature, A_6 is a better constant than A_5 and fits within the limits of experimental error. This was rather surprising, since the use of the same function to represent both the configurational energies of liquid and vapor (see Eq. (21)) was originally considered a dubious approximation.

However, a reconsideration of Eq. (16) indicates a possible explanation for the behavior of the quantities A_5 and A_6. A large part of the total expansion of the liquid takes place in a short temperature interval in the neighborhood of the critical point. In the temperature range from the melting point extending up to $T_r=0.9$ the total variation in the intermolecular liquid distances has been about 20 percent. In this small range of distances, the repulsive energies are probably large enough to overbalance the higher order dispersion terms, and $E(r)$ will probably not fall off as rapidly as r^{-6}. It should not be unexpected then to find that for this range r^{-5} provides a good representation of the intermolecular potentials.

Above a reduced temperature of 0.9 the liquid is expanded and intermolecular distances are changing rather rapidly. The repulsive forces fall off most rapidly and in this region they are probably equal to or smaller than the higher order dispersion terms. All of these terms have become proportionately smaller than the r^{-6} term and so it seems reasonable that this term should provide a good fit for both the liquid and the gas which is even more expanded. The Beattie-Bridgman equation of state gives,

$$E_c = C_1 D^2 - C_2 D. \qquad (23)$$

At large densities the first term in Eq. (23) is dominant, and the energy reduces to the form used in this paper. These large densities are certainly the case in the critical region.

Also rather surprising at first was the fact that such strongly hydrogen-bonded liquids as water, ammonia, and the alcohols (Table I) show such excellent agreement with the simple liquid model used. Of the substances reported in Table I, propyl alcohol shows the poorest agreement. Calculations not reported were made for acetic acid from Young's data (see reference to Table I) and the calculated values of E_{vap} could not be fit by any simple function of the densities. This is to be expected since it is well known that acetic acid is largely dimeric in the vapor phase, and we are dealing in this case with a rather complex system of largely associated molecules. Acetic acid is also rather anomalous in that its heat of vaporization increases with increasing temperature up to approximately the boiling point. In the case of propyl alcohol it would be of some interest to check the experimental data to see if the large deviations are real.

The good agreement for hydrogen-bonded liquids suggests that the bonding energies must vary with the intermolecular distances in the same fashion as the London forces, namely, r^{-6}. The agreement which is obtained for liquids at temperatures where it seems likely that there is restricted rotation suggests that the potential energy of the restricting barriers must show the same dependence on temperatures also.

ACKNOWLEDGMENT

The author wishes to express his thanks to Mr. Bernard Feldman of the School of Engineering for his aid in performing the many, long tedious calculations.

Chemical Forms Assumed by C^{14} Produced by Neutron Irradiation of Beryllium Nitride*

PETER E. YANKWICH
Radiation Laboratory and Department of Chemistry, University of California, Berkeley, California
(Received March 21, 1947)

The nature of the radioactive compounds formed in the production of C^{14} by neutron irradiation of beryllium nitride has been investigated. Solution of the irradiated powder gave activities corresponding to methane, carbon monoxide, carbon dioxide, hydrogen cyanide, methanol, and formic acid. Formaldehyde was not found. The distribution of activities is not affected by the acidity of the solvent. The results are considered in the light of earlier work.

AS an extension of earlier work,[1] we have made chemical fractionations of the carbon fourteen activity induced in powdered beryllium nitride by neutron bombardment. The nuclear reaction $N^{14}(n,p)C^{14}$ gives the product atom an energy of at least 40,000 ev. Though the velocity associated with such a recoil carbon fourteen atom is approximately that of an electron of 1.6-ev energy, one can expect definite chemical effects.

EXPERIMENTAL

The beryllium nitride was prepared from finely powdered beryllium metal by exposure to nitrogen at high temperature.[2,3] The powder was pressed into aluminum cans for irradiation at Hanford.

The first experiment was an analysis for total carbon radioactivity. Approximately 25 mg of the irradiated powder was placed in a small three-necked flask connected to a copper oxide-filled combustion tube. The tube was held at 650°C and was fitted with an absorption bubbler filled with 1*N* sodium hydroxide. The sample was dissolved by warming in 10 ml of 6*N* sodium hydroxide. When solution was complete a drop of methanol was added (to serve as carrier for any non-gaseous activities) along with 25 ml of saturated potassium permanganate solution. A stream of oxygen was started to sweep gases evolved into the combustion tube. The solution was brought to a boil and excess 6*N* sulfuric acid added to liberate carbon dioxide. All carbon fourteen activity was recovered by this procedure.

In the second and third experiments about 50 mg of the irradiated powder was dissolved in sodium hydroxide. The gases were swept out with a stream of oxygen and passed through an analytical train consisting of two combustion tubes, each fitted with an absorber, one at 325°, the other at 650°. Activity caused by carbon monoxide was collected in the first absorber, that from methane in the second. After these fractions were collected a small amount of inactive sodium cyanide was dissolved in the contents of the flask and the solution carefully acidified. The gases were swept first through 0.1*M* acetic acid saturated with silver acetate, and then through sodium hydroxide. Hydrogen cyanide was removed as silver cyanide in the first bubbler, and carbon dioxide was absorbed in the second.

Different procedures were used past this point in the second and third experiments. In the second, a small amount of inactive methanol was added and the total non-gaseous (oxidizable) activity collected as in the first analysis. In the third experiment, small amounts of inactive methanol, formaldehyde and formic acid were added. These compounds were then separated from the bulk of the original solution by distilling it to dryness. Formaldehyde was separated from the distillate as the 2,4-dinitrophenylhydrazone. The filtrate from this operation was made alkaline and distilled to about one-tenth its original volume. The distillate contained the methanol

* This paper is based on work performed under Contract No. W-7405-Eng-48 with the Manhattan Project in connection with the Radiation Laboratory, and the Department of Chemistry, University of California.

[1] Yankwich, Rollefson, and Norris, J. Chem. Phys. **14**, 131 (1946).

[2] Fichter and Brunner, Zeits. f. anorg. allgem. Chemie **93**, 86 (1915).

[3] The preparation was carried out by Dr. Leo Brewer and Mr. Paul Gillies. An analysis by Dr. B. M. Tolbert showed BeO 2 percent, Be 7 percent, and Be_3N_2 91 percent.

and the residue the formate. These solutions were made alkaline and the carbon compounds oxidized to carbonate with excess potassium permanganate. After acidification the carbon dioxide was swept out with oxygen and converted to barium carbonate for counting.

The radioactivities of the several samples were determined with a thin mica-window counter-tube. This tube and the method of correction for self-absorption of the beta-particles are described elsewhere.[1,4–6] The results of the fractionations are shown in Tables I and II.

A satisfactory material balance has not been obtained yet on the oxidizable fraction, through the formaldehyde is known to be inactive. In this fractionation and in subsequent experiments in which only these oxidizable activities were isolated, about 20 c/m/mg Be_3N_2 was carried by the original formaldehyde-2,4-dinitrophenylhydrazone precipitate. When twice recrystallized from hot 50 percent-ethanol this hydrazone was found to be inactive. Several other experiments gave values for the formic acid and methanol activities which were in approximately the same ratio. In an experiment in which the beryllium nitride was dissolved in 6*N* sulfuric acid, no significant departure from the activity distribution in Table I was detected.[7]

TABLE I. Distribution of activity in irradiated Be_3N_2.

	c/m/mg Be_3N_2	Percent
Total activity	31,000±700	100.0
CO	272±7	0.87
CH_4	19,700±400	62.7
CO_2	1,050±100	3.34
CN^-	1,100±100	3.50
Oxidizable	8,530±200	27.2
Not recovered	750±850	2.39

TABLE II. Activities in the "oxidizable" fraction.

	c/m/mg Be_3N_2
HCHO	0±2
CH_3OH	>200
HCOOH	>5000
Known total oxidizable	8530±200

DISCUSSION

Beryllium nitride powder of this composition has the following atomic constitution: Be, 62.8 percent, N, 36.3 percent, and O, 0.9 percent. In such an environment the first combinations of energetic carbon atoms must be with beryllium, nitrogen, or oxygen, in that order of probability. The eventual distribution of combined radiocarbon with these atomic species is not wholly predictable. No previous analysis has been carried out on substances capable of forming a metallic carbide during irradiation. However, methane is known to be the hydrolysis product of beryllium carbide, Be_2C, and it is reasonable to conclude that the active methane is derived from the radio-carbide, Be_2C^{14}, formed during the irradiation.[8] The sources of the radioactive cyanide, and at least part of the active oxides are apparent. Since they both contain hydrogen, methanol and formic acid must be produced during the hydrolysis. It is conceivable that cyanide is the source of the acid, but ordinary cyanide ion is ruled out because it hydrolyzes slowly to formic acid. Some non-ionic C−N combination trapped in the crystal lattice is probably the precursor of this activity. Similarly, radio-carbon monoxide could hydrolyze to formic acid in irradiated aqueous solutions; however, as with cyanide ion, the rate of hydrolysis of the normal compound is known to be slow at room temperature. In view of the large amount of formic acid and the 40:1 nitrogen-oxygen ratio, nitrogen-carbon combinations constitute the more probable source.

In the earlier work methanol was not found in solid hydrazine hydrochloride, and its appearance in this research was therefore not expected. Because of the highly reduced carbon atom, it is probable that the precursor of the methanol is similar to that of methane, not so much a "carbide" carbon as an isolated carbon atom trapped in the crystal. A simple path for its formation is that proposed earlier for its appearance in irradiated aqueous solutions:

$$C \rightarrow CH_2 \rightarrow CH_3OH.$$

The author wishes to acknowledge the encouragement and interest of Professors M. Calvin and G. K. Rollefson.

[4] Yankwich, Norris, and Huston, Ind. Eng. Chem., Anal. Ed. **19**, (in press).
[5] Dauben, Reid, and Yankwich (to be published).
[6] Libby, Ind. Eng. Chem., Anal. Ed. **19**, 2 (1947).
[7] Dr. B. A. Fries performed this analysis.
[8] Professor W. F. Libby first reported the production of a relatively large amount of active methane.

Photoelectric Intensity Measurements of Raman Spectra

JEN-YUAN CHIEN AND PAUL BENDER
Department of Physical Chemistry, University of Wisconsin, Madison, Wisconsin
(Received February 17, 1947)

An instrument for the direct photoelectric recording of Raman spectra of liquids is described together with the results obtained for CCl_4, $CHCl_3$, CH_2Cl_2, and C_6H_6. The precision of the results was tested by eight recorded spectrograms of $CHCl_3$. The intensity ratios of anti-Stokes to Stokes lines were found to be in good agreement with theoretical values. Approximate values of the change of the bond polarizability of the C—Cl bond in CCl_4 and the C—H bond in C_6H_6 caused by valence vibrations are calculated from the intensity data.

INTRODUCTION

QUANTITATIVE data on the relative intensities and polarization states of Raman lines are scanty and for the most part unsatisfactory in accuracy because of experimental difficulties and the inadequate theoretical treatment. Since the classical work of Placzek little progress was made in the field until recently, when Wolkenstein,[1] advanced for the calculation of intensities and polarization states for vibrational lines a semi-empirical theory which has yielded values in fair agreement with experimental results. Additional experimental data of improved accuracy are, however, essential to progress in this field.

The use of the photo-multiplier tube in the measurement of Raman line intensities and depolarization factors was introduced by Rank and his associates.[2–4] All previous experiments, except one with a photon counter,[5] employed a photographic photometric technique which is tedious and not very accurate because of the logarithmic character of emulsion response, fluctuations in background on the densitometric tracing caused by the granularity of the emulsion, fluctuations of the standard light source during emulsion calibration exposures, and local variations of the sensitivity and the degree of development of the photographic plate. According to Reitz,[6] the precision attained by the photographic method in careful experiments on Raman spectra is about ±14 percent. The experimental problem can be greatly simplified by the application of the photoelectric technique provided due care is taken to reduce fluctuations in the dark current to insignificance. The use of the photo-multiplier tube[7] is required by the extremely low level of light intensity encountered in Raman work; the linearity of its response is well established, particularly at low levels of illumination, and the only calibration required is its spectral sensitivity. The present work is a preliminary report on relative intensity measurements on the Raman spectra of CCl_4, $CHCl_3$, CH_2Cl_2, and C_6H_6 with a nine-stage photo-multiplier and d.c. amplifier system.

EXPERIMENTAL DETAILS

Photo-Multiplier and Power Supply

An RCA 1P21 photo-multiplier tube with base removed was mounted inside a glass jar fitted with a side arm carrying a glass window, in front of which was mounted a fixed slit of width 0.1 mm. Some dehydrite was placed inside the jar to minimize surface leakage. At room temperature the tube was found to have a dark current of the order of 10^{-8} ampere at an accelerating voltage of 110 volts on the dynodes; since the dark current is due mainly to thermionic emission, cooling with solid carbon dioxide was resorted to with a resultant reduction in dark current to 10^{-11} ampere. The mean fluctuation observed in the dark current was ±5 percent

[1] M. Wolkenstein and M. Eliashevich, Acta Physicochimica (URSS) **20**, 525 (1945).
[2] D. H. Rank, R. J. Pfister, and P. O. Coleman, J. Opt. Soc. Am. **32**, 390 (1942).
[3] D. H. Rank, R. J. Pfister, and H. H. Grimm, J. Opt. Soc. Am. **33**, 31 (1943).
[4] D. H. Rank, and R. V. Wiegand, J. Opt. Soc. Am. **36**, 325 (1946).
[5] V. Kudrjawzewa, Acta Physico-chimica (URSS) **3**, 613 (1935).
[6] A. W. Reitz, Zeits. f. physik. Chemie **B38**, 275 (1937).
[7] J. A. Rajchman and R. L. Snyder, Electronics **13**, 20 (1940).

with peak fluctuations amounting to ±20 percent. A heating coil was provided near the end of the side arm to prevent condensation of moisture on the window.

Since the secondary emission phenomenon depends mainly on the energy of the primary electrons, the output dark current and the overall amplification vary markedly with the accelerating voltage on the dynodes as shown in Fig. 1. It is apparent that the voltage supply must be held constant within 0.2 percent or better if 1 percent accuracy in the intensity measurement is to be possible. A special power supply was constructed for this purpose using the degenerative regulator circuit shown in Fig. 2. The output voltage was found to be constant within 0.1 percent for line voltage fluctuations from 100 to 120 volts, and the voltage supplied to the dynodes may be continuously varied by adjustment of R_{12}.

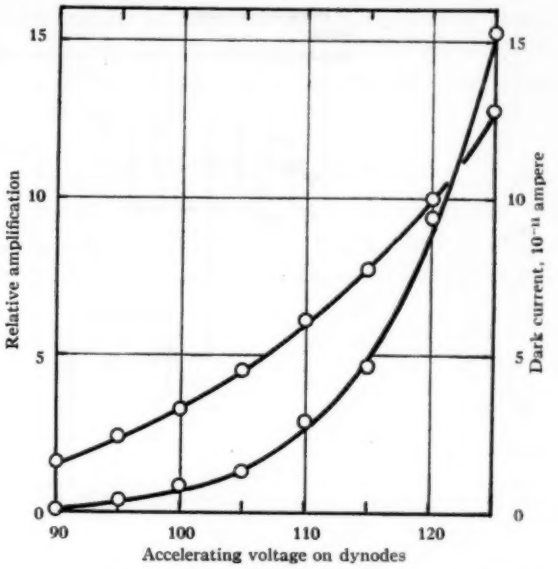

FIG. 1. Relative amplification and dark current at various accelerating voltages on dynodes.

d.c. Amplifier and Recording Device

Since the lowest current to be measured was of the order of 10^{-11} ampere, a d.c. amplifier employing standard radio tubes was adequate. Two RCA-38 tubes operating at reduced filament temperature were used in the balanced circuit shown in Fig. 3. The bias of the active tube was set at −1.20 volt, where the grid current is less than 4×10^{-12} ampere, and the bias of the balancing tube was adjusted so that a change in plate voltage supply from 20 to 30 volts would not produce a disturbance in the plate current balance greater than 0.1 microampere. Degeneration was employed to improve linearity of response. The output of the amplifier was fed

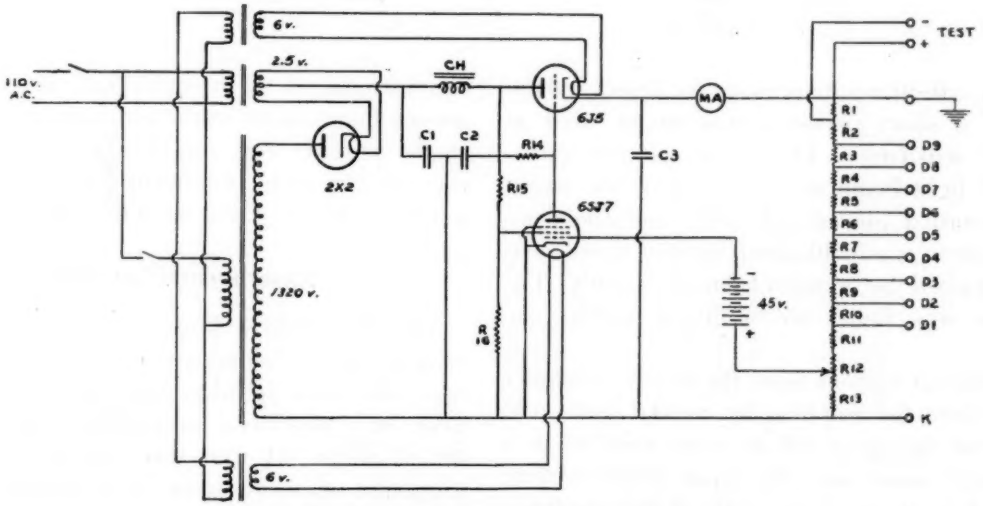

FIG. 2. Circuit of the photo-multiplier power supply.

*R*1	250 ohm	*R*14	0.5 megohm
*R*2	30000 ohm	*R*15	5.0 megohm
*R*3–*R*10	25000 ohm	*R*16	0.1 megohm
*R*11	7000 ohm	*C*1–*C*3	2 mf 2000 v
*R*12	10000 ohm	*CH*	300 H, 7.5-ma choke
*R*13	8000 ohm	*MA*	0–10-ma meter

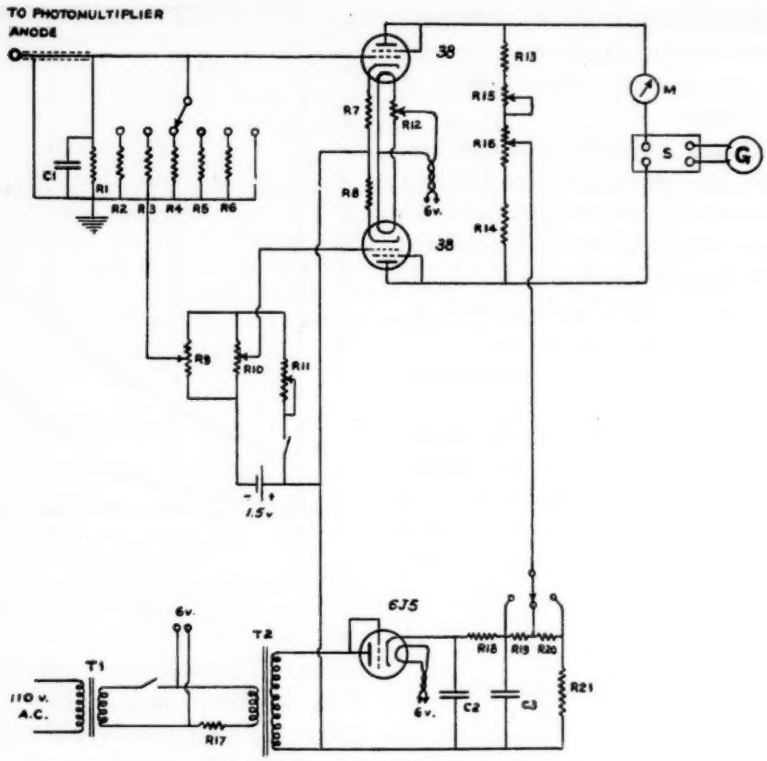

FIG. 3. Circuit for the d.c. amplifier.

*R*1	100 megohm	*R*17	5 ohm
*R*2	10 megohm	*R*18	5000 ohm
*R*3	1 megohm	*R*19, *R*20	1500 ohm
*R*4	0.5 megohm	*R*21	8000 ohm
*R*5	0.1 megohm	*C*1	.01 mf
*R*6	50000 ohm	*C*2, *C*3	24 mf, 150 v
*R*7, *R*8	1000 ohm	*T*1	6-v constant voltage transformer
*R*9–*R*11	800 ohm	*T*2	6-v filament transformer
*R*12	10 ohm	*M*	0–50 microammeter
*R*13, *R*14	50000 ohm	*S*	10000-ohm universal shunt
*R*15	400 ohm	*G*	recording galvanometer
*R*16	10000 ohm		

through a 0–50 microammeter for direct indication to a short period galvanometer used at reduced sensitivity. Deflections of the galvanometer light beam at a distance of one meter were recorded photographically, and the complete system was calibrated against input voltages supplied by a potentiometer circuit. The response was found to be linear within one percent.

The output current from the photo-multiplier was fed into the amplifier by coaxial cable; the tubes and the input circuit were shielded in a desiccated metal box. Six input resistors were provided for varying the gain of the amplifier, which is 10^4 at 100 megohm input resistance, and were selected to make convenient the change from measurement of intensity of Raman to Rayleigh scattering. A 0.01 mf shunt capacitor was introduced to integrate out the high frequency fluctuations in the photo-multiplier tube anode current. The amplifier was found to be very stable with practically no drift after a warm-up period of about 20 minutes.

Experimental Lay-Out

The Hg λ4358A line from six G.E. H-2 mercury vapor lamps was employed for excitation. The filter solution and spectrograph used have been described previously.[8] An entrance slit of width 0.1 mm was employed. The refrigerated photo-multiplier tube was mounted on a carriage constructed by Mr. L. K. Henke, laboratory chief mechanician, and scanned the focal plane of the camera lens at a speed of 1

[8] J. Y. Chien, J. Am. Chem. Soc. **69**, 20 (1947).

mm/min. The recording photographic plate or paper was moved at the rate of 5 mm/min. When the position of the exciting line was reached, as indicated by the microammeter, the gain of the amplifier was reduced manually to a lower range. The gain of the photo-multiplier was adjusted for each sample under investigation by selecting the proper accelerating voltage on the dynodes so that strong Raman lines gave a deflection of *ca* 100 mm on the recording plate. An accelerating voltage of 115 volts per stage or lower is preferable as it results in lower dark current and less fluctuations.

EXPERIMENTAL RESULTS

Several recorded Raman spectrograms of CCl_4, $CHCl_3$, CH_2Cl_2, and C_6H_6 were made as shown in Fig. 4, and the average results for peak

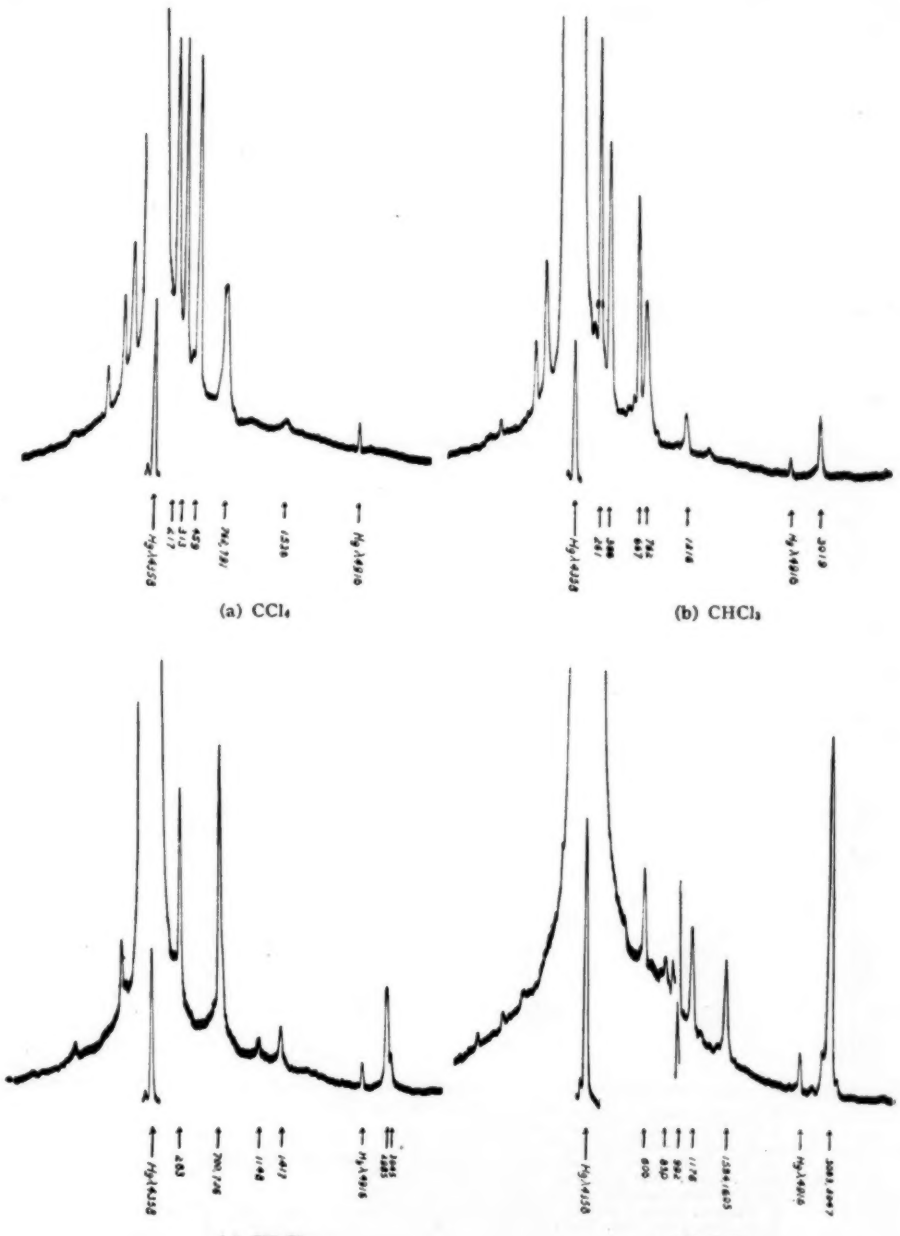

FIG. 4. Recorded Raman spectrograms of CCl_4, $CHCl_3$, CH_2Cl_2, and C_6H_6.

TABLE I. Relative peak intensities of the Raman lines.

Raman freq.	Relative intensity	Values found in the literature							
(a) CCl_4 (average of 3 runs)									
$\Delta\tilde{\nu}$	I	Carrelli and Went	Dhar	A. V. Rao	Reitz	Kowalewska	B. P. Rao	Venkateswarlu	Wolkenstein (calc.)
1536	0.4						1:7.7	0.9	
791	4.1	3.8	4.0	3.2	2.5			3.7	2.3
762									
459	10.0	10.0	10.0	10.9	10.0	10.0	10.0	10.0	10.0
313	9.3	13.8	11.3	14.3	9.3	12.9	9.0	8.1	9.2
217	8.2	11.2	6.3	11.9	8.5	10.3	8.0	6.8	13.2
0	1550	620	3330	3960			5000		
−217	3.2								
−313	2.4								
−459	1.2								

(b) $CHCl_3$ (8 runs)					
$\Delta\tilde{\nu}$	I	Dhar	A. V. Rao	Kowalewska	Wolkenstein (calc.)
3019	2.9	—	2.7		2.8
1216	1.4	—	1.2		1.9
762	4.4	3.1	2.0	(1:1.81)	(25.4)
667	7.5	4.4	8.4		13.5
366	7.5	7.4	7.6	5.5	7.6
261	10.0	10.0	10.0	10.0	10.0
0	2530	1850	4000		
−261	3.3				
−366	1.5				
−667	0.4				
−762	0.2				

(c) CH_2Cl_2 (3 runs)			
$\Delta\tilde{\nu}$	I	Wagner	Wolkenstein (calc.)
3045	1.8	—	1.0
2985	5.4	3.1	2.5
1417	1.4	0.9	0.8
1148	0.7	0.5	0.6
736	3.3	2.0	2.3
700	10.0	10.0	10.0
283	6.7	6.3	6.3
0	3080		
−283	1.9		
−700	0.5		

(d) C_6H_6 (3 runs)							
$\Delta\tilde{\nu}$	I	Carrelli and Went	Dhar	A. V. Rao	Angus Ingold Leckie	Kohlrausch	Venkateswarlu
3063	6.8	6.1	—	3.7	7.8	6.0	8.8
3047					4.4		
1605	1.4	1.7	4.0	0.6	1.4	1.2	1.0
1584					1.7	1.4	0.7
1176	1.4	2.2	4.7	1.1	2.0	1.7	1.7
992	10.0	10.0	10.0	10.0	10.0	10.0	10.0
850	0.6	0.9	2.0	0.5	0.9	0.7	0.6
606	1.3	1.2	3.7	1.0	1.8	1.5	1.4
0	2100	920	1050	2380			
−606	0.15						
−992	0.13						

A. Carrelli and J. J. Went, Zeits. f. Physik **76**, 236 (1932).
J. T. Dhar, Ind. J. Phys. **9**, 189 (1934).
A. V. Rao, Zeits. f. Physik **97**, 154 (1935).
W. R. Angus, C. K. Ingold, and A. H. Leckie, J. Chem. Soc. 925 (1936).
A. W. Reitz, Zeits. f. physik. Chemie **B38**, 275 (1937).
M. Kowalewska, Acta Phys. Polonica **7**, 279 (1938).
J. Wagner, Zeits. f. physik. Chemie **B45**, 88 (1939).
B. P. Rao, Proc. Ind. Acad. Sci. **A11**, 1 (1940).
K. W. F. Kohlrausch, *Ramanspektren* (1943) p. 359.
K. Venkateswarlu, Proc. Ind. Acad. Sci. **A21**, 126 (1945).
M. Wolkenstein and M. Eliashevich, Acta Physicochimica (URSS) **20**, 525 (1945).

TABLE II. Relative intensities of the Raman lines of $CHCl_3$ from eight recorded spectrograms.

$\Delta\tilde{\nu}$	Relative intensity No. 1	2	3	4	5	6	7	8	Average	Average deviation		Maximum deviation
3019	29	29	29	29	30	—	—	—	29±0.1	0.2	or 1%	1
1216	15	14	14	14	13	—	12	—	14±0.3	0.7	5	2
762	41	44	44	42	45	—	46	48	44±0.7	1.7	4	4
667	70	71	75	79	76	73	70	78	75±1.1	3.0	4	5
366	71	76	79	78	77	78	68	77	75±1.0	2.7	4	7
261				100					100±	—	—	—
0	235×10^2	253	276	271	264	—	240	234	253±6	15	6	19
−261	32	36	—	36	35	28	32	31	33±0.9	2.4	7	5
−366	12	16	—	17	18	15	15	11	15±0.7	1.9	13	4
−667	4	4	—	4	4	—	—	—	4±0	0	0	0
−762	3	2	—	1	2	—	—	—	2±0.3	0.5	25	1

intensities are tabulated in Table I, together with values found in the literature. In each case the intensity of the strongest line was arbitrarily fixed at 10. The frequency values of Kohlrausch[9] are used throughout, and a negative sign indicates an anti-Stokes line. The intensities of Rayleigh scattering are also indicated in the table; they are, however, subject to error as a result of wall reflections and scattering from dust particles. All the intensity values tabulated have been corrected for the spectral response of the photo-cathode according to the data of Dieke and Crosswhite.[10]

The accuracy of the measurement is indicated in Table II from the data of eight runs on $CHCl_3$. The average deviation for a single recording is ±5 percent, disregarding very weak lines. The main source of deviation is believed to be variation of the intensity of the source during the run. Further improvement may be obtained by the use of a stabilized power supply for the mercury vapor lamps.

Three runs on CCl_4 with excitation by Hg λ4047A were carried out; water instead of the regular filter solution was circulated through the filter jacket. The relative intensities found are as follows:

$\Delta\tilde{\nu}$	Relative intensity
791,762	3.7
459	10.0
313	8.3
217	8.7

The reason for the alternation in the relative intensities of $\Delta\tilde{\nu}$ 217 and 313 lines as compared to those observed by 4358A excitation is not immediately obvious.

The validity of the Placzek relation for the ratio of the intensities of anti-Stokes to Stokes lines

$$\frac{I_{AS}}{I_S}=\left(\frac{\tilde{\nu}+\Delta\tilde{\nu}}{\tilde{\nu}-\Delta\tilde{\nu}}\right)^4\exp\left(-\frac{hc}{kT}\Delta\tilde{\nu}\right),$$

when the excitation frequency ν is remote from the absorption frequency of the molecule, has been demonstrated previously[11–13] for several cases. The ratios resulting from the intensity values here presented are given in Table III, and are in excellent agreement with the calculated values. The temperature of the liquid was held at 30°C by the circulating filter solution.

TABLE III. Ratio of the intensities of the anti-Stokes to Stokes lines at 30°C.

Substance	$\Delta\tilde{\nu}$	I_{AS}/I_S obs.	calc.
CCl_4	217	0.39	0.385
	313	0.26	0.252
	459	0.12	0.118
$CHCl_3$	261	0.33	0.317
	366	0.20	0.200
	667	0.05	0.053
	762	0.05	0.035
CH_2Cl_2	283	0.28	0.288
	700	0.05	0.046
C_6H_6	606	0.11	0.066
	992	0.01	0.013

[9] K. W. F. Kohlrausch, *Raman Spektren* (Akademische Verlag, Leipzig, 1943), Edwards Bros. lithographic reprint.
[10] G. H. Dieke and H. M. Crosswhite, J. Opt. Soc. Am. 35, 476 (1945).
[11] L. S. Orstein and J. Rekveld, Phys. Rev. **34**, 720 (1929).
[12] S. C. Sirkar, Ind. J. Phys. **6**, 295 (1931).
[13] K. Venkateswarlu, Proc. Ind. Acad. Sci. **A19**, 111 (1944).

REMARKS

Assuming that the polarizability constants of a molecule can be considered as additive bond properties, as demonstrated by Denbigh[14] and assumed in the theory of Wolkenstein,[1] we can evaluate the change of polarizability at the equilibrium inter-atomic distance of the bond caused by the valence vibration of a symmetrical molecule from the intensity of the Raman line of symmetric vibration relative to that of Rayleigh line by the relation,[15]

$$\alpha_{A-B}'^2 = \alpha_{A-B}^2 \left(\frac{\tilde{\nu}}{\tilde{\nu}-\Delta\tilde{\nu}}\right)^4 \frac{I_R}{I_0} \frac{\rho RT\beta}{M} \frac{8\pi^2\mu\Delta\tilde{\nu}c}{h},$$

where α_{A-B} and α_{A-B}' are the bond polarizability and the change of polarizability $(\partial\alpha/\partial r)_{r_0}$ of the bond $A-B$, respectively, μ is the mass of the atom under symmetric vibration, and I_R/I_0 is the ratio of the intensities of Raman to Rayleigh line. The factor $\rho RT\beta/M$, in which ρ is the density, M the molecular weight, and β the isothermal compressibility of the substance, is introduced to compensate for the change of Rayleigh scattering power from the liquid to the gaseous state.[16] The result of such calculations for the case of the valence vibrations of the C−Cl bond in CCl_4 and the C−H bond in C_6H_6 is as follows:

Bond	C−Cl in CCl_4	C−H in C_6H_6	
Bond polarizability,[14] α	2.61	0.65	$\times 10^{-24}$ cc
$\alpha' = (\partial\alpha/\partial r)_{r_0}$	1.2	0.14	$\times 10^{-24}$ cc/A
Bond distance,[17] r_0	1.76	1.08	A

The compressibility data of Freyer *et al.*[18] were used in the calculation.

The lowest primary photo-current from the photo-multiplier cathode measurable by the apparatus here described is limited to *ca* 10^{-16} ampere by the fluctuations in the dark current. In the measurement of the depolarization factors of Raman lines with a more ideal set-up than one employed by Rank *et al.*,[3] the light intensity encountered would be several times weaker. A liquid air cooled photo-multiplier tube with an appropriately modified amplifier system is being tried in this laboratory.

ACKNOWLEDGMENT

One of us (J.Y.C.) wishes to express his thanks to China Institute in America, New York, for a scholarship.

[14] K. G. Denbigh, Trans. Faraday Soc. **36**, 936 (1940).
[15] R. P. Bell, Trans. Faraday Soc. **38**, 422 (1942).
[16] S. Bhagavantam, *Scattering of Light and the Raman Effect* (Chemical Publishing Company, Inc., New York, 1942) Chapter V.
[17] L. Pauling, *The Nature of Chemical Bond* (Cornell University Press, Ithaca, New York, 1940), second edition, pp. 164, 168.
[18] E. B. Freyer, J. C. Hubbard, and D. H. Andrews, J. Am. Chem. Soc. **51**, 759 (1929).

A Potentiometric Secular Equation Computer*

ARTHUR A. FROST AND MILTON TAMRES
Department of Chemistry, Northwestern University, Evanston, Illinois

(Received March 17, 1947)

An electrical computer for solving secular equations is described. The technique makes use of the linear equations from which the secular equation is derived. Each of the linear equations is successively represented by a potentiometric circuit. A series of successive approximations is carried out to arrive at the desired solutions.

INTRODUCTION

SECULAR equations make their appearance both in connection with the electronic and vibrational energies of molecules. With respect to electronic energy, the secular equation results from the use of the linear variation method for getting approximate electronic wave functions. Resonance energy calculations represent a particular case of this. With respect to vibrational energy, the secular equation is involved in the classical determination of the normal modes of vibration and fundamental vibration frequencies of a polyatomic molecule.

The manual labor involved in solving secular equations has prompted several investigators to seek time saving devices that yield solutions with a fair degree of accuracy. Several mechanical devices have been designed for the determination of vibration frequencies of molecules.[1-3] Weights and springs are interconnected to represent either directly or indirectly the vibrating molecule. More recently an electrical network analyzer has been adapted for this purpose.[4] Inductance and capacitances represent masses and force constants. The resonant frequencies of the electrical circuit then correspond to those of the molecular vibration. An electrical device has the advantage over its mechanical counterpart in being easier to interconnect for a complicated situation and easier to measure for the result.

A secular equation always has associated with it a set of simultaneous linear equations, the solution of which is equivalent to the solution of the secular equation. These linear equations are homogeneous. For the closely related problem of solving non-homogeneous simultaneous linear equations, various mechanical and electrical calculators have been constructed.[5-8] These electrical calculators have been useful in treating infra-red and mass spectrometry data in analytical work. However, they are not well adapted for the present purpose since for each different value of the energy or frequency most all of the coefficients would need to be reset. The calculator to be described is of this same type but with the incorporation into the circuits of a pair of potentiometers which takes care of the various energy or frequency values.

MATHEMATICAL CONSIDERATIONS

The secular equation in its most general form may be written:

$$\begin{vmatrix} H_{11}-ED_{11} & H_{12}-ED_{12} & \cdots & H_{1n}-ED_{1n} \\ H_{21}-ED_{21} & H_{22}-ED_{22} & \cdots & H_{2n}-ED_{2n} \\ \cdot & \cdot & \cdots & \cdot \\ H_{n1}-ED_{n1} & H_{n2}-ED_{n2} & \cdots & H_{nn}-ED_{nn} \end{vmatrix} = 0, \quad (1)$$

where in the quantum mechanical linear variation function problem the H_{ij} are matrix components of the Hamiltonian operator, the D_{ij} are matrix components of unity, and E is the energy. There will be n corresponding rows and columns if there are n functions in the linear variation, and there will result n values of the parameter E. In the molecular vibration problem the H_{ij} are

* Presented at the Second Annual Technical Conference of the Chicago Section of the American Chemical Society, January 24, 1947.

[1] C. F. Kettering, L. W. Shutts, and D. H. Andrews, Phys. Rev. **36**, 531 (1930).

[2] D. H. Andrews and J. W. Murray, J. Chem. Phys. **2**, 634 (1934).

[3] D. P. MacDougall and E. B. Wilson, Jr., J. Chem. Phys. **5**, 940 (1937).

[4] G. Kron, J. Chem. Phys. **14**, 19, (1946); G. K. Carter and G. Kron, J. Chem. Phys. **14**, 32 (1946); R. H. Hughes and E. B. Wilson, Jr., Rev. Sci. Inst. **18**, 103 (1947).

[5] J. B. Wilbur, J. Frank. Inst. **222**, 715 (1936).

[6] T. D. Morgan and F. W. Crawford, Oil Gas J. **43**, 100-105 (August 26, 1944).

[7] C. E. Berry, D. E. Wilcox, S. M. Rock, and H. W. Washburn, J. App. Phys. **17**, 262 (1946).

[8] C. C. Eaglesfield, J. App. Phys. **17**, 1125 (1946).

coefficients in the quadratic form expressing the potential energy in terms of coordinates, the D_{ij} are coefficients in the quadratic form for the kinetic energy in terms of velocities, and E equals $4\pi^2\nu^2$ where ν takes on the n values of the fundamental vibration frequency.

Associated with the secular Eq. (1) is a set of n homogeneous simultaneous linear equations:

$$\begin{aligned}
&(H_{11}-ED_{11})C_1+(H_{12}-ED_{12})C_2+\cdots \\
&\qquad\qquad +(H_{1n}-ED_{1n})C_n=0, \\
&(H_{21}-ED_{21})C_1+(H_{22}-ED_{22})C_2+\cdots \\
&\qquad\qquad +(H_{2n}-ED_{2n})C_n=0, \qquad (2)\\
&\cdots\cdots\cdots\cdots\cdots \\
&(H_{n1}-ED_{n1})C_1+(H_{n2}-ED_{n2})C_2+\cdots \\
&\qquad\qquad +(H_{nn}-ED_{nn})C_n=0.
\end{aligned}$$

This set of equations has a non-trivial solution only if the determinant of the coefficients of the variables is zero. The secular equation states just this condition. Solution of Eqs. (2) is, therefore, equivalent to solution of the secular equation, but goes further in giving relative values of the variables, C_i, which in the linear variation method are the coefficients of the wave functions and in the vibration problem give the form of the normal modes of vibration.

Solution of the linear Eqs. (2) can be carried out by a series of successive approximations such as are used in solving non-homogeneous linear equations.[6,7] This procedure is similar to the relaxation method of Southwell.[9]

If one of the correct values for E is placed in Eqs. (2) these equations become dependent so that only $n-1$ C_i's can be determined, and these only relative to the nth C_i. The n equations can then be considered as equations in $n-1$ C_i variables and the energy parameter E as the nth variable. The method then consists in first fixing one of the C_i's, say C_1, at some arbitrary convenient value. E is given an arbitrary value somewhere in the neighborhood of a value expected as a solution. The first equation is then solved for C_2; all other C_i's except C_1 and C_2 are zero unless previous information as to their probable values is at hand. Using this value of C_2 and the same values of C_1 and E, the second equation is then solved for C_3. This is continued through the sequence of C_i's, thus obtaining a value of C_n from the $n-1$st equation. The nth equation is then used to solve for a better value of E. This cycle of operations is repeated a few times until further changes in the E and C_i's are within the desired error, these final values then constituting a solution. By starting with appropriately chosen E's, the procedure will converge to the various characteristic values of E and the corresponding C_i's.

[9] R. V. Southwell, *Relaxation Methods in Engineering Science* (Oxford Univ. Press, Cambridge, England, 1940).

ELECTRICAL CIRCUIT

Consider the linear Eqs. (2) in the form:

$$\begin{aligned}
&H_{11}C_1+H_{12}C_2+\cdots+H_{1n}C_n \\
&\qquad =E(D_{11}C_1+D_{12}C_2+\cdots+D_{1n}C_n), \\
&\cdots\cdots\cdots\cdots\cdots \qquad (3)\\
&H_{n1}C_1+H_{n2}C_2+\cdots+H_{nn}C_n \\
&\qquad =E(D_{n1}C_1+D_{n2}C_2+\cdots+D_{nn}C_n).
\end{aligned}$$

The left-hand side may be represented electrically in the manner described by Berry, Wilcox, Rock, and Washburn.[7] A single product term, such as $H_{11}C_1$, is obtained by setting a potentiometer to represent the value of one factor, the voltage tapped off being applied to a second potentiometer which is set to the other factor. The potential from the second potentiometer is then proportional to the product of the two factors. The summation of terms is obtained by connecting the potentials representing products through a set of "addition resistors" to a common point. This common point has then a potential which is the average of the several product potentials and is, therefore, proportional to their sum.

The right-hand side of an equation of set (3) differs in form from the left-hand side by having multiplication by E. This is accomplished by having an extra addition resistor, in the form of a potentiometer, which is connected to ground potential and with a sliding contact to tap off a fraction E of the average potential representing the sum of terms.

When the equation is satisfied the two potentials representing the right and left sides, respectively, will be equal. This situation may be determined with the aid of any null detector commonly used in potentiometric work.

In any given problem the setting of the potentiometers representing the H_{ij}'s and D_{ij}'s may result in a value of E beyond the range of the E

potentiometer. To take care of this possibility the equations are considered in the form (4):

$$\begin{aligned} &A(H_{11}C_1+H_{12}C_2+\cdots+H_{1n}C_n) \\ &\qquad =B(D_{11}C_1+D_{12}C_2+\cdots+D_{1n}C_n), \\ &\cdots\cdots\cdots\cdots\cdots\cdots \\ &A(H_{n1}C_1+H_{n2}C_2+\cdots+H_{nn}C_n) \\ &\qquad =B(D_{n1}C_1+D_{n2}C_2+\cdots+D_{nn}C_n). \end{aligned} \tag{4}$$

The sides of each equation are now symmetrical and are represented electrically in the same manner as the right side of an equation of set (3). E is obviously the ratio B/A. The full positive range of E may be obtained in two steps. If A is set to its maximum value (considered as unity), B will be equal to E and will cover the range from 0 to 1 (on an arbitrary scale). If B is set to unity, the various values of A from 1 to 0 will correspond to E varying from 1 to infinity. In practice, to avoid confusion, A and B potentiometers are labeled $1/E$ and E, respectively, it being understood that the potentiometer not being varied must be kept at its maximum setting.

The calculator as actually constructed is shown in Fig. 1. It will handle up to six linear equations or a sixth degree secular equation. Figure 2 shows the circuit for the case of two equations with two variables. The extension to more equations is apparent. The calculator involves a bank of seventy-two 100-ohm wire-wound radio volume controls for the H's and D's, thirty-six for each. There are six 100-ohm potentiometers to represent the six C's in a given equation. A reversing switch for each C potentiometer allows for plus and minus signs for the C's. The addition resistors, R, are each approximately 100,000 ohms and are carefully matched to each other by taking series pairs of properly chosen 50,000-ohm resistors. The E potentiometers (E and $1/E$) are 100,000 ohms and are not necessarily matched to the addition resistors but must be matched to each other.

A twelve-pole six-position gang switch, serving as an *Equation Selector*, permits switching any particular set of six H's and six D's of a given equation to the addition resistors. A four-pole two-position gang switch, as a *Function Selector*, serves to connect the *Null Detector* either for balancing an equation or for connecting it together with a *Standard Potentiometer* for the

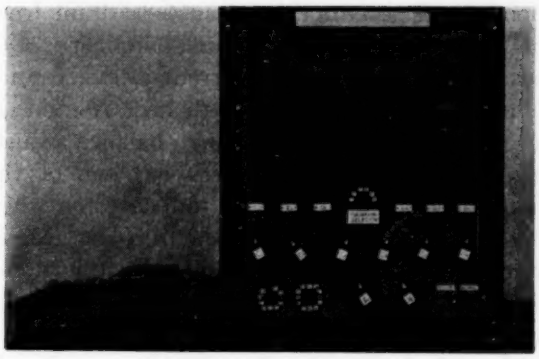

FIG. 1. Secular equation computer.

purpose of measuring final values of C's and E or $1/E$ of a solution or for setting the original values of the H's and D's. A one-pole ten-position gang switch serving as a *CE Selector* connects the standard potentiometer and detector (when the function selector is set at "standard") to any of the six C potentiometers or two E potentiometers for the purpose of measuring each individually. This selector also has a contact connected to ground to make possible a check on the balance between positive and negative sides of the power source, and a contact marked "$H-D$" to connect the *HD Selector*. This H and D selector is a one-pole twelve-position gang switch which with the aid of the equation selector makes it possible to set or measure any one of the seventy-two H_{ij}'s or D_{ij}'s.

All circuit elements are mounted on the panel illustrated except the power source, null detector, and standard potentiometer. The circuit was designed for either a.c. or d.c. operation but so far only d.c. has been used. The power source consists of two 2-volt storage cells of large capacity connected in series, the common connection being taken as zero potential. On both the $+2$ v and -2 v sides are placed rheostats to allow for making the magnitude of the voltage on both sides of zero identical. As the C potentiometers are varied or the signs are reversed, there will be differences in the current drained from the battery and the zero may shift with respect to the midpoint between the two extreme potentials. This variation is partially compensated by introducing fixed 100-ohm resistors, C', at the sign switches to cause a current drain from one cell when the corre-

sponding C potentiometer causes a drain from the other cell. This will not take care of a variable drain caused by current drawn from a C potentiometer by its attached H and D potentiometers. A complete zero balance adjustment is accomplished by varying one of the rheostats so as to balance the null detector, when the CE selector is set on the zero or ground contact mentioned above. This adjustment can be made conveniently once in each cycle of the successive approximations.

The null detector is a box-type lamp and scale galvanometer, and the standard potentiometer is a slide wire accurate to 0.1 percent. It should be noticed that the standard potentiometer and an equal series resistance are connected directly across the total voltage supplied to the C potentiometers. A zero setting on the potentiometer then corresponds exactly to the midpoint between the two extreme potentials and the full-scale setting is exactly equal to the maximum positive potential applied to the C's. There is, therefore, no need to standardize the potential measurement since relative values are sufficient.

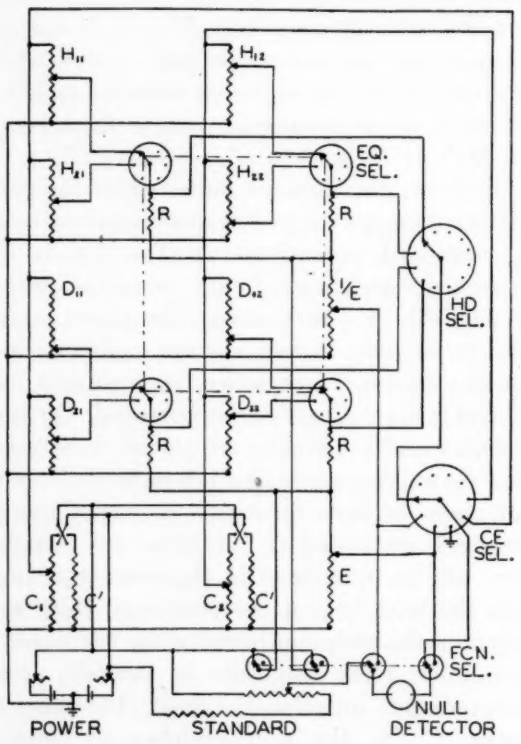

FIG. 2. Circuit diagram of the secular equation computer.

OPERATIONAL ROUTINE

1. *Arrange the mathematical problem in a form convenient for the calculator.* Since the scale on the measuring potentiometer runs from 0 to 1000 and the full-scale reading on the various component potentiometers matches a full-scale setting of the measuring potentiometer, the units for expressing the H's and D's are conveniently chosen so the maximum H_{ij} and the maximum D_{ij} are 1000 or shortly under.

2. *Set each of the H and D potentiometers to their appropriate values.* To do this, have the function selector on "Standard," the sign switches on "+," and the C potentiometers at their maximum values. With the CE selector on "zero" and the standard set to 0, adjust the balancing rheostat at the power source. This zero balance would be expected to remain the same during setting of the H's and D's, but should be occasionally checked as a precaution. Now set the CE selector to "$H-D$," the equation selector to the first equation, and the HD selector to H_1. With the standard set to the numerical value for H_{11}, adjust the H_{11} potentiometer to balance as shown by the null detector. Next with the HD selector set to H_2, the H_{12} potentiometer may be set, etc.

3. *Set the E or 1/E potentiometer to an assumed approximate value.* The function selector gang switch on the "Standard" position connects the maximum positive voltage across the E and $1/E$ potentiometers so that here again full-scale on these correspond to full-scale on the standard. However, for this purpose it is preferable to divide the standard reading by 1000 to make the maximum value unity. The CE selector is set on "E" or "$1/E$" and the corresponding potentiometer balanced.

4. *Proceed to balance the equations successively until all are balanced simultaneously.* A typical step in this procedure would be carried out as follows. The function selector is set on "Balance." Any one C or E potentiometer is varied to balance a given equation chosen by the equation selector. The settings of the CE and HD selectors and the standard potentiometer are immaterial during this operation, but since the zero must be checked occasionally it saves time to have the CE selector on "Zero" and the standard set to 0

so that by merely flipping the function selector to "Standard" the zeroing rheostat may be adjusted to balance. In balancing a given equation a particular C potentiometer might be required to go beyond its range. If it must go through zero the corresponding sign switch is flipped. If a value beyond the maximum is required, that particular potentiometer is left at maximum setting and other C's are later reduced in value. "Cut-and-try" methods are useful in obtaining rapid convergence to a solution. It may turn out that changing a given potentiometer either more or less than that corresponding to balance is preferable to an exact balance. The order of balancing of the equations may be varied at will. Also it is unnecessary to vary one particular variable in balancing a particular equation. The only requirement is that at the end of the successive approximations all equations are balanced simultaneously within the error inherent in the problem or in the calculator.

5. *Read the values of the C's and E which constitute the solution.* This is done with the standard potentiometer. The function selector is set on "Standard" and the CE selector is set on "E" and "$1/E$" to determine these. To measure the C's first throw all sign switches to the positive direction after recording which are negative. The zero must be readjusted. Then each of the C's are read by setting the CE selector to the appropriate C and setting the standard potentiometer to obtain a null.

6. *Search for other solutions, if desired.* The solutions for maximum and minimum values of E are most easily obtained. Solutions for intermediate E's are obtained quickly if reasonably good initial values of E and the C's are used. A more definite procedure to follow is to solve secular equations of successively increasing degree from the second degree up to the maximum. This involves no change in the settings of the H's and D's, but merely keeping certain C's zero and disregarding a corresponding number of equations. Since the $n+1$ E values which are solutions for an $(n+1)$st degree secular equation are interleaved with the n roots of a preceding nth degree secular equation,[10] it is possible to make an estimate of the former from the latter.

[10] L. Pauling and E. B. Wilson, Jr., *Introduction to Quantum Mechanics* (McGraw-Hill Book Company, Inc., New York, 1935), p. 188.

TABLE I. Signs of matrix elements and of E.

	H	D	E	Operation
1	+	+	+	Set up directly
2	+	−	−	Reverse signs of D and E
3	−	+	−	Reverse signs of H and E
4	−	−	+	Reverse signs of H and D
5	+	+	−	Substitute for E to get type 1
6	+	−	+	Reverse signs to get type 5 and substitute for E
7	−	+	+	
8	−	−	−	

POSITIVE AND NEGATIVE SIGNS

In the design of the calculator there appears to be a limitation on the algebraic signs that can be used for the H's, D's, and E's. Although sign switches are provided for taking care of both positive and negative C's, no such provision is made for possible negative H's, D's, and E's, although with a more complicated circuit that would have been possible. As will be shown, however, the calculator can, in principle, handle all possible combinations of signs, but in practice certain combinations may be inconvenient.

Consider first the situations where all H's have like signs, all D's have like sign, and all E's have like sign. Eight possible combinations are shown in Table I. In the first four combinations the sign of an H_{ij} is the same as that of the corresponding product ED_{ij}. These cases can be handled by merely reversing the signs of certain pairs as indicated. The justification for this is that it amounts to no more than a possible change in sign of the secular determinant which is zero anyway. The E's obtained as solutions must be given the appropriate sign depending upon whether or not it was reversed in setting up the problem on the calculator. In the last four combinations in the table the sign of an H_{ij} is the opposite of the sign of the product ED_{ij}. The quantity $H_{ij}-ED_{ij}$ is then a sum of two positive numbers or a sum of two negative numbers. The circuit as designed will handle only differences rather than sums. However, the following algebraic substitution in the original secular equation will put the problem in a suitable form. Consider case 5 to which the last three can be transformed by reversal of signs. Now let $E=E'-E_0$ such

that E' is positive and variable, E_0 being a positive constant greater than the maximum absolute value of E. Then

$$H_{ij}-ED_{ij}=H_{ij}+E_0D_{ij}-E'D_{ij}=H_{ij}'-E'D_{ij}$$

where each $H_{ij}'=H_{ij}+E_0D_{ij}$ is calculated for an arbitrarily chosen $E_0\geq|E|_{\max}$ and then set on the secular equation calculator instead of the original H_{ij}. The terms are all now of type 1.

Secular equations having matrix components of mixed sign types 1 to 4 may require merely a change in sign of some rows and columns of the secular equation determinant. The corresponding C's would then come out with reversed signs. If this is not possible or convenient the following trick may be used. Any term of type 4 mixed with type 1 or of type 3 mixed with type 2 can be set up as for positive H and D, but when used in balancing a linear equation the corresponding C sign switch is reversed. This procedure requires care in changing the appropriate sign switches each time a new equation is switched into the circuit. Mixtures of sign types 5 to 8 are treated in the same way but with the preliminary substitution for $E=E'-E_0$ as above.

The most general type of mixture of signs may be handled as follows: Consider the four possibilities where E is positive. (E is the same throughout a given secular equation for a given solution. If E is negative a similar procedure applies.) Let $E=E'-E_0$ where again E' and E_0 are positive, but now $E'\geq E_0$. This substitution converts terms of type 6 and 7 into 4 and 1, respectively, if $E_0>|H_{ij}/D_{ij}|_{\max}$ where the maximum is for all terms of types 6 and 7. This substitution does not change the type of terms of types 1 and 4 and so gives a secular equation of only types 1 and 4 which can be handled by the method given in the preceding paragraph. If the maximum ratio $|H_{ij}/D_{ij}|$ is very large, there might be difficulty in getting accurate solutions. There is no need to worry about a zero D_{ij} causing an infinite ratio since such a term could be considered to be directly of type 1 or 4.

ACCURACY

Errors inherent in the electrical circuit include lack of ability to set the potentiometers precisely, loading effects on potentiometers, lack of perfect balance in the addition resistors, contact resistances, and lack of balance between positive and negative voltages from the power supply. The 1000-ohm radio volume controls used for the H's and D's have each about 300 turns of wire making it impossible to set a given value to better than 0.3 percent of the maximum. Helical potentiometers would be preferable, but were not considered for this application since part of the aim in building the calculator was to minimize expenditure consistent with reasonable accuracy. For the C potentiometers 0.3 percent precision in setting was not critical inasmuch as in problems of this type a given percent error in the C's will result in a somewhat smaller percent error in the E. The 100,000-ohm E potentiometer can be set to 0.1 percent.

There are large loading effects on the C potentiometers since the effective resistance of twelve 1000-ohm H and D potentiometers connected in parallel is 83 ohms, even smaller than the 100 ohms of the C potentiometer to which they are attached through the sliding contact. Current drain through the H's and D's causes a non-linearity in the setting of the C's but no difficulty arises since measurement of the actual potential is always made under the loaded condition. The loading effect on the H and D potentiometers is negligible, the current drain through a 100,000-ohm addition resistor affecting the potential at the sliding contact by less than 0.2 percent. The E potentiometers have no load when balance is obtained.

The addition resistors were matched to within a maximum deviation from the mean of less than 0.2 percent, and the two E potentiometers were found to check within 0.1 percent. Possible error caused by lack of balance of positive and negative voltages has been eliminated by the zero adjustment described earlier. No difficulties with contact resistances have been encountered.

The error in the final solution is expected to be of the order of 0.5 percent of the full scale reading for the E or $1/E$ and at best 1 percent of the maximum value for each C. Perhaps the best way of indicating accuracy of solution is to compare solutions obtained with the calculator with those already known for a given secular equation. Such an example is the following.

AN EXAMPLE

The example chosen for illustration is that of the determination of resonance among the two Kekulé and three Dewar structures of benzene.[11,12]

Although this fifth degree secular equation is easily reduced through considerations of symmetry to a product of three first degree and one second degree equation, it is used here in its unreduced form as a test of the calculator since the solutions are accurately known.

The secular equation as set up by Pauling and Wheland may be written in simpler form by dividing the equation by $(3\alpha/2)^5$ and defining a new parameter, $E=-(Q-W)/(3\alpha/2)$, where W is the energy, Q the coulombic integral, and α the exchange integral. The result is:

$$\begin{vmatrix} 1-E & 1-E/4 & 1-E/2 & 1-E/2 & 1-E/2 \\ 1-E/4 & 1-E & 1-E/2 & 1-E/2 & 1-E/2 \\ 1-E/2 & 1-E/2 & -E & 1-E/4 & 1-E/4 \\ 1-E/2 & 1-E/2 & 1-E/4 & -E & 1-E/4 \\ 1-E/2 & 1-E/2 & 1-E/4 & 1-E/4 & -E \end{vmatrix} = 0.$$

This equation appears to be in suitable arrangement for the calculator, the H_{ij}'s and D_{ij}'s being all positive and having maximum values of unity. However, it is known that the correct solutions are $E=2/3[(13)^{\frac{1}{2}}-1]$, 0, $-4/3$, $-4/3$, $-2/3[(13)^{\frac{1}{2}}+1]$. Only the positive solutions would be found if the problem were set up on the calculator in this form. By substituting $E=4-4E'$ and dividing each row of the secular equations by -4 the resulting equation is such that

$$\|H_{ij}\| = \begin{bmatrix} 3/4 & 0 & 1/4 & 1/4 & 1/4 \\ 0 & 3/4 & 1/4 & 1/4 & 1/4 \\ 1/4 & 1/4 & 1 & 0 & 0 \\ 1/4 & 1/4 & 0 & 1 & 0 \\ 1/4 & 1/4 & 0 & 0 & 1 \end{bmatrix},$$

$$\|D_{ij}\| = \begin{bmatrix} 1 & 1/4 & 1/2 & 1/2 & 1/2 \\ 1/4 & 1 & 1/2 & 1/2 & 1/2 \\ 1/2 & 1/2 & 1 & 1/4 & 1/4 \\ 1/2 & 1/2 & 1/4 & 1 & 1/4 \\ 1/2 & 1/2 & 1/4 & 1/4 & 1 \end{bmatrix}.$$

[11] L. Pauling and G. W. Wheland, J. Chem. Phys. **1**, 362 (1933).

[12] H. Eyring, J. Walter, and G. E. Kimball, *Quantum Chemistry* (John Wiley and Sons, Inc., New York, 1944), pp. 249–254.

TABLE II.

	E	C_1	C_2	C_3	C_4	C_5
Correct	0.5658	(1000)*	1000	434	434	434
Calc.	0.560	1000	1000	407	411	422
Correct	1.0000	(1000)	−1000	0	0	0
Calc.	1.00	1000	−1000	0	0	0
Correct	1.3333	0	0	(754)	−754	0
Calc.	1.32	0	0	754	−755	0
Correct	1.3333	0	0	(650)	(−908)	258
Calc.	1.325	0	0	650	−908	255
Correct	1.7676	(1000)	1000	−768	−768	−768
Calc.	1.76	1000	1000	−782	−750	−762

* Parentheses indicate C values arbitrarily chosen equal to the value on the computer.

All E' values are positive. Table II shows values of E' and the C's as found by the calculator as compared with those obtained algebraically.

The third and fourth solutions constitute a twofold degeneracy. Since in such a case any linear combination of the wave functions also is a solution with the same energy, it is obvious that any number of different sets of C's could have been found. The two sets of C's shown in the table were obtained using previous knowledge that certain C's could be set equal to zero.

The accuracy of the calculations is about that expected.

COMPARISON OF CALCULATORS

The only other calculator particularly adapted to secular equations is the network analyzer which has, in principle, the advantage that the solutions are obtained directly rather than through successive approximations. Such an advantage is of minor importance since the time required to obtain convergence to a solution using the potentiometer computer is somewhat smaller than the time required to set up the problem. To set all seventy-two H's and D's for a given secular equation takes less than an hour. To obtain a particular solution then takes only a few minutes in most cases.

A serious limitation of the network analyzer is that there can be no off-diagonal D_{ij}'s. The potentiometric computer will handle any case of non-orthogonality and also problems with assymmetrical H_{ij} and D_{ij} matrices should they be of

any interest. The setting of a given H_{ij} in the potentiometric computer, which involves merely adjusting a potentiometer, is much simpler than connecting together several standardized condensers or coils as in the network analyzer.

The potentiometric secular equation computer can also solve non-homogeneous linear equations by setting the E and $1/E$ potentiometers at unity, using H_{ij}'s to represent positive matrix components and D_{ij}'s to represent negative matrix components, and keeping one C_i at unity, the corresponding H's and D's representing the constant terms in the equations.

This investigation was supported by a grant from the Abbott Fund of Northwestern University.

THE JOURNAL OF CHEMICAL PHYSICS VOLUME 15, NUMBER 6 JUNE, 1947

Multilayer Gas Adsorption on Composite Surfaces

W. G. McMILLAN*
Institute for Nuclear Studies, University of Chicago, Chicago, Illinois
(February 19, 1947)

The equation of Brunauer, Emmett, and Teller (BET) for the adsorption of a gas on a free plane homogeneous surface is extended to the case of a mixture of two such surfaces, in an attempt to explain the observed deviations below one monolayer. The resulting equation may be greatly simplified for the case that the adsorption energy parameter, c, for each component surface, is large with respect to unity, as is usually the case in low temperature adsorptions of nitrogen, argon, etc. This approximate form of the equation is applied to the nitrogen isotherm on an inorganic salt and gives substantially better agreement with experiment than does the simple BET equation. The region of agreement between the experimental and BET isotherms is discussed on the basis of a two-component surface, and conditions are given under which one might obtain *two* distinct regions of the isotherm which are fitted by the BET equation by the use of two sets of parameters. It is suggested that it is the lower of these two regions which gives rise to the occasionally observed "saturation adsorption" values corresponding to only small fractions of a monolayer.

INTRODUCTION

FOR gas adsorption in the range below about 0.8 monolayer it is commonly observed that the theoretical isotherm of Brunauer, Emmett, and Teller[1,2] (BET) for a free plane homogeneous surface, based on the rectilinear plot fitting best in the neighborhood of one monolayer, predicts too low an adsorption. A typical example of this behavior is shown in Fig. 1 for the nitrogen adsorption isotherm at 78°K on an inorganic salt; Fig. 2 gives the corresponding rectilinear plot. The departure from the theoretical curve is usually attributed[3] to an inhomogeneity of the surface, which leads to preferential adsorption on those areas which have high energies of adsorption, and which therefore justly belong to higher values of the energy parameter,[4] c, than that given by the best fit near one monolayer—i.e., on the more "uniform" part of the surface. Most calorimetric data[3,5] for adsorptions below one monolayer lend support to this interpretation, as do also the abnormally large c values obtained, for example, by Armbruster[6] and co-workers at very low relative pressures in the low temperature adsorption of inert gases on metals.

If surface inhomogeneity is indeed responsible for these low adsorption discrepancies, it poses an

* Guggenheim Fellow, 1946–1947. Present address: Department of Chemistry, University of California, Los Angeles, California.

[1] S. Brunauer, P. H. Emmett, and E. Teller, J. Am. Chem. Soc. **60**, 309 (1938).

[2] An excellent review of the theory is contained in Brunauer's book, *The Adsorption of Gases and Vapors, Vol. I, Physical Adsorption* (Princeton University Press, Princeton, 1943), p. 151 *et seq.*

[3] Reference 2, pp. 158, 335.

[4] The energy parameter, c, is given by Brunauer, Emmett, and Teller as $c=\exp(E_1-E_L)/RT$, where E_1 and E_L are, respectively, the energy of adsorption into the first layer and the energy of liquefaction.

[5] See, for example, W. D. Harkins and G. E. Boyd, J. Am. Chem. Soc. **64**, 1145 (1942); W. D. Harkins and G. Jura *ibid.* **66**, 919 (1944), Fig. 8.

[6] M. H. Ambruster, J. Am. Chem. Soc. **64**, 2545 (1942); M. H. Armbruster and J. B. Austin, *ibid.* **66**, 159 (1944).

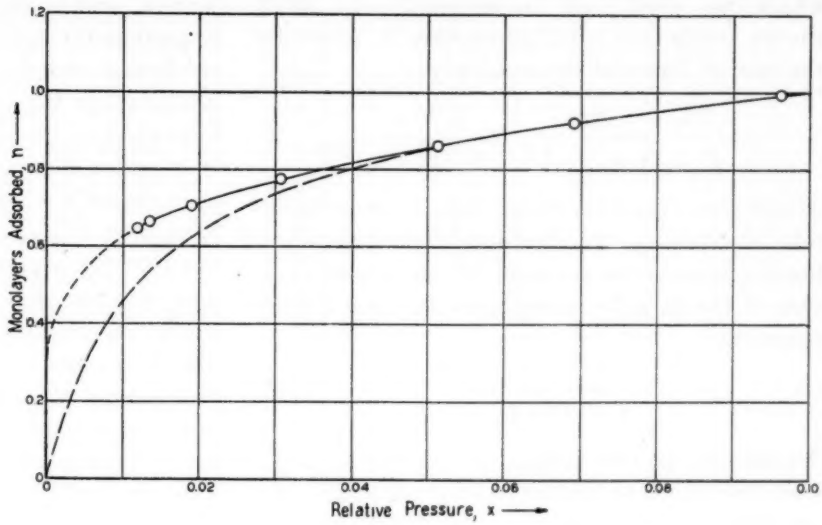

FIG. 1. Comparison between experimental (solid line) and theoretical BET (dashed line) isotherms in the low relative-pressure region in the adsorption of nitrogen on an inorganic salt. (For data see Table I.) The abscissa letter "n" should be replaced by "ν."

interesting question as to why the BET equation, derived on the assumption of uniformity of surface, fits the data even approximately. However, with inhomogeneous surfaces being the general rule, it is not surprising that for such definitely non-uniform substrates as promoted catalysts the BET plots are, by and large, rectilinear over as wide a range as for samples of high purity.

By directing attention to the discrepancies in the low relative pressure range there is no intention of minimizing the importance of those existing at higher pressures, which are generally larger in absolute magnitude though of the same order percentually. However, attempts to improve the theory in the higher range encounter difficulties which are probably unimportant at low relative pressures by virtue of the fact that here there is little multilayer adsorption, and the theoretical result is relatively independent of any inaccuracies[7] in the model of the adsorbed phase for large adsorptions. It thus appears fruitful to examine the low pressure discrepancies in the light of a somewhat generalized BET theory obtained without making any fundamental changes in the assumed mechanism of the adsorption process.

The rather evident generalization to be proposed, then, is to take account of the surface inhomogeneity, as specified by several sets of the surface parameters c_i, v_{mi}, and θ_i, where the first two have their usual meanings[4,8] and θ_i is the fraction of the total sample surface which is of type i:

$$\theta_i = v_{mi}/\Sigma v_{mj}, \quad \Sigma\theta_i = 1.$$

In itself, the assumption of surface inhomogeneity is not new, having been suggested originally by Langmuir[9] and applied to the Langmuir equation by Zeldowitsh,[10] who obtained the Freundlich isotherm in this way on the basis of a rather special distribution of the heat of adsorption over the surface. In the present treatment it will be assumed that the BET theory is correct for a perfectly uniform surface, and the discussion will be limited to the case of unrestricted adsorption on plane surfaces.

THE GENERAL TWO-COMPONENT SURFACE

The simplest type of heterogeneous surface for our purpose can be imagined to consist of a mechanical mixture of two solid components, perhaps in finely-divided form, but such that the faces of the ultimate crystallites of each component are plane surfaces whose adsorptive properties do not vary radically among the various crystal forms present. (The particles should, of course, be large enough that edge effects may be neglected.) For such a two-component surface—

[7] Cf. T. L. Hill, J. Chem. Phys. **14**, 263 (1946).

[8] v_m is the volume of gas (usually at S.T.P.) which corresponds to a complete closely packed monolayer.

[9] I. Langmuir, J. Am. Chem. Soc. **40**, 1371 (1918); cf. reference 2, pp. 77ff.

[10] J. Zeldowitsh, Acta Physicochimica (URSS) **1**, 961 (1934).

which we shall call "composite"—the BET theory predicts a total adsorption, v, given by the sum of terms of the usual type:

$$v=\frac{xv_m}{1-x}\left\{\frac{\theta_1 c_1}{1+(c_1-1)x}+\frac{\theta_2 c_2}{1+(c_2-1)x}\right\}, \quad (1)$$

wherein $v_m=v_{m1}+v_{m2}=\theta_1 v_m+\theta_2 v_m$, and x is the relative pressure, obtained by dividing the equilibrium adsorption pressure by the vapor pressure of the liquefied adsorbate. The usual BET equation,

$$v=\frac{xv_m}{1-x}\left\{\frac{c}{1+(c-1)x}\right\}, \quad (2)$$

determines the two surface parameters v_m and c from the region of linearity of the rectifying plot (cf. Fig. 2). Since for a given adsorbate v_m is essentially a geometric property of the surface, the value so obtained will be assumed to be correct, and is the one to be used in Eq. (1). Experimental deviations from Eq. (2) are thus attributed entirely to the inconstancy of c. If we substitute in Eq. (2) an isotherm relation of the form $v=f(x)$, c is implicitly defined as a function of x and will be written $c(x)$ to distinguish it from *the* BET *c constant* obtained from the rectifying plot. The plan will be to use Eq. (1) for the function $f(x)$ and to compare the behavior of the resulting function $c(x)$ with that obtained by employing the experimental isotherm for $f(x)$. This procedure is more convenient than a direct comparison of Eq. (1) with the experimental isotherm, since it gives a second-order correction to the first approximation, i.e., the BET equation, and will clearly show how $c(x)$ may be constant over a range[11] of x.

By inverting and rearranging Eqs. (1) and (2) we obtain:

$$\frac{xv_m}{v(1-x)}=\left[\frac{c(x)-1}{c(x)}\right]x+\frac{1}{c(x)} \quad (3)$$

$$=\left[\theta_1\left(\frac{c_1}{c_1-1}\right)+\theta_2\left(\frac{c_2}{c_2-1}\right)\right]^{-1}x+\frac{1}{c_0}\left\{1+\frac{\theta_1\theta_2 c_0\left(\frac{1}{c_2}-\frac{1}{c_1}\right)^2\left[\theta_1\left(\frac{c_2-1}{c_2}\right)+\theta_2\left(\frac{c_1-1}{c_1}\right)\right]^{-3}}{x+\frac{c_0}{c_1c_2}\left[\theta_1\left(\frac{c_2-1}{c_2}\right)+\theta_2\left(\frac{c_1-1}{c_1}\right)\right]^{-1}}\right\}^{-1}, \quad (4)$$

where

$$c_0=\frac{\left[\theta_1\left(\frac{c_1}{c_1-1}\right)+\theta_2\left(\frac{c_2}{c_2-1}\right)\right]^2}{\frac{\theta_1}{c_1}\left(\frac{c_1}{c_1-1}\right)^2+\frac{\theta_2}{c_2}\left(\frac{c_2}{c_2-1}\right)^2}. \quad (5)$$

Equation (4) follows exactly from Eq. (1) and is written in this form to display its similarity to Eq. (3). On equating the right sides of Eqs. (3) and (4) it will be possible to cancel the two terms linear in x for large values of $c(x)$, c_1, and c_2, where unity is negligible, and thereby obtain

$$c(x)=c_0\left[1+\frac{\theta_1\theta_2 c_0(1/c_2-1/c_1)^2}{x+c_0/c_1c_2}\right], \quad (6)$$

where the same approximation gives

$$c_0=(\theta_1/c_1+\theta_2/c_2)^{-1}. \quad (7)^{12}$$

In this connection it is noteworthy that for low temperature adsorptions of nitrogen, argon, carbon monoxide, etc., BET c constants much below 50 are seldom observed.

With the restriction to large c-values, both the expressions $\theta_1\theta_2 c_0(1/c_2-1/c_1)^2$ and c_0/c_1c_2 will be of the order of 10^{-2} or less. It may thus be seen qualitatively from Fig. 1 that Eq. (6) furnishes the correct type of behavior for $c(x)$ as calculated from Eq. (2), using the lower portion of the experimental isotherm: at large $x(\sim 0.2)$, $c(x)$ is essentially a constant, c_0, and

[11] We shall find no theoretical *upper* x-limit to the fit, since the BET theory has been assumed exact for each individual component at all x, and the surface heterogeneity introduces deviations only at small x; cf. Eq. (6).

[12] This expression is easily generalized to a larger number of component surfaces by considering the first *pair* as one component, then adding a third, and so on; thus,

$$\frac{1}{c'}=\left(\frac{\theta_0}{c_0}+\frac{\theta_3}{c_3}\right)=\left[\theta_0\left(\frac{\theta_1}{c_1}+\frac{\theta_2}{c_2}\right)+\frac{\theta_3}{c_3}\right]=\left(\frac{\theta_1'}{c_1}+\frac{\theta_2'}{c_2}+\frac{\theta_3'}{c_0}\right).$$

increases with decreasing x, corresponding to the increasing difference between the theoretical and experimental curves. The linearity of Eq. (4) and the constancy of $c(x)$ thus depend upon the value of the second term in brackets in Eq. (6). If c_1 and c_2 are both very high, this term is negligible with respect to unity and $c(x)$ becomes essentially c_0.

A conclusion which seems somewhat odd at first sight is that for given values of θ_2 and c_2, the larger the value of c_1, the less it affects the value of c_0 as given by Eq. (7). The reason for this is that for large c_1, the adsorption on this part of the surface (hereafter called "surface 1") is essentially complete at a very low value of x, so that the graphically-determined c constant deals only with changes in the adsorption on surface 2 and in the second and higher layers of surface 1 (which by hypothesis have the c constant unity).

The most interesting applications of these results arise when $c_1 \gg c_2$ (or *vice versa*), since if they are nearly equal Eq. (1) reduces to Eq. (2) almost identically. With this inequality, which will be assumed throughout the rest of the paper, we have from Eq. (7)

$$c_0 \approx c_2/\theta_2, \tag{8}$$

provided θ_2 is not much less than θ_1. A further result is that for values of $x \gg c_0/c_1c_2$ we would expect the quantity $[c(x)/c_0-1]x$ from Eq. (6) to be nearly constant. Then with the help of Eq. (8) we have

$$c_0[c(x)/c_0-1]x \approx \theta_1/\theta_2, \tag{9}$$

which permits the experimental evaluation of θ_1 and θ_2. Here $c(x)$ is to be obtained by substitution of the experimental isotherm into Eq. (2), as described earlier, and c_0 is essentially the BET c constant. Actually we later note a small difference between c_0 and c and also use an indirect method for calculating $[c(x)/c_0-1]x$.

THE LOWER LIMIT OF FIT OF THE BET EQUATION

Before turning to the experimental comparison it is perhaps appropriate to investigate the lower limit of fit of the BET equation for the case just considered. Emmett[13] has often emphasized the usefulness of the rule-of-thumb that, for low

[13] P. H. Emmett, J. Am. Chem. Soc. **68**, 1784 (1946); see also reference 2, p. 336.

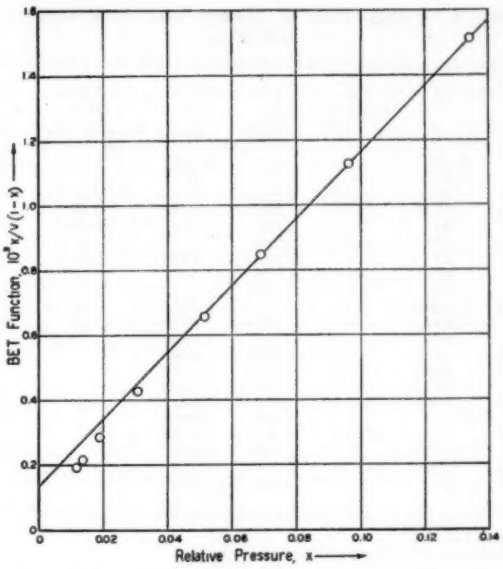

FIG. 2. BET rectilinear plot for nitrogen adsorption at 78°K on an inorganic salt. (For data see Table II.)

temperature adsorptions at least, the region of agreement is generally about $0.05 \leqslant x \leqslant 0.35$.[11] Intuitively, however, it would seem that these limits should be specified rather in terms of the number, $\nu = v/v_m$, of adsorbed layers, since this quantity is more directly related to the state of the adsorbed phase than is the relative pressure. In fact it is easily seen from Eq. (9) that the fractional deviation of $c(x)$ from c_0 is a function of the product (c_0x) rather than of x alone; we wish now to find its dependence on the amount adsorbed.

In order that Eq. (2) hold in a given range, it is necessary that throughout that range c be constant within some specified allowable deviation. To determine the order of magnitude of this variation, it must be translated into the variation in ν. For this purpose, the derivative of Eq. (2) gives the relation

$$d \ln \nu = [1-\nu(1-x)]d \ln c. \tag{10}$$

(Although we specifically permit small variations in c, it will not differ appreciably from the BET c constant and will be so treated in these order-of-magnitude calculations.) The quantity $\nu(1-x)$ is the fraction of the layer adjacent to the substrate which is completed (not to be confused with "the fraction of the surface covered by *exactly* one layer"). In other words, the quantity

TABLE I. Comparison of theory with experiment: the isotherm.

I p (mm)[a]	II x[a]	III v_{ads} (cc. STP)	IV ν_e (exp)[b]	V ν (BET)	VI $10^2x\cdot$ $[c(x)/c_0-1]$[b]	VII ν' (Eq. (23))
—	0.005	—	—	0.2912	—	0.5364
—	.01	—	—	.4552	—	.6104
9.1	.0118	61.58	0.6450	.5013	9.33†	.6320
10.4	.0135	63.34	.6634	.5330	9.54†	.6507
—	.015	—	(.687)	.5613	(10.39)	.6658
14.6	.0189	67.17	.7035	.6224	7.95†	.7008
—	.02	—	(.712)	.6364	(7.86)	.7098
—	.025	—	(.743)	.6929	(6.57)	.7462
—	.03	—	(.770)	.7373	(4.06)	.7766
23.6	.0306	73.87	.7737	.7431	5.06†	.7800
—	.04	—	(.817)	.8040	(3.00)	.8262
—	.05	—	(.856)	.8530	†Av. =8.0	.8659
39.6	.0513	82.17	.8606	.8605		.8705
53.3	.0690	87.79	.9195	.9212		.9249
—	.075	—	(.934)	.9385		.9409
74.4	.0964	94.75	.9924	.9921		.9910
—	.1	—	(1.000)	1.0002		.9993
103.6	.1342	102.61	1.0747	1.0700		1.0670
—	.15	—	(1.100)	1.0997		1.0965
149.6	.1938	112.39	1.1772	1.1799		1.1764
—	.2	—	(1.189)	1.1913		1.1878

[a] $p_0=772$ mm.
[b] Values in ( ) obtained by interpolation.

$[1-\nu(1-x)]$ is the fraction of the total surface which is uncovered; or in the BET notation, s_0/A, where A is the total surface area and s_0 the area covered by exactly zero layers. That this follows directly from the BET relations,[2]

$$s_1=cxs_0, \tag{11}$$

$$s_i=xs_{i-1} \quad (i>1), \tag{12}$$

$$s_i=cx^is_0 \quad (i\geq 1), \tag{13}$$

is shown by:

$$s_0/A=s_0\Big/\sum_{i=0}^{\infty}s_i=s_0\Big/s_0\Big(1+c\sum_{i=1}^{\infty}x^i\Big)$$

$$=(1-x)/[1+(c-1)x]$$

$$=1-\nu(1-x). \tag{14}$$

TABLE II. Comparison of theory with experiment: the BET rectifying plot.

x	$10^2x/\nu(1-x)$ Experimental	BET[a]
0.0118	0.194	0.251
.0135	.216	.269
.0189	.287	.325
.0306	.427	.446
.0513	.658	.659
.0690	.845	.843
.0964	1.126	1.126
.1342	1.511	1.517
.1938	2.139	2.133

[a] Calculated from the least-squares line, Eq. 18, based on the last five experimental points of this table

For values of c, say in excess of 20, this quantity, $[1-\nu(1-x)]$, will be less than 0.2 for all $\nu>0.85$, as is readily proved from Eqs. (11)–(13). Employing this result in Eq. (10), one sees that under these conditions a change of ± 10 percent in c is equivalent to ± 2 percent in ν, a reasonable figure for the agreement between theory and experiment. A variation in c outside this rather arbitrary permissible range of 20 percent will therefore determine the limit of fit.

We are now in a position to convert Eq. (6), or rather its approximate form, Eq. (9), into a form which depends primarily on the amount adsorbed. From Eq. (2) we have

$$(1/xc)=[\nu(1-x)]^{-1}-1. \tag{15}$$

This is seen to be just the ratio of uncovered to covered surface and again, for reasonably high c values, is less than 0.25 for all $\nu>0.85$. Since for the range in which we are interested $c\approx c_0$, use of Eq. (15) in (9) gives the fractional difference in $c(x)$ as

$$[c(x)/c_0-1]\approx\frac{\theta_1}{\theta_2}\left(\frac{1}{c_0x}\right) \tag{16}$$

$$\approx\frac{\theta_1}{\theta_2}\{[\nu(1-x)]^{-1}-1\}. \tag{17}$$

Now Emmett's value for the lower limit of fit at $x=0.05$ is obtained for samples with c (or c_0) ~ 100. By Eq. (16) this would give a 20 percent deviation in $c(x)$ from c_0 if $\theta_1\sim\theta_2$, and it is not unreasonable to expect that this latter condition might hold in a large fraction of the cases. If so, a large c constant implies a fit to very low values of x, and this has been the general rule in the experience of the writer. (Of course, we assume all along that $c_1\gg c_2$.) By Eq. (17), under the same condition that $\theta_1\sim\theta_2$, the lower limit of fit corresponding to a 20 percent deviation in $c(x)$ would be at about 0.9 monolayer. These figures are, of course, very dependent upon the ratio θ_1/θ_2, and it appears possible on the basis of the equations to obtain agreement with experiment to very low x, or low adsorptions, regardless of the magnitude of c, if the surface is highly uniform. Indications are, however, that such surfaces are most exceptional.

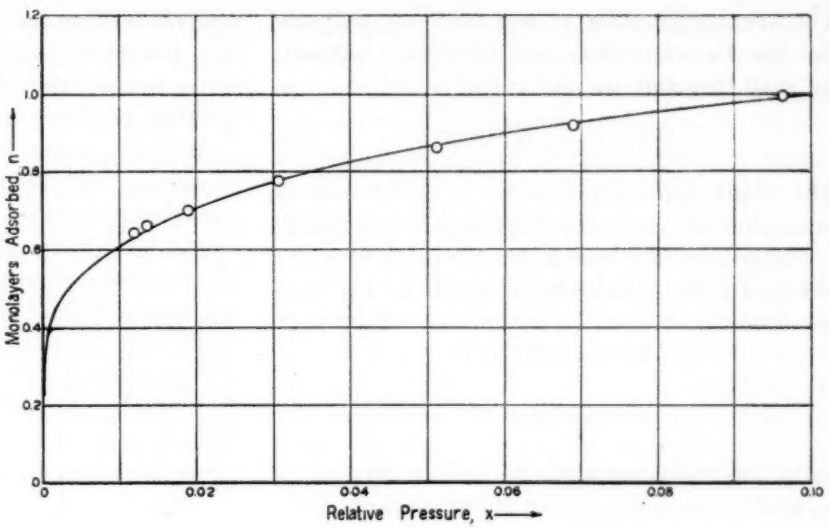

FIG. 3. Comparison between experimental points and theoretical isotherm (full line) based on extension of the BET theory to a two component surface. (For data see Table I.) The abscissa letter "n" should be replaced by "ν."

APPLICATION TO AN EXPERIMENTAL ISOTHERM

The data plotted in Figs. 1 and 2 are given in the first five columns of Table 1. The least-squares line, namely,

$$x/v(1-x)=10^{-2}(1.035x+0.0129), \quad (18)$$

through the last five points of Table II gives the BET constants: $v_m=95.47$, $c=81.2$. These have been employed in calculating the number of adsorbed layers experimentally observed (ν_e) and predicted by the BET theory (ν), listed respectively in columns IV and V of Table I. The last column contains the isotherm figures calculated on the basis of the two-component surface, as will be described presently.

The quantity $[c(x)/c_0-1]x$ of Eq. (9), tabulated in column VI, was calculated from the relation

$$[c(x)/c_0-1]x=\left(\frac{1}{\nu}-\frac{1}{\nu_e}\right)x\Big/\left(\frac{1}{\nu_e}-1+x\right). \quad (19)$$

This is derived from the two equations obtained from Eq. (2) on replacing c and ν ($=v/v_m$) first by c_0 and ν (the BET ν), and then by $c(x)$ and ν_e, and evidently involves the assumption that c_0 equals the BET c constant. While this is by no means exact (*v.i.*), it is sufficient for calculating in first approximation the difference between c and c_0. For greater accuracy one can use the value of c_0, so obtained, to calculate a more exact difference, and so on, although the rapid convergence of this process and the crudeness of the experimental data may not warrant the use of the higher approximations. The values obtained from Eq. (19) are evidently not very constant, since at low values of x the term (cf. Eq. (6)) c_0/c_1c_2 may be important, while at higher x values the small (and thus inaccurately estimated) difference between the experimental and BET curves introduces a large error; therefore, only those values were averaged which correspond to actual experimental points, the average being $[c(x)/c_0-1]x\approx 0.008$.

In order to obtain a better figure for c_0 we note that Eq. (9) now has the form

$$c(x)\approx c_0(1+0.008/x), \quad (20)$$

and hence the value of $c(x)$ exceeds c_0 by a quantity ranging from about 16 percent at $x=0.05$ to 4 percent at 0.2. Since the c constant ($=81.2$) obtained from the least-squares line, Eq. (18), is presumably an average of $c(x)$ over this range, a correction of about 10 percent must be applied to it to obtain c_0; this gives $c_0=73.2$. To go a step further, the average value 0.008 should now be corrected upward, since the actual value of c_0 is less than the c constant assumed for it in Eq. (19). In fact, if only c_0 is varied,

$$d\ln[c(x)/c_0-1]x = -\{1+x/[c(x)/c_0-1]x\}d\ln c_0,$$

so that at $x\sim 0.015$ where the average was obtained, a change of -10 percent in c_0 causes a change of about $+25$ percent in $[c(x)/c_0-1]x$.

The average found is at best very approximate, but the θ's are rather insensitive to it anyway; we shall therefore use the value

$$[c(x)/c_0-1]x\approx 0.01. \tag{21}$$

The third approximation to c_0 could now be made, but the correction is evidently quite small.

Employing the value of $c_0=73$ in Eq. (9) along with the average value given by Eq. (21), we obtain

$$\theta_1/\theta_2\approx(0.01)(73)$$

or

$$\theta_2\approx 0.6. \tag{22}$$

With this result one finds a fair fit to the experimental points using a c_1 of 50,000; however, this has a rather improbable shape at small x values, approaching the volume axis too rapidly. Trial and error shows that a much better fit is obtained by using $\theta_2=0.55$, which corresponds (cf. Eq. (9)) roughly to the highest values of column VI of Table I, and a c_1 of approximately 10,000. About c_1 we know only that it has to be much larger than c_2 to have a large effect on the shape of the isotherm in the low x region, since in the experimental example given—unfortunately the only one available at present—there are insufficient data in the low pressure region to fix c_1 accurately. Besides it is certainly an oversimplification to treat a randomly chosen surface as being composed of only two types, so we should probably not find an exact fit in any case.

The values of v' found in the last column of Table I are therefore calculated according to the formula (cf. Eq. (1))

$$v'=\left(\frac{x}{1-x}\right)\left[\frac{(0.45)(10{,}000)}{1+10{,}000x}+\frac{(0.55)(40.2)}{1+39.2x}\right], \tag{23}$$

in which c_2 is obtained from Eq. (8) as $(0.55)\times(73.2)=40.2$. The isotherm so obtained is plotted in Fig. 3, along with the experimental points. Comparison with Fig. 1 shows considerable improvement over the BET equation in the low pressure range.

It might be remarked in defense against the criticism that any equation which contains additional parameters *should* fit the data better than the simple BET theory, that Eq. (1) seems to be a logical first step in attempting to improve the theory for low relative pressures, and that the parameters introduced turn out to have quite reasonable values in the light of the independent evidence mentioned in the introduction.

Without going into the subject of the disagreement between calorimetric heats of adsorption and those obtained from c, it should be noted that if the above example is typical and the interpretation correct, the heat of adsorption up to nearly half a monolayer should be larger than that appropriate to $c=81$ by an amount $RT\ln(10000/81)$. At 78°K this is over 0.7 kcal./mole, a sizable fraction of the heat of liquefaction, 1.5 kcal./mole, of the nitrogen adsorbate. This correction is in the right direction to improve the agreement between the two methods, but is probably not the only difficulty[13,14] to be met.

THE CASE IN WHICH SURFACE 1 PREDOMINATES[15]

Another possible application of the equations for the two component surface is the case in which the adsorption on one part of the surface is negligibly small under the experimental conditions. With reference to Eq. (1) this will occur at such relative pressures that

$$\theta_1c_1/[1+(c_1-1)x]\gg\theta_2c_2/[1+(c_2-1)x]. \tag{24}$$

Besides the trivial case in which $\theta_2\to 0$, resulting in Eq. (2) (which seldom occurs if the agreement of Eq. (2) with experiment throughout the range of 0–1.5 monolayers is a proper criterion), this may also happen when $\theta_2\sim\theta_1$, provided $c_1\gg c_2$ and x so restricted that $x\ll 1/c_2$. Evidence for this behavior should thus again be sought in the region below the usual range of fit of the BET theory.

A most interesting consequence of these conditions is that one is led to predict that Eq. (2) will apply in two distinct portions of the isotherm with two distinct sets of the parameters v_m and c. One portion corresponds to the one just mentioned, in which the adsorption on surface 2 is a negligible fraction of the total; and the other corresponds to the case discussed in the previous section, wherein the adsorption in the first layer

[14] A. B. D. Cassie, Trans. Faraday Soc. **282**, 450 (1945).

[15] Since Eq. (2) reduces to the Langmuir equation at $x\ll 1$, the results of this section are very similar to that given for the Langmuir equation; see reference 2, pp. 74, ff.

on surface 1 is essentially complete.[16] Under these conditions the ratio of the v_m values found will be simply θ_1, i.e. $v_{m1}/(v_{m1}+v_{m2})$.

Experimental results of this type have been frequently found, notably by Armbruster[6] who obtained values of v_s, the Langmuir[17] saturation adsorption (equivalent to $\theta_1 v_m$ or v_{m1}, if the present theory applies), corresponding to θ_1 values in the range 0.2–1 for argon, nitrogen, carbon monoxide, etc. on silver foil at 78 and 90°K, based on the assumption that v_m equals the apparent geometric area. While such figures are not unreasonable, this leaves unexplained the "coefficient of thermal expansion," $d \ln v_s/dT$, observed in that work. On the basis of the inhomogeneity hypothesis the temperature dependence of v_s would probably also be connected with the properties of surface 2, but a complete test of such an explanation must await measurements which extend throughout the range of about 0.05 to 1.5 monolayers (based on the largest v_m value obtained).

This extension of the BET equation appears to offer no explanation of the observed low roughness factors recently reported by Emmett,[18] since these occur at relative pressures of 0.1 or above.

In conclusion, the author wishes to thank Drs. P. H. Emmett and S. W. Weller for several helpful discussions of this work. Grateful acknowledgment is made to the John Simon Guggenheim Memorial Foundation, which supported this investigation.

[16] Here we had best make again the restriction $c_2 \gg 1$, for otherwise c_0 will be low, and, correspondingly, the value of $x_m = 1/[1+(c)^{\frac{1}{2}}]$ so large that the usual deviations at large x may appear despite the approximate constancy of c as given by Eq. (6).

[17] Reference 2, pp. 60, ff.

[18] Reported at the Chicago meeting of the American Chemical Society, September 1946; See Abstracts of Papers, 110th Meeting, No. 44, p. 25E.

THE JOURNAL OF CHEMICAL PHYSICS VOLUME 15, NUMBER 6 JUNE, 1947

Thermodynamics of Crystallization in High Polymers. I. Crystallization Induced by Stretching*

PAUL J. FLORY
Research Laboratory, Goodyear Tire and Rubber Company, Akron, Ohio

(Received February 12, 1947)

A theory of oriented crystallization in elongated polymers having network structures (e.g., in vulcanized rubber) is developed through the application of statistical mechanical procedures similar to those employed in rubber elasticity theory. Expressions are derived which, within the limitation imposed by the simplifying assumptions, relate the incipient crystallization temperature with the elongation, the degree of crystallinity with the elongation and temperature, and the retractive force at crystallization equilibrium with the elongation at constant temperature. The reciprocal of the absolute temperature for incipient crystallization is predicted to decrease linearly with a simple function of the elongation and the average number of chain segments between cross linkages. Only moderate degrees of crystallinity are predicted at equilibrium. In conformity with requirements of the second law of thermodynamics, equilibrium crystallization decreases the tension in the stretched specimen.

Apparent discrepancies between some of these predictions and various observations are attributed to severe departure from equilibrium crystallization when the polymer undergoes crystallization *during* the stretching process. A better approach to equilibrium should be achieved by stretching under conditions which prevent crystallization (e.g., at elevated temperature), then allowing crystallization to proceed at fixed elongation. Few experiments have been performed in this manner, but such results as are available confirm qualitatively the predictions of the theory.

Reasons for the rapid increase in tension which is observed when crystallization occurs during ordinary stretching of rubber are discussed. It is pointed out that crystalline and amorphous regions preferably should not be regarded as separate phases. Likewise, the conversion of amorphous to crystalline polymer does not conform to the definition of a phase transition.

INTRODUCTION

THE tendency for a high polymer to crystallize may be greatly enhanced by deformation. This is particularly true if the polymer possesses a network structure, in which case the deformation imposes on the structure an orientation which cannot be dissipated by ordinary

* The work presented in this paper comprises a part of a program of fundamental research on rubber and plastics being carried out under contract between the Office of Naval Research and the Goodyear Tire and Rubber Company.

internal relaxation processes. Thus, vulcanized rubber, which does not crystallize at ordinary temperatures, becomes highly crystalline when sufficiently elongated, even at temperatures above 100°.[1] Similarly, butyl rubber develops a high degree of crystallinity when stretched at temperatures below 50°,[2] although so far as is known it does not crystallize at all when cooled without stretching.

The reasons for the effects of deformation on crystallization are fairly obvious. When the polymer having a network structure is stretched, chains between network junctions are deformed from their most probable configurations, most of them being elongated. The configurational entropies of these chains consequently are decreased. Less entropy remains to be sacrificed in passing to the crystalline state, where the configurational entropy can be taken as zero. Crystallization will occur when $T\Delta S_f < \Delta H_f$. Consequently, crystallinity may develop at a higher temperature the smaller ΔS_f becomes as a result of elongation.

Alfrey and Mark[3] attempted to give quantitative expression to this concept. Their treatment, which resembles in certain respects the one presented here, applies only to an individual chain, and cannot, therefore, be related to the composite network structure elongated by a factor, α. Recently James[4] has considered the problem in one dimension. The application of his results to actual three-dimensional network systems is of doubtful significance.

In the present paper the influence of stretching on crystallization will be treated by an extension of the statistical mechanical theory of rubber elasticity as it is applied to three-dimensional network structures.[5–10] Because of the approximations introduced for the purpose of simplification, the quantitative validity of some of the relationships which are derived is questionable. Regardless of this deficiency it is felt that the present treatment clarifies the nature of the problem and that the results deduced should at least be valuable as a guide for appropriate future experiments in this field.

THEORETICAL DEVELOPMENT

Consider a network structure composed of long polymer chains joined together at cross linkages. (A "chain" is defined[10] as that portion of the network extending from one cross linkage to the next.) The number of chains united at one "cross linkage" need not necessarily be four; if the cross linkages are trifunctional, or of higher functionality than four, the theory presented here need not be modified. In the development which follows it is considered implicitly that crystallization occurs *after* the polymer has been elongated to the final relative length, α. Experimentally this condition would be fulfilled if the sample were elongated at an elevated temperature at which crystallization would not occur, then cooled gradually. Thus, the final state is to be achieved by two separate and distinct steps, namely, stretching and crystallization, which occur in this order. If crystallization occurs simultaneously with stretching, as indeed ordinarily is the case, the present treatment cannot be expected to apply directly.

Crystallites formed in stretched network polymers (e.g., in vulcanized natural rubber) are observed to be well oriented with their fiber axes parallel to the direction of stretch. This experimental observation is one of the premises of the theory presented below.

As is customary in dealing with the properties of semiflexible chain molecules,[8–12] it is assumed that the behavior of the polymer chains can be approximated satisfactorily by a hypothetical chain composed of a large number of relatively

[1] Unpublished results of Kirsch referred to in *Advances in Colloid Science* (Interscience Publishers, Inc., New York, 1946), Vol. II, p. 67.

[2] W. O. Baker and N. R. Pape, unpublished results submitted to the Office of the Rubber Director.

[3] T. Alfrey and H. Mark, J. Phys. Chem. **46**, 112 (1942).

[4] H. M. James, unpublished work described by Guth, James, and Mark in *Advances in Colloid Science* (Interscience Publishers, Inc., New York, 1946), Vol. II, pp. 279–285.

[5] W. Kuhn, Kolloid Zeits. **76**, 258 (1936); W. Kuhn and F. Grün, J. Polymer Sci. **1**, 183 (1946).

[6] F. T. Wall, J. Chem. Phys. **10**, 132 (1942); **10**, 485 (1942); **11**, 527 (1943).

[7] L. R. G. Treloar, Trans. Faraday Soc. **39**, 36 (1943).

[8] H. M. James and E. Guth, J. Chem. Phys. **11**, 455 (1943); J. App. Phys. **15**, 294 (1944); E. Guth, H. M. James, and H. Mark in *Advances in Colloid Science* (Interscience Publishers, Inc., New York, 1946), Vol. II, p. 253.

[9] P. J. Flory and J. Rehner, Jr., Ann. N. Y. Acad. Sci. **44**, 419 (1943); J. Chem. Phys. **11**, 512 (1943).

[10] P. J. Flory, Chem. Rev. **35**, 51 (1944).

[11] W. Kuhn, Kolloid Zeits. **87**, 3 (1939). W. Kuhn and H. Kuhn, Helv. Chim. Acta, **29**, 1095 (1946).

[12] L. R. G. Treloar, Trans. Faraday Soc. **42**, 77, 83 (1946).

small rigid segments joined together by bonds which permit a considerable latitude of freedom in the disposition of one segment relative to the preceding one in the chain. Because of thermal agitation, these segments are assumed to shift at a rapid rate from one position to another, consistent with their attachments to neighboring segments of the same chain and the availability of free space in their immediate environment. Under these circumstances the occasional transitory occurrence of σ segments of neighboring chains arranged in a close packed array in a plane perpendicular to the direction of elongation is not improbable. Such a temporary arrangement can be regarded as a potential crystallite nucleus. If successive neighboring segments of these same chains also align themselves similarly in planes parallel to the first, a crystallite is formed with its fiber axis parallel to the direction of stretch. The potential nuclei referred to may exist momentarily under any conditions, but crystallites are stable thermodynamically only when propagation of this arrangement through consecutive segments of these chains is accompanied by a decrease in free energy.

It should be noted that the formation of crystal nuclei as described above involves no significant configurational entropy change. Alignment of the segments in a planar array ordinarily will require merely that segments intersected at a given instant by the hypothetical plane be shifted by small distances, less than the dimensions of the segments themselves. The selection of chains and the selection of which segment of each of these chains shall occur in the planar array are essentially arbitrary. Any one of a large number of segments of a given chain may be assigned to the planar array, or crystal nucleus, and the σ segments from the σ chains can be permuted over the cross section without altering appreciably the macro-state.[13a] If the crystal nucleus grows, these segments become fixed in this particular array. The locations of these fixed segments generally will correspond approximately to a most probable group of configurations for their respective chains. This is essentially a "freezing in" process unaccompanied by change in entropy.

On the other hand, those potential nuclei in which the particular array of segments is most conducive to crystal growth under the conditions of deformation will be the ones which survive. Here the element of selection enters to some extent, and a corresponding entropy decrease should be considered. No means for estimating the magnitude of this entropy change is evident. In the belief that it is relatively small, it is neglected here. In effect, it is assumed, as an approximation, that the crystal nuclei are formed without change in entropy.[13b]

As the crystal nucleus grows in either direction parallel to the axis of elongation, which is taken as the z-axis, two contributions to the entropy change must be considered. A segment entering the crystallite sacrifices all freedom of orientation relative to the preceding segment of the same chain. The entropy must decrease accordingly. A further entropy change arises from the alteration of the distance traversed ("displacement length"[10]) by the remaining amorphous portions of the chain. As the crystal grows parallel to the axis of elongation (z-axis), the z-component of this distance, or displacement length, is decreased while at the same time the number of amorphous segments available to traverse the required distance is diminished. At the onset of crystal growth, the chains having had their z-components increased by stretching, this change permits the amorphous portion of the chain to assume a greater number of configurations, since the displacement length is decreased out of proportion to the decrease in number of amor-

[13a] The latter half of this statement is not strictly true when the chains are directionally unsymmetrical, as for example is the case in natural rubber. In a bundle of parallel rubber chains, some will have their methyl groups to the right of the double bond and some to the left. The crystalline array doubtless includes the two orientations in equal numbers arranged in regular array. (Compare, C. W. Bunn, in *Advances in Colloid Science* (Interscience Publishers, Inc., New York, 1946), Vol. II, p. 113). Since the arrangement of "right" and "left" chains is systematic in the crystal, the entropy of nucleation in polymers such as natural rubber should include the term $-k\sigma \ln 2$. This term is neglected here.

[13b] It might appear necessary to consider that each chain has been separated at the crystallite into two chains. The crystallite does in fact fix the positions of segments at the ends of the crystallites, hence, computation of the number of configurations available when the crystallite is present would require consideration of two separate sub-chains with coordinates fixed by the location of the crystallite. However, the crystallite is permitted to form at *any* convenient location. In order to include all potential configurations (for the same macro-state) it is necessary, therefore, to disregard both the specific location of the crystallite and the particular sequence of ζ-segments of a given chain which occur in the crystal.

phous segments. Hence, the entropy of the amorphous portion generally is increased by crystallization. As an increasing proportion of the chain joins the crystallite, a condition may be reached where this is no longer true, or at any rate where this source of entropy gain with further crystallization is diminished. It is evident that this must be so inasmuch as the elongated z-component of the displacement length of the amorphous portion is rapidly decreased by the lengthening of the crystallite, while fewer amorphous segments are available to traverse the unaltered x and y distances. The computation of the net entropy change in the amorphous portion of the chain is the major problem to be solved.

The desired total entropy change accompanying crystallization might be obtained by computing the separate entropy changes as detailed above. Instead, calculation of an "absolute" configurational entropy of the semi-crystalline stretched polymer will be carried out, taking the hypothetical totally crystalline (single crystal) polymer as the standard state.

The dependence of the relative number of configurations (configurational probability) of an amorphous chain on the distance of separation of its ends, or chain displacement length, is assumed to be a Gaussian function of this distance $r[=(x^2+y^2+z^2)^{\frac{1}{2}}]$, i.e.,[14,15]

$$W(xyz)=(\beta/\pi^{\frac{1}{2}})^3\exp[-\beta^2(x^2+y^2+z^2)] \quad (1)$$

where x, y and z represent the coordinates of one end of the chain with respect to the other and $1/\beta$ equals the most probable value of the chain displacement length, r. The cross linkages are introduced into the polymer while it is in its undeformed state, in which the molecules are free to assume random configurations. Hence, the above function must also represent the distribution of chain coordinates which exists before stretching.

After stretching along the z-axis by a factor, α, the volume remaining constant, the distribution of chain coordinates becomes

$$\nu(xyz)=\sigma(\beta/\pi^{\frac{1}{2}})^3\exp[-\beta^2(\alpha x^2+\alpha y^2+z^2/\alpha^2)] \quad (2)$$

where σ is the total number of chains under consideration.

We shall adopt as our hypothetical model a chain composed of rigid segments connected by bonds which permit complete freedom of orientation of one segment relative to the one preceding it in the chain.[8–12] For such chains the reciprocal most probable displacement length is given by

$$\beta=(3/2n)^{\frac{1}{2}}/l \quad (3)$$

where l is the length of each segment and n is the number of segments per chain. The product nl is taken equal to the maximum extension L of the actual chain consistent with bond angles and dimensions and with steric interferences of substituents. The quantities n and the corresponding value of $l=L/n$ are fixed by the further stipulation that the Gaussian function must give the best possible fit to the actual distribution of chain displacement lengths, except, of course, for values of r approaching the maximum extension L, where the Gaussian function necessarily is a poor approximation.

If an alternative model chain were chosen in which the segments are connected by valence bonds at fixed tetrahedral angles about which rotation is completely free, then [14–16]

$$\beta=(3/4n)^{\frac{1}{2}}/l. \quad (4)$$

In this case, in order to match the configuration distribution of the actual chain, it would be necessary to make l smaller and n correspondingly larger than in the case of the previously considered chain model. It is evident that the distribution function is preserved if n for the second model is twice that for the first, l being decreased to one-half.

When ζ of the n segments of the chain occur in a crystalline region, the relative number of configurations available to the remaining $n-\zeta$ segments becomes

$$W'(xyz')=(\beta'/\pi^{\frac{1}{2}})^3\exp[-(\beta')^2(x^2+y^2+z'^2)] \quad (5)$$

where

$$\beta'=[\text{Const.}/(n-\zeta)l^2]^{\frac{1}{2}}=\beta[n/(n-\zeta)]^{\frac{1}{2}} \quad (6)$$

and z' is the algebraic sum of the z displacement lengths of the (two) amorphous sections of the chain. The x and y displacements are unaffected

[14] W. Kuhn, Kolloid Zeits. **68**, 2 (1934).
[15] E. Guth and H. Mark, Monats. f. Chem. **65**, 93 (1934).
[16] H. Eyring, Phys. Rev. **39**, 746 (1932).

by the formation of crystallites with axes parallel to the direction of elongation, but z in general will be altered by an amount ζl. If α is sufficiently greater than unity, then in most cases the chain will traverse the crystallite in the same direction as the displacement between the ends of the chain located at cross linkages, which are assumed to be fixed at their most probable positions,[17] the coordinates of one with respect to the other being x, y, and z. As an expedient, though regrettable, approximation, it is considered here that all chains traverse the crystallite in the same direction as the z displacement of one end of the chain with respect to the other; i.e., it is assumed that

$$z' = \pm(|z| - \zeta l) \tag{7}$$

where the plus sign is to be used for $z>0$ and the minus for $z<0$. For small values of z this approximation is a particularly poor one. However, the z' term enters the summations which follow as the square, and the contributions of these small z terms consequently are of minor importance. The consequences of this approximation will be dealt with later.

For the calculation of the configurational entropy with respect to the totally crystalline polymer, two hypothetical steps are considered: (a) melting of $n-\zeta$ of the segments of each of σ chains composed of n segments, the ends of the chains being free (i.e., not attached to cross linkages) to occupy most probable locations such that the distribution of displacement lengths x, y, and z' for the amorphous portions is given by

$$\nu'(xyz') = \sigma W'(xyz') \tag{8}$$

and (b) assignment of the ends of the chains to the locations of the cross linkages within the elongated polymer, as prescribed by Eq. (2). The entropy change for the first of these steps is given by

$$S_a = \sigma(n-\zeta)s_f \tag{9}$$

where s_f is the entropy of fusion per segment.[18a] According to the lattice theory[18b] of thermodynamic properties of high polymers

$$s_f = k[\ln(\gamma-1)-1] \tag{10}$$

where k is Boltzmann's constant and γ is the coordination number of the lattice; at any rate Eq. (10) should represent that portion of the entropy of fusion arising from the randomness of arrangement of the segments in space, but not including entropy contributions from internal changes within the segments during melting, or from enhanced freedom of oscillation within a cell of the liquid lattice.

The entropy change S_b in step (b), arises from the transformation of the chain length distribution for the amorphous portion from $\nu'(xyz')$ given by Eq. (8) to $\nu(xyz)$ given by Eq. (2). Employing the Boltzmann relationship[19] $S = k\sum \nu \ln W$,

$$S_b = k\sum_{xyz} \nu(xyz)\ln W'(xyz') - k\sum_{xyz'} \nu'(xyz')\ln W'(xyz').$$

Converting to integrals and substituting the previously given expressions for the various functions

$$S_b = \sigma k(\beta/\pi^{\frac{1}{2}})^3 \int_{-\infty}^{\infty}\int\int \exp[-\beta^2(\alpha x^2+\alpha y^2+z^2/\alpha^2)][A'-\beta'^2(x^2+y^2+z'^2)]dxdydz$$

$$-\sigma k(\beta'/\pi^{\frac{1}{2}})^3 \int_{-\infty}^{\infty}\int\int \exp[-\beta'^2(x^2+y^2+z'^2)][A'-\beta'^2(x^2+y^2+z'^2)]dxdydz'$$

[17] See reference 9; also H. M. James and E. Guth, J. Chem. Phys. **11**, 478 (1943).

[18a] Under the plausible assumption that cross linkages (i.e., ends of chains) are prohibited for stereochemical reasons from occurring within crystallites, a further entropy term $\sigma k \ln (n-\zeta+1)/n$ should be added to account for the limitations on the choice of the sequence of ζ crystalline segments. The effect of this term is small when n is large. Hence, it has not been considered of sufficient importance to merit incorporation in the present treatment.

[18b] P. J. Flory, J. Chem. Phys. **10**, 51 (1942).

[19] The alternate treatment of Wall[6] in which interchangeability of chain elements is taken into account leads to results insignificantly different from those deduced here by merely summing over the *a priori* probabilities for the individual chains. In this connection see also, Kuhn and Grün[5] and Kuhn and Kuhn.[27]

where $A'=\ln(\beta'/\pi^{\frac{1}{2}})^3$. The second integral expression can be integrated at once to $-\sigma k(A'-\frac{3}{2})$. In accordance with Eq. (7), the integral over z in the first expression can be separated into two parts, one from 0 to ∞, where $z'=z-\zeta l$, and the other from $-\infty$ to 0, where $z'=z+\zeta l$. With appropriate further rearrangement, there is obtained

$$S_b=8\sigma k(\beta/\pi^{\frac{1}{2}})^3\int_0^\infty\int\int\exp[-\beta^2(\alpha x^2+\alpha y^2+z^2/\alpha^2)]\{A'-\beta^2[n/(n-\zeta)][x^2+y^2+(z-\zeta l)^2]dxdydz$$
$$-\sigma k(A'-\tfrac{3}{2})\}.$$

After carrying out the integrations

$$S_b=-\sigma k[(\zeta\beta l)^2 n/(n-\zeta)-2\alpha(\zeta\beta l/\pi^{\frac{1}{2}})n/(n-\zeta)+(\alpha^2/2+1/\alpha)n/(n-\zeta)-\tfrac{3}{2}]. \tag{11}$$

For small degrees of crystallinity and low elongations Eq. (11) assigns a small positive value to S_b; it is negative for all higher elongations. For example, if α is less than about 2, then for a certain range of small degrees of crystallinity S_b as computed from Eq. (11) is positive. Obviously, S_b should always be zero or negative since the final state may not have higher entropy than the most probable state. This failure of Eq. (11) at low elongations seems to arise, in large part at any rate, from the approximation introduced in Eq. (7).

The configurational entropy of the σ chains involved in the crystallite is the sum of S_a+S_b, or

$$S=\sigma k[(n-\zeta)s_f/k-(\zeta\beta l)^2 n/(n-\zeta)+(2\alpha\zeta\beta l/\pi^{\frac{1}{2}})n/(n-\zeta)-(\alpha^2/2+1/\alpha)n/(n-\zeta)+\tfrac{3}{2}]. \tag{12}$$

Letting h_f represent the heat of fusion per segment of the polymer, the heat change accompanying the fusion of $n-\zeta$ of the segments per chain is $\sigma h_f(n-\zeta)$. The second step in the hypothetical procedure for forming the partially crystalline polymer may be assumed to occur without change in internal energy. Hence, the free energy of the system, taking the perfectly ordered, totally crystalline chains as the standard state, becomes

$$F=\sigma kT[\zeta(s_f/k-h_f/kT)+(\zeta\beta l)^2 n/(n-\zeta)-(2\alpha\zeta\beta l/\pi^{\frac{1}{2}})n/(n-\zeta)$$
$$+(\alpha^2/2+1/\alpha)n/(n-\zeta)-\tfrac{3}{2}-n(s_f/k-h_f/kT)]. \tag{13}$$

It is convenient to employ the following substitutions:

$$\lambda=(n-\zeta)/n$$

and

$$\theta=s_f/k-h_f/kT.$$

Converting to molar quantities, for which the same symbols will be employed, and setting $h_f/s_f=T_m^0$, the "incipient crystallization temperature" for the undeformed polymer,

$$\theta=(h_f/R)(1/T_m^0-1/T).$$

The free energy function then assumes the form

$$F=\sigma RT[n\theta(1-\lambda)+(n\beta l)^2(1-\lambda)^2/\lambda-(2\alpha n\beta l/\pi^{\frac{1}{2}})(1-\lambda)/\lambda+(\alpha^2/2+1/\alpha)/\lambda-\tfrac{3}{2}-n\theta]. \tag{13'}$$

The condition for equilibrium with respect to the degree of longitudinal growth of the crystallite can be stated as $(\partial F/\partial\zeta)_a=0$, or $(\partial F/\partial\lambda)_a=0$. Differentiating Eq. (13') with respect to λ

$$(1/\sigma RT)(\partial F/\partial\lambda)_a=-[n\theta+(n\beta l)^2(1/\lambda^2-1)-(2\alpha n\beta l/\pi^{\frac{1}{2}})/\lambda^2+(\alpha^2/2+1/\alpha)/\lambda^2] \tag{14}$$

which on equating to zero gives

$$\theta\lambda^2+n\beta^2 l^2(1-\lambda^2)=\varphi(\alpha)$$

where

$$\varphi(\alpha)=2\alpha\beta l/\pi^{\frac{1}{2}}-(\alpha^2/2+1/\alpha)/n. \tag{15}$$

Solving the above equation for the equilibrium value of λ

$$\lambda = \{[n\beta^2 l^2 - \varphi(\alpha)]/[n\beta^2 l^2 - \theta]\}^{\frac{1}{2}}. \tag{16}$$

Substituting from Eq. (3) for β

$$\varphi(\alpha) = (6/\pi)^{\frac{1}{2}}\alpha/n^{\frac{1}{2}} - (\alpha^2/2 + 1/\alpha)/n \tag{17}$$

$$\lambda = \{[\tfrac{3}{2} - \varphi(\alpha)]/[(\tfrac{3}{2} - \theta)]\}^{\frac{1}{2}}. \tag{18}$$

Before proceeding with the interpretation and application of the relationships derived above, it may be well to recapitulate as follows the assumptions and approximations employed in their derivation:

(1) Crystallization is assumed to occur in a thermodynamically most favorable manner, i.e., a state of equilibrium is assumed.

(2) Possible small entropy changes associated with the formation of nuclei are neglected. Thus, for example, the tendency for chains having comparatively large z components in the undeformed state to crystallize selectively is disregarded.

(3) Crystallites are considered to be oriented parallel to the axis of elongation.

(4) Each chain is assumed to traverse the crystallite in the direction of the displacement of its ends with respect to the z-axis. See Eq. (7).

(5) The Gaussian distribution is employed to represent the relative number of configurations although it is known to be unsatisfactory for this purpose at high extensions of the chains.

Finally, the approximate invariance of these equations (and those deduced from them in subsequent sections of this paper) with change of model should be pointed out. If, for example, a model for the chain is adopted in which the segments are attached by tetrahedrally disposed valence bonds about which rotation is unrestricted, β will be given by Eq. (4), in place of (3). However, this chain of the same contour length nl as the chain composed of freely orienting segments necessarily will have to be made up of a greater number of smaller segments in order to conform to the actual chain. Perusal of the equation given above will show that they remain unchanged when βl is replaced by its value (see Eq. (4)) for tetrahedrally bonded segments, provided that n is doubled while l, and likewise h_f and s_f, are halved. Thus, it appears that the conclusions to be drawn are not sensitive to the type of chain model selected.

DEGREE OF CRYSTALLINITY

The quantity $1-\lambda$ represents the fractional degree of crystallinity of the σ chains under consideration. To the extent that these chains are typical of the network as a whole, $1-\lambda$ may be regarded as the degree of crystallinity in the entire system. This interpretation of λ may be reasonably satisfactory for low degrees of crystallinity, but it is beset with doubts, partly of intuitive origin, when a substantial fraction of the material becomes crystalline. A literal extension of the above description of the formation of a single crystallite to the system as a whole would imply that nucleation is restricted to the initial crystallization interval, further crystallization thereafter being restricted to *longitudinal* growth of existing crystallites. Actually nucleation doubtless occurs simultaneously with growth of existing crystalline regions, and these may grow laterally as well as longitudinally. As a result of this course of the crystallization, a given chain may pass through several crystalline regions. Fundamentally, the above treatment is also applicable to chains which pass through several crystalline regions of total length ζ. However, these several crystalline regions generally will not be co-linear, and if $1-\lambda$ is relatively large, additional "x and y" restraints consequently may be imposed. Consideration of this factor and others arising from the various assumptions previously introduced (especially assumption (4)) casts doubt on the quantitative validity of equilibrium degrees of crystallinity computed from the present theory. On the other hand, it seems likely that such calculations may represent useful approximations.

In Fig. 1, the degree of crystallinity computed from Eq. (18) is plotted against the elongation α for arbitrary values of the parameters. The number of segments n has been taken as 50. The heat of fusion h_f has been assigned a value of $600R$ and the incipient crystallization tempera-

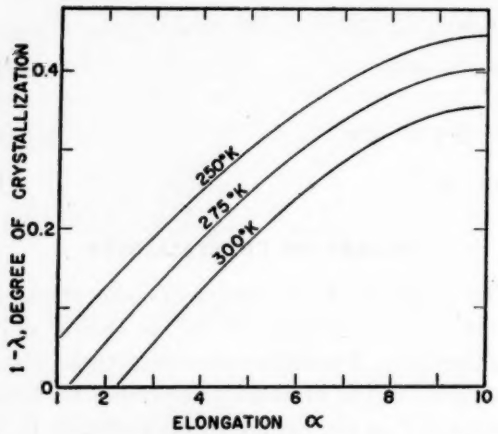

FIG. 1. Degree of crystallization $(1-\lambda)$ at equilibrium *vs.* elongation at the three temperatures indicated. Curves calculated from Eq. (18) taking $n=50$, $h_f=600R$ and $T_m^0=250°K$.

ture T_m^0 for the unstretched polymer has been taken as 250°K. Accordingly,

$$\theta=600(1/250-1/T).$$

These values have been chosen so as to obtain relationships which may resemble the behavior of vulcanized rubber.[20] The uppermost curve represents the calculation for $T=T_m^0$, corresponding to $\theta=0$; the middle and lowest curves represent crystallization at $T=275°K$ and 300°K corresponding to $\theta=0.2182$ and 0.4000, respectively.

It will be observed that the $T=T_m^0=250°K$ curve fails to fall to zero crystallinity at $\alpha=1$. This is a result of the failure of Eq. (11) at low elongations as already noted. Presumably all of the curves give values of $1-\lambda$ which, at low elongations at any rate, are somewhat too high. The maxima in the curves in Fig. 1 near $\alpha=(2n)^{\frac{1}{2}}$ are of dubious significance in view of the inadequacy of the Gaussian distribution for highly extended chains and in view also of other approximations.

According to these calculations the equilibrium degree of crystallinity induced by stretching is never large. This prediction of the theory might appear to be at variance with the established highly crystalline character of stretched vulcanized rubber.[21] However, the calculations refer to an equilibrium crystalline state which ordinarily is not reached when crystallization occurs simultaneously with elongation; under these circumstances crystallinity may exceed the equilibrium value (compare the following).

INCIPIENT CRYSTALLIZATION TEMPERATURE

In consideration of the expectation that the present theory should apply with optimum validity when the equilibrium degree of crystallinity is very small, calculation of the dependence of the incipient crystallization temperature T_m on the elongation α is particularly appropriate. Placing $\lambda=1$ in Eq. (16)

$$\theta\equiv(h_f/R)(1/T_m^0-1/T_m)=\varphi(\alpha)$$

from which it follows that the reciprocal of the incipient crystallization temperature should vary linearly with the function φ of the elongation α in accordance with the relationship

$$1/T_m=1/T_m^0-(R/h_f)\varphi(\alpha). \qquad (19)$$

Here again an incongruity arises as a result of the failure of Eq. (11) at low elongations: $\varphi(\alpha)$ retains a small positive value when α is decreased to unity and as a result T_m at $\alpha=1$ is predicted to be less than T_m^0. It may be presumed that a more accurate theory would replace $\varphi(\alpha)$ with a function which would equal zero at $\alpha=1$, thus removing the inconsistency just mentioned. The important present result is the form assumed by Eq. (19) relating incipient crystallization temperature to the heat of fusion and to a function of the elongation, although the latter admittedly is not given accurately by the present theory.

The function $\varphi(\alpha)$ as given by Eq. (17) depends on the structure of the network in a particularly simple manner. Except at quite low elongations, Eq. (17) can be written, approximately,

$$\varphi(\alpha)\cong(6/\pi)^{\frac{1}{2}}(\alpha/n^{\frac{1}{2}})-(\tfrac{1}{2})(\alpha/n^{\frac{1}{2}})^2 \qquad (17')$$

from which it is evident that the effect of increasing n, the number of segments between

[20] The value assigned to T_m^0 is some 50 to 60° lower than the crystallization temperature for raw rubber. (See L. A. Wood and N. Bekkedahl, J. App. Phys. **17**, 362 (1946); also, reference (24)). The incipient crystallization temperature probably is lowered somewhat, though perhaps not this much, by vulcanization or, more accurately, by the chemical changes accompanying vulcanization. Similarly, the value of h_f employed here may be rather larger than would be expected in view of the low heat of fusion of crystalline rubber. (See L. A. Wood, N. Bekkedahl and R. E. Gibson, J. Chem. Phys. **13**, 475 (1945)).

[21] J. E. Field, J. App. Phys. **12**, 23 (1941).

cross linkages, by a factor a can be compensated by increasing the elongation by $a^{\frac{1}{2}}$.

EFFECT OF CRYSTALLIZATION ON FORCE OF RETRACTION

Under assumptions paralleling those employed in the computation of the equilibrium degree of crystallinity, the retractive force f after the stretched rubber has been allowed to crystallize can be deduced as follows.

$$f=(\partial F/\partial\alpha)_e$$

where the subscript "e" implies a condition of equilibrium with respect to degree of crystallinity (i.e., equilibrium ζ or λ). Here f is expressed in force per unit initial cross-sectional area provided that σ represents the number of chains per unit volume. In general, recalling Eq. (13′) where F is expressed as a function of α and λ,

$$dF/d\alpha=(\partial F/\partial\alpha)_\lambda+(\partial F/\partial\lambda)_\alpha(d\lambda/d\alpha).$$

At equilibrium with respect to crystallinity, $(\partial F/\partial\lambda)_\alpha=0$ (see above). Hence,

$$f=(\partial F/\partial\alpha)_e=(\partial F/\partial\alpha)_\lambda$$
$$=\sigma RT[(\alpha-1/\alpha^2)-(2n\beta l/\pi^{\frac{1}{2}})(1-\lambda)]/\lambda \quad (20)$$

where λ represents the equilibrium fraction of amorphous material calculable as a function of α and T from Eq. (16) or (18). Substituting for β from Eq. (3)

$$f=\sigma RT[(\alpha-1/\alpha^2)-(6n/\pi)^{\frac{1}{2}}(1-\lambda)]/\lambda. \quad (21)$$

When $\lambda=1$, Eqs. (20) and (21) reduce to

$$f=\sigma RT(\alpha-1/\alpha^2) \quad (22)$$

which is the expression ordinarily obtained for a network of Gaussian chains in the absence of crystallization.

In Fig. 2 stress-strain curves have been computed from Eq. (21) using the same values of the parameters employed for the calculations shown in Fig. 1. The uppermost curve corresponds to the non-crystalline material ($\lambda=1$); other curves correspond to the temperatures indicated. According to these calculations, crystallization subsequent to elongation (i.e., equilibrium crystallization) should markedly decrease the tension at extensions well above that for incipient crystallization. That the tension must be decreased by spontaneous isothermal crystallization at fixed elongation is an obvious consequence of the second law of thermodynamics. (A partial exception to this statement can be conceived in the case of a hypothetical elastic substance in which an increase in tension resulting from equilibrium crystallization at high elongations would be compensated by a decrease in tension at lower elongations.)

This deduction from theory is supported by observations of Meyer and Ferri[22] on the dependence of the tension in stretched vulcanized rubber on temperature. When samples stretched to fixed length were cooled gradually, an accelerated decrease in tension was observed on entering the crystallization range. Gradual decay in the tension at constant temperature in this region was similarly attributed to further slow crystallization. These observations were confirmed and extended by Wood and Roth.[23,24]

If temperatures somewhat lower than the temperature T_m^0 for incipient crystallization in the undeformed material are employed, the equilibrium tensions calculated from Eq. (21), using λ from Eq. (18), are found to be negative. Calculations in this range may not be quantitatively significant for the following reason. As crystallization progresses in the sample at fixed elongation α, the tension decreases steadily according to Eq. (21). When the tension becomes small, indicating negligible orientation of amorphous portions of chains, additional nuclei which may form should no longer be preferentially oriented with respect to the z-axis. Crystal growth arising from these nuclei should not, therefore, decrease (algebraically) the tension in the sample, although longitudinal growth of crystals formed earlier should be expected to do so.

Smith and Saylor[25] observed increases in length when samples of stretched rubber were cooled to −25°C. This "secondary elongation" amounted

[22] K. H. Meyer and C. Ferri, Helv. Chim. Acta **18**, 570 (1935).

[23] L. A. Wood and F. C. Roth, J. App. Phys. **15**, 781 (1944).

[24] For a thorough and comprehensive discussion of crystallization in rubber-like materials under various conditions, see "Crystallization Phenomena in Natural and Synthetic Rubbers" by L. A. Wood, in *Advances in Colloid Science* (Interscience Publishers, Inc., New York, 1946), Vol. II.

[25] W. H. Smith and C. P. Saylor, Bur. Stand. J. Research **21**, 257 (1938).

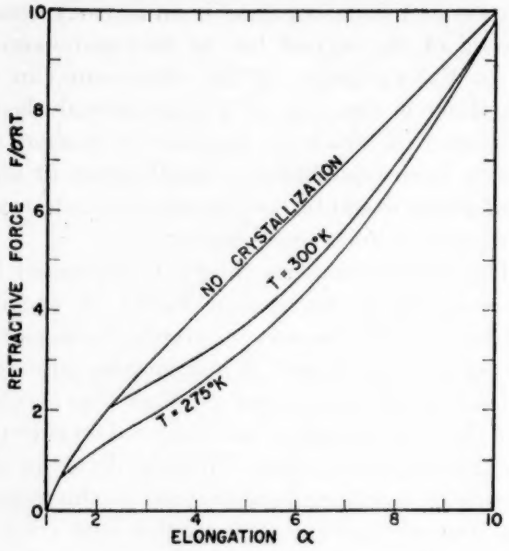

FIG. 2. Stress-strain curves, respectively, without crystallization and with equilibrium crystallization at the two temperatures indicated. Results calculated from Eq. (21) using the same parameters as those employed for computing the curves shown in Fig. 1.

to as much as 4 percent of the stretched length when the elongation was 200 to 300 percent.[24] This observation is readily explained by the present theory. It shows further that increase in crystallinity, even after the tension has been totally relieved, proceeds in part at least by longitudinal growth of existing oriented crystallites.

DISCUSSION

In attempting to characterize the effects of crystallization on elastic properties of rubber, one is faced with a superficially paradoxical situation. Abundant evidence shows that the tension in a highly elongated vulcanized rubber which has undergone crystallization during stretching is substantially greater than in another similarly vulcanized rubber (or the same rubber at higher temperature) in which no crystallization occurs at the same elongation. On the other hand, theory leads inevitably to the conclusion that crystallization should decrease the tension.[3,4] This can be deduced from a theoretical analysis such as has been set forth above, or more directly from thermodynamic (equilibrium) considerations.

As earlier remarks have indicated, the clue to the resolution of this "paradox" may be found in the limitation of thermodynamical theories to states of equilibrium. When vulcanized rubber is stretched in the customary manner, such that crystallites form during the stretching process, the equilibrium state to which the theory applies will not ordinarily be reached. This point appears to have been overlooked in previous discussions of the theory of crystallization on stretching.[3,4] For example, James[4] attributes the observed increase in tension resulting from crystallization to "filler action" of the crystallites. The following discussion attempts to show in some detail how crystallites as normally formed in stretching may markedly enhance the retractive force.

Formation of crystal nuclei at an elongation, α, occurs without significant change in entropy as pointed out above. These identical nuclei, made up of the same chain segments in the same arrangement, could not be assembled at a different elongation without decreasing the entropy. Their formation at an elongation either greater or less than α would involve assignment of the chains to configurations not in conformity with their most probable arrangement consistent with this elongation. The situation is analogous to the formation of cross linkages at an intermediate elongation; in fact, the crystal nuclei may be regarded as giant cross linkages. Random introduction of cross linkages at an elongation, α, entails no change in configurational entropy, but if the elongation is altered in either direction the entropy will be less than it would have been in the absence of these cross linkages. It becomes evident, therefore, that both the entropy S_α and $(dS/d\alpha)$ at the elongation α remain unaltered when cross linkages, or crystal nuclei (disregarding the effects of their growth to finite size), are introduced at random at the extension α. Hence, the tension at α also is unchanged. As the elongation is increased, however, the tension will be augmented by the presence of these additional cross linkages, or by the crystal nuclei.

In the ordinary "non-equilibrium" stretching of rubber, the first crystal nuclei may be presumed to form at an extension α_1 only slightly beyond the extension for incipient crystallization at equilibrium. Growth of these crystallites may actually reduce the tension somewhat at elongations not greatly exceeding α_1, in accordance with concepts set forth by Alfrey and Mark[3] and

with the above theory. As the elongation is increased to α_2, these crystallites, being of sufficient permanence to resist dissolution in favor of a crystalline arrangement more stable at the higher elongation, act in the manner discussed above to increase the tension. However, further crystallization will occur at α_2 and thus counteract this effect. The portion of this further crystallization which consists of nucleation and of attachment of chains to existing crystallites (lateral, as apart from longitudinal, growth of existing crystallites) introduces restraints which increase the tension developed in passing to a higher elongation α_3; etc. In this way a state is soon reached where the tension rises rapidly with elongation.

Under the influence of these compounded internal stresses, the degree of crystallinity ultimately reached may exceed considerably its equilibrium value as calculated above. Additional deformation is borne largely by the remaining amorphous material, and when only a small fraction remains in the amorphous condition that fraction must undergo an actual deformation exceeding correspondingly the incremental macroscopic deformation of the sample.[3,4]

Thus, we reach the conclusion that the accelerated increase in tension with elongation and the ultimate steep slope of the stress-strain curve for crystallizing rubbers are consequences of two interrelated factors: (a) sub-division of amorphous chains, or portions thereof, by attachments to crystalline regions (i.e., the "cross-linking effect"), which increases the number of elastically effective elements at all higher elongations, and (b) the small residue of easily deformable (i.e., amorphous) material at high elongations. Explanations according to which the accelerated rise in the stress-strain curve is attributed primarily to the rapid decrease in entropy as the chain approaches full extension,[5,26] or to the combined entropy decrease and internal energy increase arising from bond deformations for chains nearing full extension,[27] crystallization being disregarded as a primary factor, are rejected here. Near the breaking point unquestionably many chain elements are stretched approximately to full extension. However, in order to arrive at an adequate interpretation of the stress-strain curve at intermediate and high extensions, consideration must be given first of all to the large increase in the number of elastic elements brought about as a result of crystallization.

The non-equilibrium character of crystallinity as it ordinarily occurs in stretched rubber is confirmed by various observations. Hystersis loops are larger when the deformation cycle extends into the region of crystallization.[23,28] Rohde[29] and Braendle and Wiegand[30] compared the relaxation of stress or strain in vulcanized natural rubber subjected to repeated elongation with that which occurred in Buna-S, or in GR-S, under the same conditions. At low maximum elongations relaxation of the synthetic rubber was greater, but this order was reversed at higher elongations extending into the crystallizing range for natural rubber. The latter showed marked relaxation effects with repeated stretching to high elongations. These results can be attributed plausibly to recrystallization induced by the cyclic deformation. Some vestiges of crystallinity presumably survive the retraction phase of the cycle, and these may serve as nuclei for crystallization during the subsequent elongation. It is to be expected that more favorably located crystalline regions will be developed preferentially under these circumstances. In any event, a change in crystalline arrangement must necessarily proceed in the direction of the more stable state, and this change will diminish the tension. Braendle and Wiegand[30] emphasize the practical merit of this relaxation phenomenon in rubber when subjected to repeated stresses which approach the ultimate strength of the material (e.g., in cut growth in tire treads).

Throughout this paper the term "melting point" has been avoided, "crystallization temperature," or "incipient crystallization temperature," having been used instead. In the opinion of the author it is best to avoid designation of the amorphous and crystalline regions as separate phases. Neither would exist in the same state apart from the other. The configurational re-

[26] L. R. G. Treloar, Trans. Faraday Soc. **42**, 83 (1946).
[27] W. Kuhn and H. Kuhn, Helv. Chim. Acta **29**, 1095, 1615, 1634 (1946).
[28] I. Williams and B. M. Sturgis, Ind. Eng. Chem. **31**, 1303 (1939).
[29] E. Rohde, Kautschuk **15**, 64 (1939).
[30] H. A. Braendle and W. B. Wiegand, J. App. Phys. **15**, 304 (1944).

strictions imposed on amorphous sections of chains by the crystallites to which they are attached are evident from the above discussion.[31] The partial molal free energy of the amorphous "phase," if formulation of such a function were attempted, would depend on the amount of that phase, in direct violation of the concept that such functions are intensive only.

If the amorphous and crystalline regions were considered as separate phases, the phase rule would dictate that the system be characterized by an invariant melting temperature (at fixed pressure). High polymers invariably change from amorphous to crystalline (or *vice versa*) over a range of temperature, although the onset of crystallinity may occur at a well defined temperature. Corresponding complications arise in two component systems if the semi-crystalline polymer is counted as two phases.[32]

The present theory appears to be in satisfactory qualitative agreement with observation, although, as is evident from the above discussion, few experimental measurements have been reported on the crystallization of stretched vulcanized rubbers under conditions which assure satisfactory approach to equilibrium. It is not possible at the present time, therefore, to compare quantitative aspects of the theory with experiment. In view of the desirability of minimizing complications (both theoretical and experimental) which may enter at appreciable degrees of crystallinity, a test of Eq. (19) relating elongation with incipient crystallization temperature seems most immediately appropriate. Experiments designed to furnish data suitable for this purpose are under way in this laboratory at the present time.

[31] E. M. Frith and R. F. Tuckett, Trans. Faraday Soc. **40**, 251 (1944), have discussed the thermodynamics of crystallization in polymers in the absence of deformation. The equations (see J. Chem. Phys. **10**, 51 (1942)) which they used to express the entropy of chain elements within the amorphous region actually apply only to chains the ends of which are free to locate anywhere. The dependence of melting temperature on degree of crystallinity deduced by Frith and Tuckett originates entirely from this erroneously implied freedom of each of the amorphous chain elements with respect to the remainder of the semi-crystalline structure.

[32] R. B. Richards, Trans. Faraday Soc. **42**, 10 (1946).

On the Mass Spectra of Hydrogen and Deuterium

D. P. STEVENSON
Shell Development Company, Emeryville, California

(Received April 8, 1947)

On the basis of reasonable assumptions with regard to the probabilities of electron-impact induced transitions of hydrogen and deuterium, it is calculated that the relative intensity of H^+ in the mass spectrum of hydrogen should be 2.3 times greater than that of D^+ in the mass spectrum of deuterium for ionization by electrons of less than 35-volt energy. This value is compared with experimental values 2.8 (22-v energy), 1.5 (30-v energy), 1.9 (50-v energy), and 2.2 (100-v energy).

SOME years ago it was predicted and experimentally verified[1] that the relative intensity of H^+ in the mass spectrum of hydrogen is greater than that of D^+ in the mass spectrum of deuterium. It is the object of this note to show that a relatively simple calculation leads to a quantitative prediction of this phenomenon in agreement with experiment.

When hydrogen or deuterium is exposed to the ionizing action of electrons, as in the ionization chamber of a mass spectrometer, several processes may occur. If the energy of the electrons is less than 15.4 volts, no positive ions are formed. For electrons with energies between 15.4 and 18.0 volts only molecular ions in the stable, symmetric, $^2\Sigma^+_g$ state are formed. If the energy of the electrons is greater than 18.0 volts, the molecular ions may be formed in the $^2\Sigma^+_g$ state, but above the dissociation limit of this state, so that the molecular ions immediately dissociate into an atomic ion and a free atom. For electronic energies greater than 27 volts, excitation to the repulsive, antisymmetric, $^2\Sigma^+_u$ state of the molecular ion is possible, and these molecular ions immediately dissociate into an atomic ion and a free atom. As the energy of the ionizing electrons is further increased, other excited states of the molecular ion become accessible, and since these states are repulsive they lead to the formation of atomic ions and excited free atoms. The relative probability of each of these processes becomes essentially independent of the energy of ionizing electrons when the energy of the electrons is from 25 to 50 percent greater than the minimum energy required for the process.[2]

Inasmuch as the electronic wave functions of hydrogen and deuterium are identical to all approximations ordinarily considered, the electronic factors of the transition probabilities of hydrogen and deuterium from a given initial to a given final state will be identical for electrons of such sufficient energy that the transition probability is essentially independent of the electron energy. For ionizing electrons of only slightly more than the minimum energy, the transition probability of hydrogen will be greater than that of deuterium, since the difference in the zero point energy of hydrogen and deuterium (0.07 ev) causes the minimum energy for transitions of hydrogen to be less than the minimum energy of the corresponding transitions of deuterium.

As was stated by Bleakney, Condon, and Smith,[1] the condition for transitions to the $^2\Sigma^+_g$ state of the molecular ions above the dissociation limit is that the interatomic distance in the molecule at the instant of ionization be less than a critical value, say r_c. The value of r_c is determined by the interatomic distance in the $^2\Sigma^+_g$ state of the molecular ion at which the energy of the molecular ion equals the dissociation energy of the molecular ion. This condition follows from the equal applicability of the Franck-Condon principle to electron-impact and optically induced transitions.[1] Thus the transition probabilities to the $^2\Sigma^+_g$ state contain a factor dependent on the electronic wave functions of molecule and molecular ion. The factors dependent on the vibrational wave function amount to nothing more than the fraction of the molecules with interatomic distances less than r_c for transitions above the dissociation limit of $^2\Sigma^+_g$ and the fraction of molecules with interatomic distances greater than r_c for transitions to the

[1] Bleakney, Condon, and Smith, J. Phys. Chem. **41**, 197 (1937).
[2] W. Bleakney, Phys. Rev. **35**, 1180 (1930).

TABLE I. The fraction of hydrogen and deuterium molecules with interatomic distances $\leqslant 0.586$A and $\geqslant 0.586$A, ground vibrational state of $^1\Sigma^+_g$.

	Harmonic oscillator	Anhormonic oscillator[3]
$f_H(<r_e)$	0.0429	0.0187
$f_H(<r_e)$	0.9561	0.9813
$f_D(<r_e)$	0.0193	0.0083
$f_D(>r_e)$	0.9807	0.9917
F_H/F_D [1]	2.28±0.2 [2]	2.29±0.2 [2]

[1] $F_H/F_D=[f_H(<r_e)/f_H(>r_e)]/[f_H(<r_e)f_D(>r_e)]$.
[2] This uncertainty is that corresponding to the uncertainty in r_e, ±0.01A.
[3] *The Tables of incomplete gamma functions*, by K. Pearson, were used to evaluate the integrals.

stable levels of $^2\Sigma^+_g$. These fractions of molecules will be designated $f(<r_e)$ and $f(>r_e)$, respectively.

If the effect of the small differences in zero point energy is neglected, and the electronic transition probabilities for transitions from the ground state of hydrogen and deuterium to the $^2\Sigma^+_g$, $^2\Sigma_u{}^+$, etc., states of their molecular ions are designated by $T(^2\Sigma^+_g)$, $T(^2\Sigma^+_u)$, etc., the number of atomic ions observed in the mass spectra of hydrogen and deuterium will be

$$n(a^+)=bf(<r_e)T(^2\Sigma^+_g)+bT(^2\Sigma^+_u)+\cdots, \quad (1)$$

and the number of molecular ions will be

$$n(n^+)=bf(>r_e)T(^2\Sigma^+_g), \quad (2)$$

where b is a constant of proportionality.

The fractions, f, are given by

$$f(<r_e)=\int_0^{r_e}\psi_0{}^2(r)dr \quad (3a)$$

and

$$f(>r_e)=\int_{r_e}^{\infty}\psi_0{}^2(r)dr=1-f(<r_e), \quad (3b)$$

where $\psi_0{}^2(r)$ is the normalized, vibrational wave function for the ground vibrational level of hydrogen or deuterium. Only the ground level need be considered because the magnitudes of the fundamental frequencies of hydrogen and deuterium are so great that a negligible fraction of the molecules are vibrationally excited at the highest temperatures encountered in mass spectrometers (250–300°C).

Although the T's may be taken equal for transitions of hydrogen and deuterium, the f's of hydrogen and deuterium are different because the values of the integrals are dependent on the numerical parameters of $\psi_0{}^2(r)$, and the numerical parameters are different for hydrogen and deuterium. Two approximations to the vibrational wave function, $\psi_0{}^2(r)$, were considered in evaluating the f's for hydrogen and deuterium. These approximations were the solutions of the radial wave equation,[3] neglecting the rotational term, for the harmonic oscillator and the Morse function approximation to the potential function. For the vibrational ground state these solutions are

$$\psi_0(r)=N_0\exp[-\alpha(r-r_e)^2], \quad (4a)$$

$$\psi_0(r)=A_0\exp[-\epsilon\exp\{-a(r-r_e)\}]\cdot\exp[-a(\epsilon-\tfrac{1}{2})(r-r_e)], \quad (4b)$$

where N_0 and A_0 are normalization constants, $\alpha=4\pi^2\mu c\omega_e/h$, $\epsilon=D_e/hc\omega_e$, $a=2\pi^2\mu c^2\omega_e{}^2/D_e$, and the other symbols have their usual significance.[4] The numerical values of the various parameters were taken from the compilation by Herzberg.[4]

The value of r_e used was 0.586±0.01A. This value was obtained by interpolation from the quantal calculations of Hylleraas.[3,5] The values of the f's are given in Table I.

The ratio of the relative abundances of H^+ and D^+ in the mass spectra of hydrogen and deuterium is

$$[n(H^+)/n(H_2{}^+)]/[n(D^+)/n(D_2{}^+)]=\frac{F_H+[1/f_H(>r_e)][T(^2\Sigma^+_u/T(^2\Sigma^+_g)]+\cdots}{F_D+[1/f_D(>r_e)][T(^2\Sigma^+_u)/T(^2\Sigma^+_g)]+\cdots}, \quad (5)$$

and F_H and F_D are defined in the notes to Table I. It is known that for electrons of less than 30 to 35-volts energy $T(^2\Sigma^+_u)/T(^2\Sigma^+_g)\ll F_H$.[2] Thus for such electrons the ratio of the relative abundances of H^+ and D^+ in the mass spectra of hydrogen and deuterium should be equal to $F_H/F_D=2.3\pm0.2$.

Two experimental investigations have been made of the ratio of the relative intensities of H^+ and D^+. The first of these[1] leads to 2.8 for 22-volt ionizing electrons. The second[6] gives 1.5±0.2, 1.9±0.2, and 2.2±0.2 for 30, 50, and 100-volt

[3] Pauling and Wilson, *Introduction to Quantum Mechanics* (McGraw-Hill Book Company, Inc., New York, 1935), pp. 264–266.
[4] Herzberg, *Molecular Spectra and Molecular Structure, I.* (Prentice-Hall, Inc., New York, 1939).
[5] Hylleraas, Zeits. f. Physik **71**, 739 (1931).
[6] Bauer and Beach, J. Chem. Phys. **15**, 150 (1947).

electrons, respectively. The calculated value, 2.3 ± 0.2, is in satisfactory agreement with these experimental values.

It was remarked above that the higher zero point energy of hydrogen than of deuterium results in a lower appearance potential of H^+ in the mass spectrum of hydrogen than of D^+ in deuterium. Thus, as the energy of the ionizing electrons is lowered and it approaches 18 volts, the assumption of equality of $T(^2\Sigma^+_g)$ for hydrogen and deuterium fails. With decreasing electron energy, $T(^2\Sigma^+_g)$ of hydrogen becomes greater than $T(^2\Sigma^+_g)$ of deuterium and

$$[n(H^+)/n(H_2^+)]/[n(D^+)/n(D_2^+)]$$

should be greater than F_H/F_D in proportion.

For ionization by electrons of more than 50-volt energy, the probability of transitions to the repulsive state, $T(^2\Sigma^+_u)$, becomes very much greater than the probability of transition to the repulsive portion of the stable state, $f(<r_c)T(^2\Sigma^+_g)$.[7] There are, however, two related reasons why the mass spectrometrically observed value of the ratio of the relative abundances of H^+ and D^+ will not approach unity as rapidly as might be expected from Eq. (5) and the data of Bleakney[2,7] when the ionizing electron energy is increased. The atomic ions formed as a result of transitions to the $^2\Sigma^+_u$ state are formed with a large amount of kinetic energy. This results in an increase in the breadth of the corresponding mass spectral peaks and failure of the assumption usually made, namely, that peak height is proportional to total ion intensity. Thus using the peak height as a measure of the ion current, as is commonly done, results in underestimation of the current caused by ions with extra kinetic energy. Furthermore, the construction of ionization chambers of mass spectrometers is such that there is a disproportionate loss of ions formed with kinetic energy.[8] This too results in the underestimation of the number of atomic ions. Of these two factors the selective loss of ions with extra kinetic energy is probably the more important in the case of the measurements of Bauer and Beach.[6] Examination of their mass spectra reveals asymmetry of the H^+ and D^+ peaks such as would result from contributions of fast atomic ions.

The magnitude of

$$[n(H^+)/n(H_2^+)]/[n(D^+)/n(D_2^+)]$$

is found by Bauer and Beach[6] to increase with electron energy, rather than decrease as predicted by our theory. The failure of their mass spectrometer to record H^+ and D^+ ions with excess kinetic energy accounts for the failure of the ratio of relative intensities to decrease with increasing electron energy. That the observed ratio of relative intensities increases with electron energy, the experimental value approaching equality with the calculated value for ionization by 100-volt electrons, may be taken as indication that the assumption of equality of $T(^2\Sigma^+_g)$ for hydrogen and deuterium is not accurately valid for electrons with energies between 30 and 50 volts.

According to the assumptions that have been made, F_H and F_D should be approximately equal to the relative abundances of H^+ and D^+ in the mass spectra of hydrogen and deuterium, respectively, for ionization by electrons of less than 30 to 35-volt energy. Although the ratio of F_H/F_D is independent of the approximation to the vibrational wave function used to evaluate the integrals of Eqs. (3a) and (3b), the values of F_H and F_D are very sensitive to the nature of the wave function. Thus it is not surprising that $F_H=0.019$ and $F_D=0.008$ (anharmonic oscillator, Table I) are not in good agreement with the experimental values

$$H^+/H_2^+=0.0096, \quad D^+/D_2^+=0.0034$$

for 22-volt electrons,[1] and

$$H^+/H_2^+=0.0058, \quad D^+/D_2^+=0.038$$

for 30-volt electrons.[6] As would be expected, the anharmonic oscillator approximation to the vibrational wave function leads to better values of F_H and F_D than does the harmonic oscillator approximation.

In conclusion, the author would like to acknowledge his indebtedness to Dr. J. Y. Beach for communicating his most recent experimental results and to Dr. E. U. Condon with whom these questions were discussed during the winter of 1940–1941.

[7] See Fig. 5 of reference 2. Approximate values of the ratio $T(^2\Sigma^+_u)/f(<r_c)T(^2\Sigma^+_g)$ for 50-, 100-, and >150-volt electrons, estimated from the curves referred to, are 3, 6, and 7, respectively, for hydrogen.

[8] This has been discussed by Bleakney, reference 2.

Average Square Length and Radius of Unbranched Long-Chain Molecules with Restricted Internal Rotation

WILLIAM J. TAYLOR*
American Petroleum Institute Research Project 44, National Bureau of Standards, Washington, D. C.
(Received March 27, 1947)

EYRING[1] has derived a well-known formula for the average square length of an unbranched long-chain molecule with n bonds, each of length σ, with a fixed valence angle θ between successive bonds, and *free internal rotation* about each bond, and Debye[2] has given a formula for the average square radius of the molecule. These quantities appear as parameters in theories of the physical properties (elasticity, intrinsic viscosity, streaming double refraction, etc.) of long-chain molecules. However, the assumption of free rotation is now known to be inadequate for a quantitative treatment of properties affected by internal rotation. In actual molecules in which rotations occur, the latter are, in general, partially restricted by potential functions with one or more minima separated by intervening maxima (potential barriers).

The only published attempt to calculate the effect of a restricting potential of which the writer is aware, is that of Bresler and Frenkel,[3] who, however, considered only the special case of small torsional oscillations about the equilibrium configuration.[4] Their treatment fails for large oscillations or for potential functions with more than one minimum, so that they have not in fact treated restricted *rotation*.

The present communication reports formulas for the average square length and radius of an unbranched long-chain molecule for the case in which the rotation about each bond is restricted by the same potential function $V(\phi)$ (ϕ = angle of rotation, defined so that $\phi = 0(\pi)$ for the planar *trans* (*cis*) configuration of three successive bonds). It is assumed that there are no interactions between different rotations (because of terms in the potential function or of steric hindrance), but there are no restrictions on the form of the function $V(\phi)$, or on the extent of the rotation. The exact solution has been obtained in a very general form which allows also for variation of the bond angle and bond length. However, in actual molecules the effect of these latter variations on the length and radius should be much less important that that of internal rotation. Only the formulas for restricted internal rotation will be presented here, and, in addition, only the approximate formulas valid for long chains. The derivation (which is based on Eyring's method[1]) and the general solution will be presented in a subsequent paper.

According to classical statistics, the probability that a given bond rotation lies in the range $(\phi, \phi+d\phi)$ is $p(\phi)d\phi$, where

$$p(\phi) = C \exp[-V(\phi)/kT] \tag{1}$$

and C has a value such that,

$$\int_{-\pi}^{\pi} p(\phi)d\phi = 1. \tag{2}$$

k is Boltzmann's constant and T is the absolute temperature. The average square length and radius depend on the function $V(\phi)$, and on the temperature, only through the two parameters, a and b, defined by the equation,

$$\begin{Bmatrix} a \\ b \end{Bmatrix} = \int_{-\pi}^{\pi} p(\phi) \begin{Bmatrix} \cos\phi \\ \sin\phi \end{Bmatrix} d\phi. \tag{3}$$

a and b are clearly the average values of $\cos\phi$ and $\sin\phi$, respectively. The solution has been obtained for the general case, $a \neq 0$, $b \neq 0$. However the only case likely to be of physical interest is that corresponding to an *even* potential function, $V(\phi) = V(-\phi)$, for which $b = 0$.

---

* Research Associate on the American Petroleum Institute Research Project 44 on the "Collection, Analysis, and Calculation of Data on the Properties of Hydrocarbons."

[1] H. Eyring, Phys. Rev. **39**, 746 (1932); E. Gorin, J. Walter, and H. Eyring, J. Am. Chem. Soc. **61**, 1885 (1939); see also, F. T. Wall, J. Chem. Phys. **11**, 67 (1943).

[2] P. Debye, J. Chem. Phys. **14**, 636 (1946).

[3] S. E. Bresler and J. I. Frenkel, Acta Physicochimica U.R.S.S. **11**, 485 (1939). In English.

[4] R. Simha, in reviewing the present paper, has brought to the attention of the author a paper by B. H. Zimm, R. S. Stein, and P. Doty (Polymer Bulletin, Vol. 1, October 1945, page 109 and Eq. (64)) in which brief mention is made of a treatment of this problem by Debye. It is not immediately clear whether the result quoted agrees with Eq. (4) of the present paper.

Only the result for $b=0$ is reported here. The case of free rotation corresponds to $V(\phi)=0$, $a=b=0$. An important special case is that of a potential function with m-fold symmetry, $m \geqslant 2$, so that $V(\phi)=V(\phi+2\pi/m)$. In this case it is easily shown from Eq. (3) and Lagrange's trigonometric identity that $a=b=0$, so that the length and radius have the same values as for free rotation, as has been pointed out by Gorin, Walter, and Eyring.[1]

It is assumed that the n bonds join $(n+1)$ point masses, or atoms, of equal mass. For each possible configuration of the molecule there may be defined: (1) the *length*, L, equal to the distance from the first to the $(n+1)$th atom; (2) the *radius*, R, equal to the root-mean-square value of the $(n+1)$ radii from the center of mass to the $(n+1)$ atoms. A given configuration is defined (for a fixed valence angle θ) by the values of the ϕ's for each of the $(n-2)$ internal rotations. The probability of occurrence of the given configuration is taken to be the product of $(n-2)$ functions $p(\phi)$, one for each rotation (corresponding to the assumption that the potential energy is separable). An average of a quantity over all configurations, each weighted according to its probability of occurrence, will be denoted by the notation $\langle\ \rangle$.

For sufficiently large values of n, the average square length and radius are very nearly proportional to n, just as for free rotation, but the constant of proportionality is altered by the restricting potential. The approximate equations for large n are,[5]

$$\langle L^2\rangle = \sigma^2\left(\frac{1+\alpha}{1-\alpha}\right)\left(\frac{1+a}{1-a}\right)n, \tag{4}$$

$$\langle R^2\rangle = \tfrac{1}{6}\langle L^2\rangle \tag{5}$$

where $\alpha=\cos\theta$ and a is given by Eq. (3). Equation (5) is that given by Debye;[2] that is, the ratio of the radius to the length is unchanged to this approximation. For free rotation, $a=0$, and Eq. (4) reduces to the result reported previously.[1] The fractional errors in $\langle L^2\rangle$ and $\langle R^2\rangle$, as calculated from Eqs. (4) and (5), are of the order of magnitude of $(1/n)$ for values of α, a, and n, such that

$$n|\lambda_1{}^n|<1, \quad n|\lambda_2{}^n|<1 \tag{6}$$

where

$$\left\{\begin{matrix}\lambda_1\\ \lambda_2\end{matrix}\right\} = \tfrac{1}{2}\{\alpha(1-a)\pm[\alpha^2(1-a)^2+4a]^{\frac{1}{2}}\}. \tag{7}$$

Also $|\lambda_1|<1$ and $|\lambda_2|<1$ for $|\alpha|<1$ and $|a|<1$, so that conditions (6) are satisfied for sufficiently large n except in the limiting cases, $|\alpha|=1$ or $|a|=1$.

According to Eqs. (4) and (5), $\langle L^2\rangle$ and $\langle R^2\rangle$ are functions of the temperature, through the parameter a. As the temperature increases the rotation becomes less restricted, and $|a|$ decreases. As a result, $\langle L^2\rangle$ and $\langle R^2\rangle$ decrease (increase), if a is positive (negative), resulting qualitatively from the increasing probability of more (less) coiled configurations. There is no temperature coefficient in the case of free rotation ($a=0$).

Returning now to the results of Bresler and Frenkel[3] (hereafter referred to as BF) it will be seen that Eq. (4) is not in agreement with Eq. (35) of BF, which it should include as a special case. The writer is confident that Eq. (4) is correct, since it is obtained by an exact calculation. There are a number of approximations in the derivation of Eq. (35) of BF. The equivalent of Eq. (4) has been obtained by another method of calculation for a special case,[5] and Eq. (4) also yields the correct result for free rotation.[6]

[5] Equations equivalent to Eqs. (4) and (5) have been obtained by the writer by another method of calculation for the following special case: $\theta=109°28'$; $\phi=0, \pm(2\pi/3)$ (with unequal probabilities for the 0 and $\pm(2\pi/3)$ positions). These equations were contained in an unpublished manuscript completed September 30, 1944.

[6] *Note added in proof:* C. Sadron, J. chim. physique **43**, 12 (1946), in a paper which became available to the writer after the present paper was submitted for publication, has given an approximate formula for $\langle L^2\rangle$ for the case of *nearly free* rotation which agrees with the form assumed by Eq. (4) for this special case ($|a|\ll 1$).

Letters to the Editor

*THIS section will accept reports of new work, provided these are terse and contain few figures, and especially few halftone cuts. The Editorial Board will not hold itself responsible for opinions expressed by the correspondents. Contributions to this section should not exceed 600 words in length and must reach the office of the Managing Editor not later than the 15th of the month preceding that of the issue in which the letter is to appear. No proof will be sent to the authors. The usual publication charge (**$3.00 per page**) will not be made and no reprints will be furnished free.*

Dye Sensitization of Photographic Emulsions and the Triplet State

WILLIAM T. SIMPSON
University of California, Berkeley, California
April 20, 1947

CURRENT research has established the existence of a triplet state associated with unsaturation electrons in organic molecules.[1] The triplet state concept will be shown below to furnish a plausible explanation of dye sensitization of photographic emulsions.

The position of the "long wave-length" limit of absorption of a silver bromide crystal would ordinarily be taken as an indication of the energy of the lowest electronic excited state of the crystal. Actually, considerably less energy than would be involved in the absorption of light by silver bromide can, through the agency of an adsorbed sensitizing dye, produce a photographic latent image. Experiment seems to indicate that there is no destruction of adsorbed sensitizing dye, as would take place if the dye gave up an electron to the crystal.[2] The most reasonable alternate explanation for the phenomenon of dye sensitization is that there exists another energy level in the crystal, but one that cannot be reached by the action of light.[3] In this connection it is interesting to remember that a very stringent selection rule is the one requiring conservation of multiplicity.

A variation solution of the quantum mechanics of the silver bromide crystal requires that, in the first excited electronic state, the probability distribution of an electron be huge with respect to the size of a single-lattice element. This spread-out probability is said to fit the observed phenomenon of photo-conductivity. But a more refined calculation in which exchange integrals are considered explicitly might predict the existence of a new, lower lying, excited electron state (which is in reality a band): a triplet state. In the modified variation solution, the coefficients of atomic orbitals should become large as the orbitals are chosen nearer and nearer to the hypothetical point of ejection, the orbital proper to the atom which absorbed the excitation being represented maximally. An electron in such an excited state would not be identified with the whole crystal from the standpoint of space, but might be from the standpoint of time. The spin parallelism existing in the new low lying excited state ought to prevent the excited electron from re-pairing, a metastability existing just as with the triplet state of organic molecules.

With the aid of the concept of a triplet state in a silver halide crystal, one can propose a mechanism for dye sensitization. The surface adsorbed sensitizing dye can undergo internal conversion to the triplet state after absorption of light raises it first to the excited singlet state. The ordinarily metastable triplet state of the dye may be very short lived, for the dye returns to its ground singlet state, simultaneously transferring its energy to the silver bromide crystal in a spin conservative process. An electron is thereby ejected from a lattice bromide ion situated adjacent to the dye molecule. The ultimate result of such an excitation of the silver bromide crystal ought to be the trapping of the electron in a sensitivity speck or in a growing latent image silver speck.[4] If no such "trapping centers" exist nearby, re-pairing of electrons occurs, accompanied, of course, either by the heating of the crystal or the emission of light.

[1] G. N. Lewis and M. Kasha, J. Am. Chem. Soc. **66**, 2100 (1944).
[2] See for example the discussion by G. Kornfeld, J. Phys. Chem. **42**, 795 (1938).
[3] The most recent exposition of this viewpoint is by N. F. Mott, J. Phys. Radium **7**, 249 (1946).
[4] The Gurney and Mott theory of the latent image is accepted here without caution.

An X-Ray Examination of Cyclooctatetraene[1]

H. S. KAUFMAN, I. FANKUCHEN, AND H. MARK
Institute of Polymer Research, Polytechnic Institute of Brooklyn, Brooklyn, New York
May 5, 1947

CYCLOOCTATETRAENE is an unusual compound which was reported for the first time by Willstätter[2] and co-workers in 1911. During the last war it was prepared in Germany by the catalytic polymerization of acetylene,[3] and more recently it has been produced in this country using similar processes. An extensive x-ray investigation of this compound was undertaken in order to determine the stereochemistry of the molecule in the solid state The work proceeded to a state where all the details of the structure cannot be given, but because of the unusual interest in this material, we are presenting the data obtained to date.

Cyclooctatetraene (C.O.T.) is a golden yellow liquid of density 0.938 which freezes, at -7 degrees C, to almost colorless needle-shaped crystals. Special low temperature cameras were constructed to obtain suitable powder and single crystal x-ray diagrams using nickel filtered copper radiation. The *d*-values, observed and computed, and relative intensities of the powder diagram are given in Table I. The density, $1.04 \mp .02$, of the solid was obtained by applying an experimentally derived correction to the liquid density.

The preliminary x-ray examination was done using the Debye-Scherrer techniques. The diagram was remarkably simple in appearance and resembled the line system given by cubic materials. Indeed, all of the Debye-Scherrer lines (Table I) can be reasonably indexed using a cubic unit cell of side $a = 10.85$A. The crystals are, however, birefringent, and a cubic structure is therefore unacceptable.

A tetragonal unit cell was then considered, and all of the Debye-Scherrer lines were indexable on the basis of a primitive tetragonal unit cell with $a=7.8$A, $c=10.7$A. The pseudo-cubic character of this cell is evident; $c \leqq a(2)^{\frac{1}{2}}$.

TABLE I. Interplanar spacings and relative intensities of cyclooctatetraene from Debye-Scherrer powder diagrams.

d-A (obs.)	d-A (comp.)*	Intensity	$h\ k\ l$
5.34	5.33	m	0 0 2
4.88	4.88	s	1 1 1
3.87	3.89	m	0 2 0–2 0 0
3.49	3.49	m	1 2 0
3.30	3.30	m	2 1 1
3.14	3.14	m	2 0 2–0 2 2
2.98	2.98	m	1 1 3
2.91	2.91	m–w	1 2 2
2.65	2.66	m–w	0 0 4
2.48	2.48	w	2 1 3
2.39	2.39	m–w	3 1 1–1 3 1
2.19	2.19	m–w	2 0 4–0 2 4
2.16	2.15	vw	3 2 0
2.13	2.12	w	2 3 1
2.02	2.02	mw	1 3 3–3 1 3
1.95	1.95	w	0 4 0–4 0 0
1.82	1.82	w	4 0 2–0 4 2
1.67	1.66	w	4 2 2–2 4 2

* In those cases where two sets of indices are given the computed spacing is an average.

At this stage it appeared desirable to employ single-crystal x-ray measurements. A study of the intensities of observed reflections showed that the tetragonal unit cell was untenable. This led to the choice of an orthorhombic pseudo-tetragonal cell where $a \leqq b \leqq 7.8$A and $C=10.7$A. This revised cell permitted satisfactory indexing of all Debye-Scherrer lines (Table I) as well as of the single crystal reflections.

The lattice constants were then determined more exactly by a least-squares solution of those Debye-Scherrer lines which could be uniquely indexed. This gave $a=7.76$A, $b=7.80$A, $c=10.66$A. These values were used to calculate the spacings for the powder reflections (Table I). The agreement is good.

Systematic extinctions of the (hkl) reflections for $(k+1)$ odd, of the (hol) reflections for h odd, and the (okl) reflections for k odd were found. Two orthorhombic space groups require these extinctions; $A\ b\ a$ and $A\ b\ a\ m$.

For four molecules per cell, the x-ray density is 1.06 which may be compared to the measured value of 1.04.

Inasmuch as the space group choice is limited to $A\ b\ a$ or $A\ b\ a\ m$, the molecular centers must be located at special locations in the unit cell. In either case, the centers of the molecules are located at the points of a face centered orthorhombic lattice, and the molecule must possess at least a twofold axis of symmetry. If the space groups were $A\ b\ a\ m$, in addition, the molecule would have to have a plane of symmetry. We now feel that this latter space group is the less likely of the two.

[1] This work represents part of a dissertation to be presented by H. S. Kaufman to the Graduate Faculty of the Polytechnic Institute of Brooklyn, in partial fulfillment of the requirements for the degree of Doctor of Philosophy.

[2] Willstätter and Waser, Ber. **44**, 3423 (1911); Willstätter and Heidelberger, Ber. **46**, 517 (1913).

[3] Report by Dr. Walter Reppe on Cyclopolyolefines (Ludwigshafen on Rhine, April 28, 1944).

A New Refinement Technique for X-Ray Structure Analysis

ANDREW D. BOOTH
Institute for Advanced Study, School of Mathematics, Princeton, New Jersey

May 5, 1947

THE standard technique of Fourier refinement, which has been used with such success in many simple structure analyses, is unfortunately reaching a state in which, despite technical improvements,[1–3] the time taken for a structure analysis is increasing to a prohibitive extent. Thus, in recent determinations (on geranylamine hydrochloride[4] and penicillin),[5] times of the order of 3 years have been needed for completion.

At the root of this decline is the fact that, in order for the Fourier process to converge, a set of parameters must be found by trial and error, which are a reasonable approximation to the correct ones. Roughly speaking, the region of convergence of the Fourier method is the same as that of its differential variant.[3]

Patterson-Harker syntheses cannot be considered the complete solution to the problem of approximate structure determination since, in a wide range of cases, no useful information is obtainable from this technique; and this is especially true in complex organic structures. Similarly, molecular transforms are very difficult to apply in any but the simplest space groups.

It can be stated that the desirable features of any systematic form of structure determination are the following:

(1) Starting from any arbitrary position, it should be possible to locate the position of a molecule *considered as a rigid unit.*
(2) Having found the position of the molecule considered rigid, it should be possible to determine the individual atomic positions.
(3) If necessary, the method should be applicable to density distributions. This is particularly true for macromolecules since here, although the general shape may be known, the details may be completely obscure.

A solution to these problems is to be found *via* the method of "steepest" descents" which, although in some ways a generalization of the least-squares refinement,[6] is unlike the latter in that it can be applied to systems of any degree of complexity. In addition, it is possible to locate the position of a molecule considered either as a rigid whole or as a set of rigid parts, or to refine a density distribution given at lattice points over the unit cell.

Full details of the method in all its forms, will be published at a later date, but it is proposed to explain here the general philosophy of the attack and to give the equations for the simplest case.

In essence, the scheme is merely a procedure for minimizing either:

$$R_1 = \sum_{hkl} \| F_{\text{obs}} | - | F_{\text{calc}} \|$$

or

$$R_2 = \sum_{hkl} (F_{\text{obs}}^2 - F_{\text{calc}}^2)^2.$$

Now $R_n = \text{const.}$ represents a surface in the $3N$ dimensional space defined by the atomic parameters x_{rj} $(r=1 \cdots N;\ j=1, 2, 3)$. The method of minimization is to proceed in the direction of the normal to any given surface until the value of R_n no longer decreases. Having arrived at this

point, the procedure is repeated, and a little consideration shows that this technique leads to the minimization of R_n.

Two expressions are available for the change ϵ_{rj} in any coordinate x_{rj}:

$$\epsilon_{rj} = -2R_n(\partial R_n/\partial x_{rj})/\sum_{rj}(\partial R_n/\partial x_{rj})^2$$

or:

$$\epsilon_{rj} = -[\sum_{rj}(\partial R_n/\partial x_{rj})^2](\partial R_n/\partial x_{rj})/$$
$$\sum_{rj,r'j'}(\partial^2 R_n/\partial x_{rj}\cdot\partial x_{r'j'})(\partial R_n/\partial x_{rj})(\partial R_n/\partial x_{r'i'}).$$

The first expression should be used only so long as the coordinates are far from their final values and is particularly simple to compute; whilst the second equation applies up to the minimum itself.

A particularly interesting variant of the method is available when a sufficiently large number of planes of zero observed intensity is available (excluding zeros due to symmetry elements). In this case the expressions:

$$0_1 = \sum_{hkl} |F_{\text{calc}}|$$

$$0_2 = \sum_{hkl} F_{\text{calc}}^2$$

taken over all planes of zero observed intensity can be minimized, and the resulting calculations are much simplified.

Simple extensions enable the position of a fixed molecular shape to be found such that R_n is minimized. This is done either by referring the molecule to an axial system, whose orientation and origin are then varied, or by taking three atoms of the molecule as standards and minimizing R_n in such a way that all inter-atomic distances remain fixed. When a molecule contains known groupings related to one another by free rotations, a slightly more general approach enables the same methods to be applied.

Finally, it is possible to use the technique to obtain density distributions which minimize R_n, although there, particular care has to be taken to obtain a stereo-chemically plausible starting distribution.

[1] Booth, Trans. Faraday Soc. **41**, 434 (1945).
[2] Booth, Trans. Faraday Soc. **42**, 444 (1946).
[3] Booth, Trans. Faraday Soc. **42**, 617 (1946).
[4] Jeffrey, Proc. Roy. Soc. **A183**, 388 (1945).
[5] Crowfoot (to be published).
[6] Hughes, J. Am. Chem. Soc. **63**, 1737 (1941).

Upper Limit to the Tritium Content of Ordinary Water

MAXWELL LEIGH EIDINOFF
Department of Chemistry, Queen's College, Flushing, New York
April 23, 1947

IN 1938 Sherr, Smith, and Bleakney[1] concluded from mass spectrographic measurements, using deuterium gas, that the tritium content of ordinary water is less than one part in 10^{12}. It has been established by the experiments described below that the tritium atom fraction in ordinary water is less than one part in 10^{17}. An extension of this technique should lead to a smaller upper limit to the abundance of this isotope.

22-mm partial pressure of deuterium gas, having a D content greater than 95 percent,[2] was added to a glass envelope copper gauze cathode Geiger-counter tube having a diameter of 42 mm, an effective counting volume of 200 cc and containing 23-mm partial pressure each of argon and ethyl alcohol. The normal background count, employing a $\frac{3}{8}''$ lead shield was 2.85 counts per second. The addition of the deuterium gas did not change the the counting rate within the precision of the measurements. The average deviation of this measurement (based upon four independent experiments) was 0.03 counts per second. The latter value was used in calculating the upper limit to tritium abundance.

Using the above data and a tritium half-life of 31 years,[3] the tritium atom fraction in ordinary water is less than $1.5\times10^{-13}(T°/T)$, where $(T/T°)$ is the factor by which the tritium was enriched in the electrolysis of normal water from 99.98 percent H to the final D content. Using 95 percent for the latter, the initial-volume/final-volume water ratio was calculated from the $H-D$ cathodic separation factor. The ratio $(T/T°)$ was calculated from this volume ratio and the $H-T$ separation factor.[4] For $H-D$ and $H-T$ separation factors of 5 and 10, respectively, $(T/T°)$ equals 2.0×10^4. For corresponding factors 6.5 and 13, respectively, $(T/T°)$ equals 1.3×10^4. Taking $(T/T°)$ as 1.5×10^4, the tritium atom fraction in ordinary water is less than one part in 10^{17}. By exhaustive electrolysis of heavy water, it will be possible to decrease the magnitude of this upper limit. The latter is of interest, inasmuch as tritium is a possible reaction product in nuclear processes taking place in the earth's atmosphere.[5]

This investigation was supported by a grant from the Research Corporation.

[1] R. Sherr, L. G. Smith, and W. Bleakney, Phys. Rev. **54**, 388 (1938).
[2] From Stuart Oxygen Company, San Francisco, California.
[3] R. D. O'Neal and M. Goldhaber, Phys. Rev. **58**, 574 (1940).
[4] M. L. Eidinoff, J. Am. Chem. Soc. **69**, 977 (1947).
[5] E.g., W. F. Libby, Phys. Rev. **69**, 671 (1946).

Patterson-Harker Maps of Molecular Crystals

A. D. BOOTH
Institute for Advanced Studies, Princeton, New Jersey, and Birkbeck College, University of London, London, England
AND
DOROTHY WRINCH
Smith College, Northampton, Massachusetts
May 15, 1947

THE interpretation of the x-ray data obtained from megamolecular crystals presents a new and difficult problem in cases where the structure and even the composition of the molecular units are unknown. If an attack be attempted by way of Patterson and Patterson-Harker maps, computed from the experimental data, a useful, even necessary preliminary is the study of the Patterson maps of various structure types.[1] A fundamental difficulty, however, arises at the outset owing to the overlapping in Patterson space S_2 of the Pattersons of individual molecules in the crystal in atomic space S_1[2]. The purpose of this note is to draw attention to and indicate some of the implications of the fact that there is always a region about the

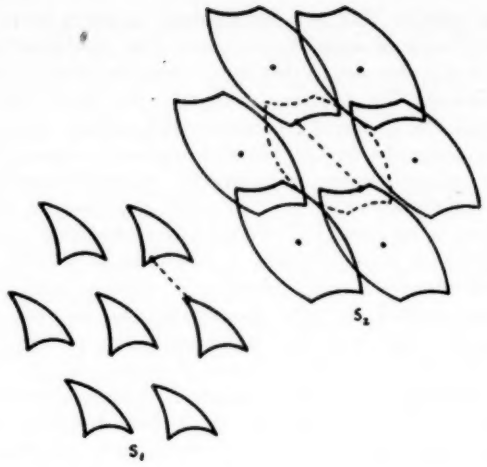

FIG. 1.

origin in S_2 which records the Patterson of a single unit of pattern, provided there is a minimum distance of approach of the units of pattern in neighboring cells in S_1.

Figure 1 depicts the case of a two-dimensional crystal with a single molecule as its unit of pattern. With a minimum approach k between molecules, there is an "intra-molecular" region about the origin in S_2 which extends at least to a circle of radius k. To define this region more precisely, we take a number of directions in turn and observe the closest approach of molecules in each case. Erecting these vectors at the origin in S_2, we get points on the boundary of the region—actually pairs of points, since the Patterson map has a center of symmetry in the origin. For the corresponding three-dimensional cases, the situation may be described in similar terms.

The question then arises as to the type of information, if any, which is implicit in this restricted part of the Patterson map of an individual molecule. The answer is clear on general grounds. All entries in a Patterson map in the neighborhood of the origin are caused by local situations within the molecule, i.e., by the fine structure of the molecule. As an example of a case in which the Patterson near the origin bears marks of the fine structure of a point set in S_1, we give in Fig. 2 the central section of the Patterson normal to a trigonal axis of a 96-point set on the surface of an octahedron.[3]

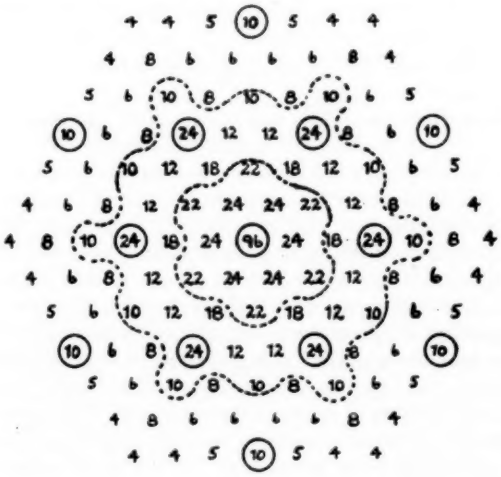

FIG. 2.

In the case of a molecular crystal with more than a single molecule in its unit of pattern, the case is more complicated but there is still the possibility of obtaining some hint from the Patterson map of the crystal regarding the fine structure, if any, of the molecules. It is still true that the Patterson near enough to the origin depends only upon local situations within the unit of pattern, i.e., upon neighborhood situations within the individual molecules. For, suppose there are two molecules A and B in the unit of pattern which are not necessarily parallel displacements of one another and may even be different structures. The Patterson of $A+B$ is the Patterson of A plus the Patterson of B plus the Patterson interactions of A on B and of B on A.[4] If the nearest approach of A and B is k', the cross interactions do not come nearer to the origin than k'. There is, therefore, a region around the origin in which the Patterson is simply the sum of the individual Pattersons of A and B; the same type of situation obtains with any number of molecules in the unit of pattern.

[1] A. D. Booth and D. Wrinch, J. Chem. Phys. **14**, 503 (1946).
[2] D. Wrinch, Phil. Mag. **27**, 490 (1939).
[3] D. Wrinch, "Fourier Transforms and Structure Factors," Monograph of the Am. Soc. for X-Ray and Electron Diffraction, pp. 57–62, 1946.
[4] I. Langmuir and D. Wrinch, J. Am. Chem. Soc. **60**, 2247 (1938).

Application of Radioactive Isotopes to the Problem of Diffusion of Electrolytes in Aqueous Solutions

LAWRENCE B. ROBINSON AND JAMES B. DREW
Department of Physics, Howard University, Washington, D. C.
April 30, 1947

THE diaphragm cell has been used extensively in studying the problem of the diffusion of ions in solution. The method reduces the problem to a one dimensional case. The starting point in one dimensional diffusion studies is usually

$$\frac{\partial c}{\partial t}=\frac{\partial}{\partial x}\left(\mathfrak{D}\frac{\partial c}{\partial x}\right), \tag{1}$$

where $\mathfrak{D}$ is the diffusion coefficient. $\mathfrak{D}$ is then taken as a first approximation to be independent of concentration, whence Fick's law results:

$$\frac{\partial c}{\partial t}=\mathfrak{D}\frac{\partial^2 c}{\partial x^2}. \tag{2}$$

Equation (2) has been integrated in many forms, and it is evident the equation involves an average or integral diffusion coefficient, as it is known experimentally that $\mathfrak{D}$ is not independent of c. The diffusion coefficient of an electrolyte at infinite dilution was first calculated by Nernst[1] to be

$$\mathfrak{D}^\circ=17.863\times10^{-10}T\left(\frac{\lambda_+^\circ\lambda_-}{\Lambda^\circ}\right), \tag{3}$$

where the symbols have their usual meaning. By using the Debye-Hueckel theory, Onsager and Fuoss[2] were able to obtain the following equation for the dependence of the diffusion coefficient on concentration:

$$\mathfrak{D} = 16.632 \times 10^{+10} T \left(\frac{\bar{m}}{c}\right)\left(1 + c\,\frac{\partial \ln y_{\pm}}{\partial c}\right), \qquad (4)$$

where $y_{\pm}$ is the mean ionic activity coefficient, and the mobility term $(\bar{m}/c)$ is a complicated function of the viscosity, the concentration, and the equivalent conductance at infinite dilution of the ions and compound. The slowness of diffusion makes it so that experiments are quite difficult and of long duration. Because of the difficulty in obtaining accurate analytical data, experiments in the region where the Debye-Hueckel theory is taken to be valid have been heretofore almost impossible. Onsager and Fuoss[2] were unable to obtain results below $0.05N$ with which to test their equation. Greater dilutions have been studied by experimenters, using optical methods for analysis, but Longsworth[3] says: ". . . This probably indicates that the optical methods in current use for the study of free diffusion, while capable of yielding results that are accurate within a few percent, we are not yet sufficiently sensitive for work of high precision, especially in the regent of dilute solutions for which the theory is valid."

In the Physics Laboratory at Howard, studies on diffusion of ions in solution have been undertaken using the radioactivity of isotopes as the analytical tool. The explicit assumption is made that the radioactive isotope behaves in exactly the same way as the non-radioactive isotope (in spite of the slight difference in mass). A given amount of active salt was added to a liter of $0.1M$ solution, in preliminary tests, and several more dilute solutions were prepared from this. It was found that the counts per minute, registered on a Geiger-Mueller counter and scaling circuits, from a definite quantity of each solution were a linear function of the concentration, as would be expected. Preliminary trials have indicated that this technique will give better results than any of the previous analytical methods. We have found it possible to work with solutions of $10^{-5}M$ without difficulty. Results obtained will be reported to this journal soon.

[1] W. Nernst, Zeits. f. physik. Chemie **2**, 613 (1888).
[2] L. Onsager and R. L. Fuoss, J. Phys. Chem. **36**, 2689 (1932); H. S. Harned and B. B. Owen, *The Physical Chemistry of Electrolytic Solutions* (Reinhold Publishing Corporation, New York, 1943), pp. 178–182.
[3] L. G. Longsworth, Ann. N. Y. Acad. Sci. **46**, 211 (1945).

Propagation of Ultrasonic Waves Through Liquid Mixtures and the Dynamics of Their Molecular Interaction

R. PARSHAD
Physical Laboratory, Council of Scientific and Industrial Research, University Buildings, Delhi, India
April 28, 1947

IN some previous papers,[1,2] a theoretical background was developed for discussing the variation of ultrasonic velocity with molecular structure of pure liquids and liquid mixtures. It was shown that it is compressibility and not sound velocity that is a fundamental property from the point of view of molecular structure. One significant conclusion was that association would raise the value of compressibility. The mixtures analysed were water alcohol (methyl ethyl, propyl), benzene-ethyl alcohol, benzene-carbon tetrachloride, butyl alcohol-heptane, benzene-ether, ethyl acetate-carbon tetrachloride, chloroform-acetone, and chloroform-ether.[1,3,4] On the experimental side, maxima of velocity (and minima of compressibility) were obtained for water alcohols, a minimum of velocity for chloroform-ether, and inflexion of velocity curve for benzene-alcohol. It was shown that in water-alcohol mixtures, there is mutual depolymerization of the components that gives rise to minima of compressibility.

Experimental data for a number of other mixtures were taken as far back as in 1940, at the Bose Institute, Calcutta, and their analysis has recently been completed.[5] They are ethyl alcohol-chloroform, ethyl alcohol-carbon tetrachloride, benzene-chloroform, ether-alcohol, water-glycerine, chloroform-carbon tetrachloride and sodium chloride+water+ethyl alcohol. Moreover, analysis of experimental data of other workers for acetone-water and acetic acid-water[7] has also been attempted. In the following we state some of the more important experimental facts and derivations therefrom.

Alcohol-Chloroform.—The velocity and compressibility curves are inflected, the compressibility being less than the ideal values on the alcohol-rich side, and greater than the ideal on the chloroform-rich side. It is concluded that the chloroform molecules can partially depolymerize alcohol association on the alcohol-rich side, without all the molecules so dissociated being attached to chloroform molecules. These dissociated molecules are in strong force-fields and cause lowering of compressibility. The finding is in direct contrast to that of Raymond and Scatchard.[6] Because of the tendency of alcohol molecules to associate with themselves and, simultaneously, with chloroform, a dynamical equilibrium results, resulting in part of the moecules being dissociated. Because of tendencies for a particular class of molecules to associate in two different systems, what actually results depends upon the strength of the two tendencies, and the structure of the different possible association systems. The name "dynamics of liquid mixtures" has been proposed to denote this sort of dynamical interaction.

Water-Glycerine.—The velocity is more and compressibility less than the ideal values all through the range. It is derived that the association of water is broken down, but that of glycerine incompletely, because of its relatively great strength.

Chloroform-Carbon Tetrachloride.—The velocity curve shows a slight minimum, and the compressibility is greater than the ideal values. It is derived that the value of compressibility of chloroform in the pure state, lower than that of carbon tetrachloride, is not directly due to its dipolar activity, but due to the greater intermolecular action involved because of its particular molecular shape. Two Cl atoms of a chloroform molecule can approach two Cl atoms of another molecule because of the dip in its otherwise symmetrical molecular shape, caused by the small size

of H. This two-to-two contact between neighboring molecules causes greater London dispersion forces,[9] than the one-to-one contact only possible in the tetrachloride.

Acetone-Water.—There is a maximum of velocity and minimum compressibility. This is again a case of dynamical interaction, when effective depolymerization of water is produced due to the opposing tendencies for the formation of water-water and water-acetone associations. But acetone-water associations may also be formed in some measure, as there is no opposing action of formation of acetone-acetone associations.

Acetic Acid-Water.—The maximum of velocity and minimum of compressibility is caused by the dynamical equilibrium producing effective depolymerization of both the components due to the mutually opposing tendencies of acid-acid, water-water, and acid-water associations. While the depolymerization of water may be thought to be complete, especially at the middle ranges, that of the acid is not expected to be so, on account of the much greater strength of the acid association than that of water.

Sodium Chloride+Water+Alcohol.—The system is of course very complex. But as the minimum of compressibility of water alcohol mixtures was derived to be due to depolymerization, it was surmised that by depolymerizing the water used for the mixture, say by dissolving a salt like sodium chloride in it, the minima of compressibility would be reduced in depth and shift towards the extreme of 100 percent salt water. This is actually found to be so, and there is left no minimum at all for 3N salt water.

From the foregoing it follows that maxima of velocity and minima of compressibility would be produced when an associated liquid is depolymerized by another associated liquid (water-alcohol) or by an unassociated but dipolar and active liquid (water-acetone). Minima of velocity and maxima of compressibility would be produced in a mixture whose components cannot have comparable mutual interactions to that in the pure state of each component, because of diversity of and mutual non-reactivity of elements in their molecular structures.

[1] R. Parshad, Ind. J. Phys. **15**, 323 (1941).
[2] R. Parshad, Ind. J. Phys. **19**, 47 (1945).
[3] R. Parshad, Ind. J. Phys. **16**, 1 (1942).
[4] R. Parshad, Ind. J. Phys. **16**, 389 (1942).
[5] R. Parshad, Doctorate thesis 1946, Punjab University.
[6] Salcelau, Comptes rendus **208**, 83 (1939). Recent determinations for this mixture are, Willard, J. Acous. Soc. Am. **12**, 438 (1941); Ramachandra Rao, Proc. Ind. Acad. Sci. **25**, 190 (1947).
[7] Smith and Ewing, J. Chem. Phys. **7**, 632 (1939).
[8] Raymond and Scatchard, J. Am. Chem. Soc. **60**, 1278 (1938).
[9] F. London, Trans. Faraday Soc. **33**, 8 (1937).

Influence of Neighbor Bonds on Additive Bond Properties in Paraffins

JOHN R. PLATT
Physics Department, University of Chicago, Chicago, Illinois
March 21, 1947

LEAST-SQUARES empirical formulas have been worked out for the variations among acyclic paraffin isomers in molar refractivities, molar volumes, heats of formation, and boiling points to fit the beautiful data in the API Tables of Properties.[1] The fit is about as good as that in the analyses of Taylor, Pignocco, and Rossini (TPR),[2] but it is believed that the physical significance of the present parameters is clearer.

The properties of the bonds are conceived to be strictly additive, but the contribution of each C−C or C−H bond is supposed to be slightly altered by the influence of its next C−C or C−H neighbors, by its second neighbors, third neighbors, and so on to the tips of the molecular skeleton. For the αth C−C bond, the contribution p_α to the property G is

$$p_\alpha = p_0 + p_1 f_{\alpha 1} + p_2 f_{\alpha 2} + \cdots + q_1 g_{\alpha 1} + q_2 g_{\alpha 2} + \cdots .$$

For the βth C−H bond, the contribution s_β is

$$s_\beta = s_0 + s_1 i_{\beta 1} + s_2 i_{\beta 2} + \cdots + r_1 h_{\beta 1} + r_2 h_{\beta 2} + \cdots ,$$

where p_j is the effect of a jth neighbor C−C bond on the C−C property, q_j of a C−H bond on the C−C, r_j of a C−C on the C−H, s_j of a C−H on C−H; and where there are $f_{\alpha j}$ of the C−C bonds at a distance of j bonds along the skeleton from the αth C−C, etc.

Summing these contributions for the whole molecule, the total property G can be shown to be of the form

$$G = A + a_0(N-1) + a_1 \sum_\alpha f_{\alpha 1} + a_2 \sum_\alpha f_{\alpha 2} + \cdots ,$$

where the a_1, a_2, $\cdots$ are linear combinations of the p_j, q_j, etc., and where N is the number of carbon atoms.

Additional quadratic terms were found to be necessary to obtain a good fit:

$$G = A + a_0(N-1) + a_1 \sum_\alpha f_{\alpha 1} + a_2 \sum_\alpha f_{\alpha 2} + a_3 \sum_\alpha f_{\alpha 3} + a_{11} \sum_\alpha f_{\alpha 1}^2 + a_{12} \sum_\alpha f_{\alpha 1} f_{\alpha 2} + a_{22} \sum_\alpha f_{\alpha 2}^2 .$$

The expressions for $\Sigma f_{\alpha 2}$ and $\Sigma f_{\alpha 1} f_{\alpha 2}$ will be found to correspond to the coefficients of TPR's k_1 and k_2. The least-squares parameters obtained from the data on the C_5 to C_8 paraffins by use of this last formula are shown in Table I, together with a comparison of the deviations from experimental values obtained with this analysis and with TPR's.

TABLE I. Neighbor-sum parameters.

	R ml/mole at 20°C	V ml/mole at 20°C	BP °C at 760 mm	$Hf°$ kcal/mole at 25°C (for gas from graphite and H_2)
A	6.448	48.45	—	−17.584
a_0	4.744	15.68	(about 45° near C_8)	− 2.116
a_1	.0239	1.090	−8.23	− 1.570
a_2	−.0741	− .505	−2.34	− .545
a_3	−.0015	+ .160	−1.43	− .140
a_{11}	−.0039	− .120	+ .76	+ .120
a_{12}	+.0070	− .100	+1.03	+ .235
a_{22}	−.0020	− .035	+ .14	+ .070
	Deviations, C_5–C_8			
TPR				
M.D.	±.013	± .16	± .55	—
σ	±.016	± .20	± .70	—
Max. dev.	.037	.49	1.71	—
Neighbor-sums				
M.D.	±.0106	± .22	± .67	± .19
σ	±.012	± .26	± .85	± .24
Max. dev.	.022	.60	2.41	.75

TABLE II. Predicted deviations of C_1 to $n-C_4$ from line of homologues.

	$\Delta\Sigma f_{\alpha 1}$	$\Sigma f_{\alpha 2}$	$\Sigma f_{\alpha 3}$	$\Sigma f_{\alpha 1}{}^2$	$\Sigma f_{\alpha 1} f_{\alpha 2}$	$\Sigma f_{\alpha 2}{}^2$	R	V	δ	BP	δ	$Hf°$	δ
C_1	2	4	6	6	10	12	−.235	−1.02		−17.86	2.53	−2.25	−.30
C_2		2	4	2	6	8	−.136	−1.49		− 1.58	2.26	.56	−.54
C_3			2		2	4	.003	− .02	(−.38)	− .24	.00	.47	−.10
C_4						2	−.004	− .07	(−.20)	+ .28	− .17	.14	.16

The n-paraffin molar volumes require an additional exponential term in the formula as follows,

$$\delta V = 10^{(1.939-.387N)},$$

to take account of the thermal enlargement of the lighter molecules. The n-paraffin boiling points are not additive. They lie within ±.17° of the curve

$$BP = 936.43° - \frac{1162.91°}{1+.074189N^{.88}};$$

and the formula for G can only be used for differences among isomers.

The fit in the neighbor-sum solution is better than the TPR fit for R, even when applied to the older data used by TPR, and it is within the claimed experimental error for $\Delta H_f°$. It is worse for the "phase properties" V and BP, indicating perhaps that these properties require the more detailed description of local structure furnished by the TPR analysis. Conversely, the descriptive advantage of the present scheme lies in its ignoring such details, so that its parameters do not multiply so rapidly with increasing N. Still more important, additional parameters such as TPR introduced, are not needed here to handle special cases such as methane and ethane and molecules with maximum branching.

The a_j values for BP and H seem to fall off smoothly, about $1/j^2$. Reversals of sign are present in R and V, which conceivably indicate steric effects between second neighbors.

The quadratic terms behave qualitatively like a saturation effect, if we consider that the influence of the C−C bonds on each other is the dominant effect. With this in mind, we would set

$$p_\alpha = p_0 + (p_1 f_1 + p_2 f_2) - \eta(p_1 f_1 + p_2 f_2)^2$$
$$= p_0 + p_1 f_1 + p_2 f_2 - \eta p_1{}^2 f_1{}^2 - 2\eta p_1 p_2 f_1 f_2 - \eta p_2{}^2 f_2{}^2.$$

The a_{11}, a_{12}, a_{22}'s are indeed in the ratio $p_1{}^2 : 2p_1p_2 : p_2{}^2$ within about 10 percent. But the ratio $p_1 : p_2$ so determined does not fit the $a_1 : a_2$ by factors of 2 and more; and a more general treatment is required to obtain a good fit.

The value of a_0 does not represent the whole increment between successive n-paraffins, since the $\Sigma f_{\alpha j}$ and $\Sigma f_{\alpha j} f_{\alpha k}$ all depend on N. Below C_5 this dependence is not linear, and the more distant neighbor sums successively become zero. Consequently, C_1 to C_4 should deviate from the line of the higher n-paraffins by the amounts shown in Table II. The columns marked δ give the additional correction necessary to match the experimental value. The big deviations in BP and $\Delta H_f°$ of methane are predicted almost within the original accuracy of fit of the neighbor-sum solution on the C_5 to C_8 isomers. Such a prediction was not possible from the TPR analysis.

Tabulations of the neighbor sums and expressions for the relations between the $\Sigma f_{\alpha j}$, $\Sigma g_{\alpha j}$, etc., and their relations to branching in the molecule will be given in detail in a forthcoming paper.

I am indebted to Dr. H. B. Klevens for his initial suggestion that the paraffin refractions deserved more study.

[1] American Petroleum Institute Research Project 44 at the National Bureau of Standards. Selected Values of Properties of Hydrocarbons. Tables 1a–4a, 1b–4b, dated June 30, 1945; 1p–3p, April 30, 1945 and November 30, 1946.

[2] W. J. Taylor, J. M. Pignocco, and F. D. Rossini, J. Res. Nat. Bur. Stand. **34**, 413 (1945).